Open access • Journal Article • DOI:10.1080/01614940.2020.1743420

Catalytic partial oxidation of methane to syngas: review of perovskite catalysts and membrane reactors — Source link

Abdalwadood H. Elbadawi, Lei Ge, Zhiheng Li, Shaomin Liu ...+2 more authors

Institutions: University of Queensland, University of Southern Queensland, Beijing University of Chemical Technology, University of Adelaide

Published on: 02 Jan 2021 - Catalysis Reviews-science and Engineering (Taylor & Francis)

Topics: Membrane reactor, Partial oxidation, Syngas, Hydrogen production and Catalysis

Catalytic Partial Oxidation of Methane to Syngas: Review of Perovskite Catalysts and Membrane Reactors

AbdAlwadood H. Elbadawi,[a] Lei Ge,[b*] Zhiheng Li,[a] Shaomin Liu,[c] Shaobin Wang[d], Zhonghua Zhu[a,*]

[a]School of Chemical Engineering, The University of Queensland, Brisbane, QLD 4072, Australia

[b]Center for Future Materials, University of Southern Queensland, Springfield Central, QLD 4300, Australia

[c]Department of Chemical Engineering, Curtin University, GPO Box U1987, Perth, WA 6845, Australia

[d]School of Chemical Engineering, The University of Adelaide, Adelaide, SA 5005, Australia

*Correspondent author: z.zhu@uq.edu.au (Zhonghua Zhu)

Catalytic Partial Oxidation of Methane to Syngas: Review of Perovskite Catalysts and Membrane Reactors

Abstract

Partial oxidation of methane (POM) offers a promising option to produce syngas for downstream processes such as hydrogen production and Fischer-Tropsch processes. POM in fixed-bed reactors requires an oxygen separation plant with high operation cost and safety risks. On the contrary, membrane reactors can provide an improved process by integrating both oxygen separation and catalytic reaction processes. With many advantages including high purity and efficient oxygen separation from the air at the catalytic reaction conditions, mixed ionic-electronic conducting membranes (MIEC) caught great attention in the scientific research field over the past two decades. In this review, POM using different catalysts in fixed-bed reactors was firstly summarised with emphasizing on perovskite-based catalysts, and then the material screening of MIEC membrane reactors was introduced and linked to the selection of conventional and perovskite catalysts. The catalytic activity, reaction mechanisms, and emerging challenges have been analyzed. Furthermore, future research directions have been outlined by highlighting the effect of electronic properties, continuous reduction-oxidation in the presence of oxygen flux, and chemical reaction mechanism on membrane/catalyst.

Keywords: Partial oxidation, Syngas, Membrane reactors, Mechanism

Table of Contents

1. Introduction	**5**
1.1 Methane to Syngas Processes	**6**
1.2 POM Reactors Configurations	**10**
2. Supported Catalysts for POM	**14**
2.1 Cobalt Catalysts	**15**
2.2 Nickel Catalysts	**16**
2.3 Rhodium and Ruthenium Catalysts	**23**
2.4 Other POM Catalysts	**24**
2.5 Perovskite Catalysts for POM	**27**
2.5.1 B-site Cation Selection	**28**
2.5.2 A-site doping in perovskite catalytic activity	**33**
3. Membrane Reactor Configurations for POM	**34**
3.1 Symmetric Membranes	**35**
3.2 Asymmetric Membranes	**38**
3.2.1 Porous catalysts layer effects on membrane catalytic activity	**38**
3.2.2 Dual-Functional Membranes Reactors	**45**
3.2.3 Overview of Catalyst Layer Coating Methods	**47**
3.2.4 Effect of Catalyst Layer on Oxygen Permeation	**48**
3.2.5 Effect of Oxygen Flux on Syngas Production	**50**
4. Thermodynamic Analysis and Mechanism of POM in Membrane Catalysis	**51**
4.1 Overview of POM Thermodynamics	**51**
4.2 POM Reaction Mechanism	**53**
5. Membrane Reactor Stability in POM	**60**

5.1 Membrane Structure and Thermodynamic Stability **60**

5.2 Stability of Perovskite Catalysts and Membrane Reactors During POM **61**

5.3 Carbon deposition **65**

5.4 Stability of Membrane Catalyst Layer in the Asymmetric Membrane Reactor **67**

6. Conclusion and Future prospective **68**

6.1 Conclusion **68**

6.2 Future prospective **70**

6.2.1 Understanding POM Mechanism in Membrane Reactors **70**

6.2.2 Taking Advantages of Oxygen Vacancies in POM Membrane Reaction **71**

6.2.3 Bridging Electronic Properties with Catalytic POM Reaction **73**

7. Funding Details **75**

8. Acknowledgment **75**

9. Appendix **75**

10. References **78**

1. Introduction

In the past decades, researchers have been focusing on alternatives to petroleum-based derivatives as energy sources, and natural gas is an attractive option. The methane in natural gas (typically 95%) can be utilized to produce hydrogen and syngas. Consequently, hydrogen from natural gas is utilized in the production of urea, heavy water, and fuel cells. Natural gas has also been a reliable feedstock for syngas production in industries, which will be further utilized to produce a variety of value-added chemicals (Figure 1). Besides, syngas can be produced from other feedstocks such as coal, biomass, and oil. However, natural gas is a more feasible source of syngas since it is environmentally friendly, easy to be transported, and abundant in onshore and off-shore locations [1]. Currently, many mature and new processes are available for CH_4 conversion to syngas. In the following section, we will focus on the methane reforming processes for syngas production from natural gas.

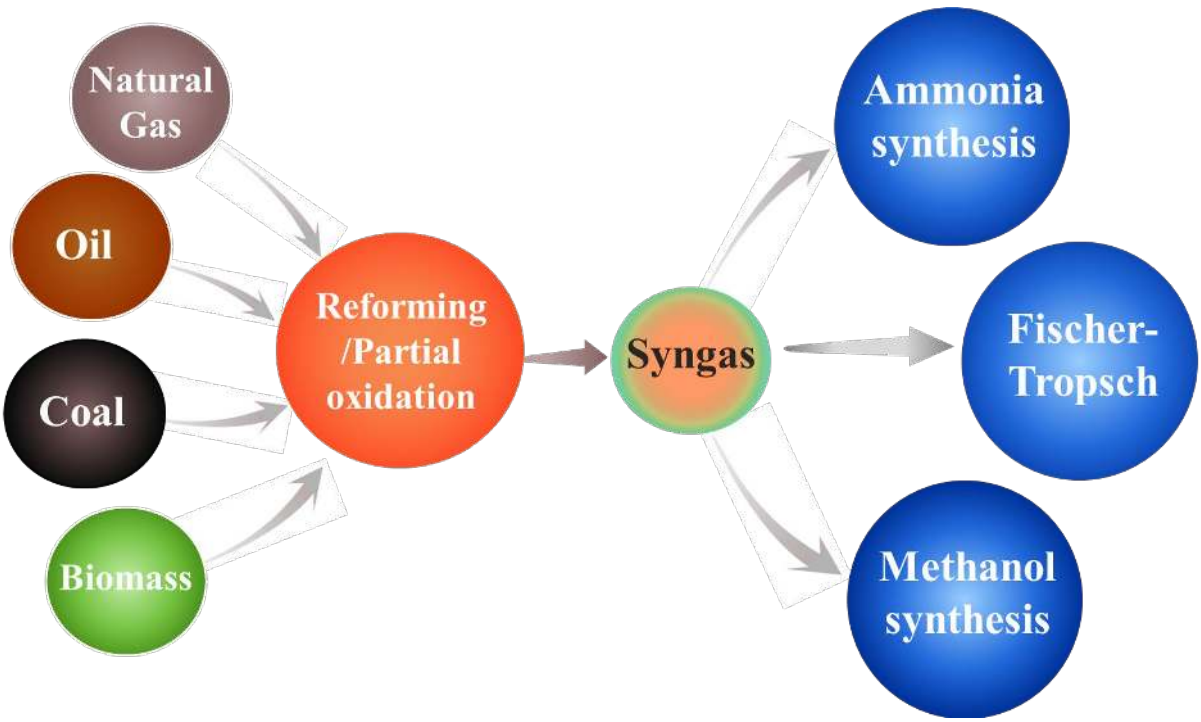

Figure 1. Valued-added chemicals produced from syngas.

1.1 Methane to Syngas Processes

1.1.1 Steam Methane Reforming (SMR)

Steam methane reforming (SMR) contributes majorly to worldwide hydrogen production from natural gas. In steam methane reforming (SMR), methane reacts with steam at high temperature (800- 900 ºC) in the presence of metals as catalysts [2]. However, one disadvantage associated with SMR is the water-gas shift reaction. This reaction is considered as an undesired side reaction since it consumes CO to produce CO_2 and H_2, as shown in Equation 2. Moreover, SMR is an endothermic reaction that requires higher temperature operation, leading to an increase in the operation cost.

$$CH_4 + H_2O \leftrightarrow CO + 3H_2, \Delta H^o_{298} = 206\ kJ \cdot mol^{-1} \quad (1)$$

$$CO + H_2O \leftrightarrow CO_2 + H_2, \Delta H^o_{298} = -41.2\ kJ \cdot mol^{-1} (2)$$

1.1.2 Auto-Thermal Reforming of Methane (ATR)

In auto-thermal reforming, several reactions take place including combustion, reforming, and partial oxidation [1]. An ATR reactor usually has two reaction zones, combustion zone (T ≈1927 ºC) and reforming zone (T ≈ 900-1100 ºC). ATR strat with CH_4 combustion reaction as in Equation 3, then partial oxidation and steam reforming reactions take place in the catalyst bed zone [1].

$$CH_4 + O_2 \rightarrow CO_2 + 2H_2O, \Delta H^o_{298} = -801\ kJ \cdot mol^{-1} (3)$$

The produced H_2/CO ratio from ATR depends on the natural gas ratio in the feed and can vary from 1 to 2. Compared to steam and dry reforming, ATR process requires less energy. However, the direct combustion of methane as a side reaction can cause feed loss.

1.1.3 Dry Methane Reforming (DMR)

Dry reforming uses CO_2 to replace steam due to the relatively low cost of CO_2. Equation 4 shows the methane dry reforming reaction. However, the syngas ratio from the dry methane reforming process is less than one due to the high carbon to hydrogen ratio in the reactants, which limits its application in chemical industries [2]. Furthermore, the reaction is more endothermic than steam reforming, which makes the process more energy-intensive.

$$CH_4 + CO_2 \leftrightarrow 2CO + 2H_2, \Delta H^o_{298} = 247\ kJ \cdot mol^{-1} (4)$$

Furthermore, the presence of CO_2 raises the chances of coke formation on the catalyst by producing CO and consuming H_2 via reversible water-gas shift reaction as in Equation 2. CO produces carbon by Boudouard reaction (Equation 6). It is worth mentioning that carbon deposition reduces the catalyst activity and lifetime and that it is a great challenge for this process[3].

$$CO_2 + H_2 \leftrightarrow CO + H_2O (5)$$

$$CO \leftrightarrow CO_2 + C (6)$$

1.1.4 Partial Oxidation of Methane (POM)

In POM, syngas is produced via partial oxidation by feeding non-stoichiometric CH_4/O_2 to the reactor [2, 4, 5] as in Equation 7. In addition to partial oxidation reaction, several possible reactions are involved in the partial oxidation as shown in Table1. As can be noticed from Equation 7, POM is an exothermic reaction. Hence, it requires less energy than steam reforming and dry reforming. An additional advantage of partial oxidation is that syngas is produced with H_2/CO ratio around 2, which is suitable for various chemical production processes such as Fischer-Tropsch and also for solid oxide fuel cells [6]. However, it suffers from drawbacks of pure oxygen supply and high safety risk. It is also noteworthy that catalytic partial oxidation is

severely affected by sulfur content in the feed. Therefore, de-sulphurization of feed should be carried out firstly; otherwise, catalysts would be poisoned.

Table1. Reactions involved in methane partial oxidation [3]

Reaction	ΔH^{o}_{298} (kJ.mol^{-1})
$CH_4 + \frac{1}{2}O_2 \rightarrow CO + 2H_2 (7)$	-36
$CH_4 + 2O_2 \rightarrow CO_2 + 2H_2O (8)$	-802
$CH_4 + H_2O \leftrightarrow CO + 3H_2 (9)$	206
$CH_4 + 2H_2O \leftrightarrow 2CO_2 + 4H_2 (10)$	165
$CH_4 + CO_2 \rightarrow 2CO + 2H_2 (11)$	247
$CO + H_2O \leftrightarrow CO_2 + H_2 (12)$	-41

1.1.5 Bi-Reforming of Methane

Bi-reforming is a process that utilizes CO_2 and steam to convert methane into syngas as in Equation 13 [7]. Bi-reforming is a promising commercial alternative to steam and dry reforming processes as it consumes less energy. Furthermore, unlike dry reforming, H_2/CO ratio is flexible and can be changed by adjusting the CO_2/H_2O ratio. This gives the bi-reforming process the advantage of being suitable for producing syngas feed for chemical synthesis processes such as Fischer-Tropsch.

$$3CH_4 + CO + 2H_2O \leftrightharpoons 4CO + 8H_2, \Delta H^o_{298} = +151\ kJ \cdot mol^{-1} (13)$$

Moreover, compared to steam and dry reforming, recent studies showed that bi-reforming has the potential to produce higher-value chemicals such as methanol [8]. Another advantage of bi-reforming is the lower carbon deposition compared to dry reforming due to the presence of steam as an oxidant [7]. Nevertheless, the standing challenges are to develop a catalyst that can stand the long operation in a steam-rich environment and the high operation cost required to operate the independent steam plant.

1.1.6 Tri-Reforming of Methane

In tri-reforming, flue gases contain CO_2, N_2, O_2, and H_2O can be directly utilized to reform methane without separation of CO_2 [5]. In this process, a combination of reactions of dry reforming, steam reforming, and partial oxidation are used to reform methane[5]. This process is designed to lower the cost and greenhouse gases emissions compared to the process using pure CO_2 in dry reforming. However, the tri-reforming process faces some challenges such as minimizing SO_x and NO_x effects. In addition, the process depends mainly on CO_2 reforming, H_2/CO ratio is close to 1. Therefore, further treatment is required prior to application in Fischer-Tropsch or methanol synthesis processes.

1.1.7 Comparison among Different Methane Reforming Processes

H_2 to CO ratio (i.e. syngas ratio) is an important factor in choosing a suitable process for methane reforming. This is because the next process into which syngas will be fed depends essentially on the syngas ratio. For instance, for chemical synthesis processes such as Fischer–Tropsch, the optimum syngas ratio is 2-2.5, while for hydrogen and ammonia production is 3 or higher. Table 2 compares the syngas ratio produced by the different processes and the corresponding application. Furthermore, each process has it is own advantages and disadvantages due to different operation conditions, reaction mechanism, feed and catalyst used.

Overall, by considering syngas for chemicals production processes such as Fischer–Tropsch, partial oxidation and steam reforming of methane processes are preferred. Although steam methane reforming has high efficiency, it is less economically feasible due to the high operating temperature, and also it suffers from greenhouse gases emissions [1]. As well, catalytic partial oxidation of methane also faces several challenges including the need for a separate oxygen plant as mentioned earlier.

Table 2. Syngas ratio from different processes and the corresponding application [2,3].

H_2/CO	Proposed Process	Application
> 3	Steam reforming or water-gas shift	H_2 and ammonia
2-3	Steam reforming	Methanol synthesis
2-2.5	Steam reforming or partial oxidation	Fischer–Tropsch for gasoline and light olefins
1.7-2	Steam reforming or partial oxidation	Fischer–Tropsch for waxes and diesel
1.5	Hydroformylation	Aldehydes and alcohols
≤ 1	Auto thermal reforming or dry reforming	Acetic acid, polycarbonates

1.2 POM Reactors Configurations

1.2.1 Fixed Bed and Fluidized Bed Reactors

Although several different reactor configurations for POM have been reported, the fixed-bed reactor is the most commonly used configuration. Generally, partial oxidation of methane can be achieved at a high temperature (1200-1500 ºC) without a catalyst and the reaction temperature can be reduced significantly (800-900 ºC) by the introduction of a suitable catalyst [9,10]. Therefore, catalyst selection and development are crucial to the reduction of the reaction temperature in fixed-bed reactors.

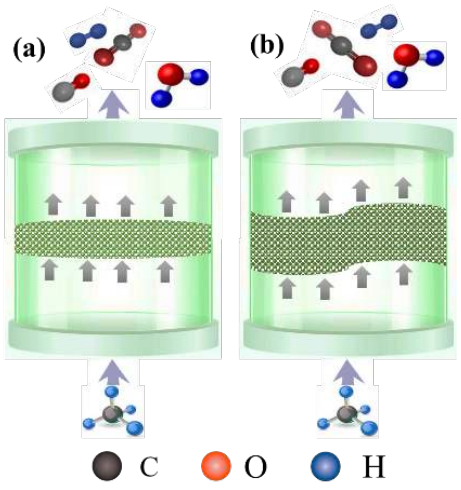

Figure 2. Schematic of (a) Fixed bed and (b) Fluidized bed reactors

In addition, due to mild exothermicity of the reaction, a large temperature gradient can be observed in fixed-bed reactors because of the high reaction rate of catalytic partial oxidation (CPO) to cause hot spots in the catalyst bed and interfere with the accuracy of the experimental data [11]. The hot spot issue causes difficulties in reactor scale-up and industrial applications. Fluidized bed reactors use a fluidized solid catalyst as an internal heat carrier within the bed can resolve the hot spot problem and provide a uniform reactor temperature profile [11]. Preliminary experiments show that excellent performance could probably be achieved in a properly designed riser reactor with much higher throughputs [12].

1.2.2 Chemical-Looping Partial Oxidation

Recent developments have been introduced to partial oxidation of methane such as chemical-looping partial oxidation to eliminate the need for the addition of pure O_2. In the chemical looping process (Figure 3), oxygen is provided by an oxygen carrier catalyst [13, 14]. Accordingly, an additional reactor is desired for catalyst regeneration (oxidizer) by air at a high temperature. In the case of chemical looping methane reforming, the required temperature is 820-930 ^{o}C. Nevertheless, similar to steam reforming, soots and carbon deposition were detected in this process. Oxygen carriers are in oxides forms mostly, resulting in complete combustion rather than partial oxidation [3, 15-18]. Therefore, controlling catalyst oxidation degree is crucial for syngas selectivity and overall yield. In addition, there are some issues yet to be resolved regarding chemical looping reforming such as carrier attrition and difficulties in reactor scale-up [13].

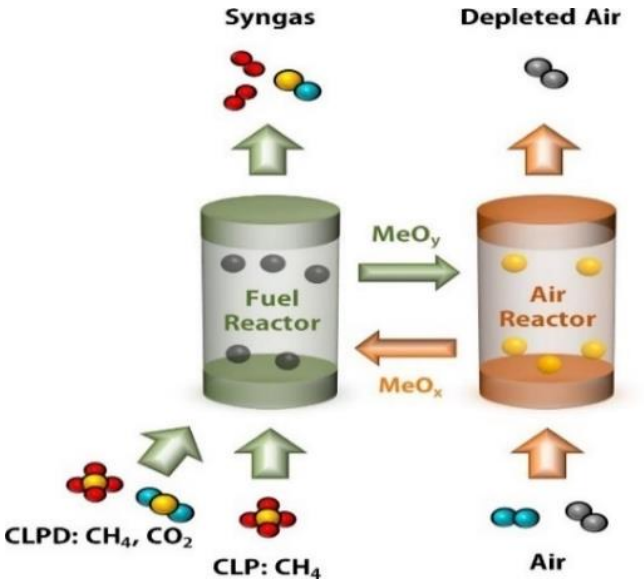

Figure 3. Chemical-looping reforming concept. Reproduced with permission from reference [14]. Copyright 2018, Elsevier.

1.2.3 Short Contact Time Catalytic Partial Oxidation (SCT-CPO)

Short contact time in reaction has been introduced to catalytic partial oxidation recently to achieve high conversion of methane to syngas [2, 3]. The feed flows through the gas-solid contact zone for 6-10 seconds at a temperature of 600-1200 ºC, which facilitates the selective syngas formation and inhibits chain reactions in the gas phase.

Furthermore, short contact time catalytic partial oxidation (SCT-CPO) is conducted in very small reactors with a high tolerance for flow variation. Several hydrocarbon feedstocks in addition to CH_4 can be fed to the reactor for syngas production. However, the implementation of this technology embraces limitations including product capacity, energy consumption and reduction of CO_2 formation.

1.2.4 Membrane Reactors

Membrane reactors are attractive for POM due to their ability to combine oxygen separation and chemical reaction in a single unit without hot spots [13]. Mixed ionic-electronic conducting

membrane reactors are the most suitable type for POM due to the continuous and controllable oxygen supply (Figure 4). Hence, this process reduces operation cost in comparison with conventional POM reactors and reduces safety risks [13]. Besides, a compact membrane module allows access to different types of natural gas sources such as offshore reservoirs. However, the challenge for the membrane reactors in POM is their stability in reducing CO_2, CO, H_2, H_2O, and CH_4 species.

In most cases, membrane reactor modules are designed based on planner-disk or cylindrical modules. Therefore, the most common types are disk and tubular membranes (Figure 4). Disk membrane reactors are can be easily fabricated and they are less expensive. However, they suffer from stability issues due to their low mechanical strength and consequently, their scale-up process is challenging [18-21]. On the other hand, the tubular membrane module has the advantage of higher stability and they can be easily scaled-up [19]. Yet, they have a higher fabrication cost. Another difference between disk and tubular membrane modules that in disk membrane the reactant is introduced from one side while air is introduced from the opposite side. However, in the case of the tubular membranes, the confined configuration makes their cleaning process more difficult compared to disk membranes[19].

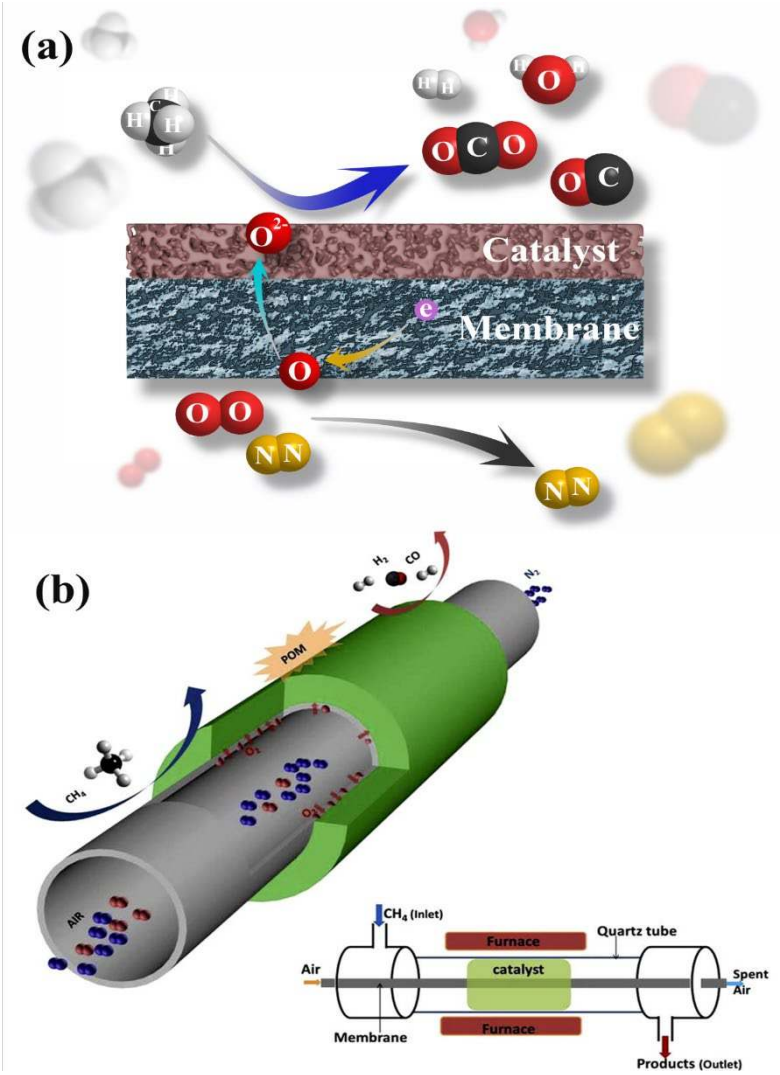

Figure 4. (a) Disk membrane module and (b) Tubular membrane module. ((b) Reprinted with permission from reference [19]. Copyright 2017, Elsevier.

2. Supported Catalysts for POM

Prettre et al. firstly reported catalytic partial oxidation of methane (CPOM) over supported Ni at 973-1173 K and 1 atm [22] and they suggested that syngas production occurred via combustion of CH_4, followed by CO_2 and H_2O reforming. Partial oxidation was raised in a much interest since the 1990s [23], initially focusing on catalyst screening and reaction condition and then catalyst stability and performance. Up to now, different catalysts including bulk metal oxides, supported metal oxides, and perovskite catalysts have been investigated in

catalytic partial oxidation of methane. The following sections will briefly discuss the activities of the catalysts in terms of CH_4 conversion and syngas selectivity.

2.1 Cobalt Catalysts

Cobalt catalysts are reported to be promising POM catalysts. The conversion and syngas selectivity on a Co/Al_2O_3 catalyst were reported to be close to theoretical equilibrium. However, it suffers from deactivation due to the rapid oxidation of metallic cobalt and formation of $CoAl_2O_4$ [24, 25]. The reducibility of these formed Co oxides follows an order of Co_3O_4>$CoAlO_4$> $CoAl_2O_4$ [26].

Different catalyst supports have been studied for Co-catalysed POM. For example, MgO and $MgO\text{-}Al_2O_3$ catalyst supports were investigated by Choudhary et al. [27]. $CoO\text{-}MgO\text{-}Al_2O_3$ exhibited 95% CH_4 conversion with 99% CO selectivity and syngas ratio of 2:1 at 850 ºC. Another study reported that Co/MgO catalyst showed higher CO conversion and H_2 selectivity in comparison with Co/CaO, Co/BaO and Co/SiO_2 [28], attributing to the presence of CoO-MgO phase. Other Co supports such as LnO_x (lanthanide oxides) [29], alkaline earth, rare earth, SiO_2 [30], Y_2O_3 or ZrO_2 [31], TiO_2 [32], UO_2/ThO_2 [33] were reported to have lower activity in POM. Furthermore, $Co/ZrO_2\text{-}Al_2O_3$ was reported to achieve 85% CH_4 conversion, 98% CO selectivity at 700 ºC. It was highlighted that metal-support interaction played a key role in active site sintering, which enhanced catalyst activity [34].

Addition of promoters can be useful in improving the reducibility and deactivation. Swann et al. added Zn promoter to Co/Al_2O_3 and Co/SiO_2 catalysts[34]. CH_4 conversion was 99% with 99% CO selectivity at 900 ºC. $Pt\text{-}Co/\alpha\text{-}Al_2O_3$ catalyst was tested by Tang et al. [35]. It was found that Pt turned to have better reducibility and lower temperature to 700 ºC. Enger et al. [16] used a series of metals including Ni, Fe, Cr, Re, Mn, V, W, Mo and Ta for modification of $Co/\alpha\text{-}Al_2O_3$. V, W, Mo had a negative effect on methane conversion and syngas selectivity

due to the low availability of Co active sites. Cr, Re and Mn promoted the catalyst deactivation at a higher gas hourly space velocity. On the contrary, Ni addition improved the stability at higher gas hourly space velocity.

Although Co-based catalysts showed relatively lower performance than Ni-based catalysts, no carbon deposition occurred on most of the Co-based catalysts [31]. Moreover, CoO addition to Ni-based catalysts can significantly reduce carbon deposition [3]. Co suffers from rapid oxidation, which lowers syngas selectivity in POM, it was suggested that reduced Co phase could maintain well dispersion and hence have higher syngas selectivity [36].

2.2 Nickel Catalysts

Nickel-based catalysts have drawn the major attention in POM due to the high activity in the reaction. Nickel-based catalysts can achieve >95% CH_4 conversion and > 96% syngas selectivity, while carbon deposition is the major issue [16]. Carbon deposition can reduce performance and increase feed stream pressure [37]. Another issue of Ni catalysts is the loss of metal active species by sintering and corrosion. Similar to Co-based catalysts, the change of surface morphology by the formation of undesired oxides (such as $NiAl_2O_4$) will favor CO_2 formation. Therefore, a considerable number of studies have been dedicated to improve Ni-based catalysts stability and performance and to reduce carbon formation including support modification, doping with promoters, new synthesis method, and different reaction conditions (feed ratio, temperature, pressure, and reaction time).

This section is focused on the effect of support and metal promoters on the performance of Ni-based catalysts. In this context, one approach to enhance catalyst stability and activity is the screening of appropriate metal-support pairs. Many supports have been studied extensively in the literature to prevent the formation of undesired oxides species or carbon deposition. NiO was supported on different oxides, MgO, CaO, SrO, BaO, Sm_2O_3, and Yb_2O_3 [38, 39].

Excellent performance (95% CH_4 conversion, 97.5% CO selectivity and 95% H_2 selectivity) was obtained with MgO at 800 ºC. The formation of $MgA1_2O_4$ protective layer reduced the interaction between Ni and support and the deposited NiO [38]. On the contrary, Ni-NiO_x interaction with Al_2O_3-$NiAl_2O_4$ nanofibrous support was reported to reduce Ni aggregation. in this case, 98.5% CH_4 conversion, 98.5% CO selectivity, and 97.4% H_2 selectivity were achieved at 850 ºC [40].

NiO was directly deposited on Al_2O_3/SiO_2 supports and it was noticed that CH_4 conversion and syngas selectivity significantly decreased due to the formation of $NiAl_2O_4$. Boukha et al. confirmed that MgO addition to $NiAl_2O_4$ catalyst prevented metallic Ni deposition on catalyst surface [41]. Likewise, Ni/Al_2O_3/MgO and Ni/sorbacid catalysts showed good activities in POM at 500 and 600 ºC. It was suggested that high basicity favored water-gas shift reaction and inverse Boudouard reaction [42]. Moreover, Ni/TiO_2 performance was reported in methane partial oxidation and dry reforming [43]. 86.3% CH_4 conversion was obtained with 88.2% CO and 99.7% H_2 selectivities. TPR experiments and XRD results demonstrated that surface nickel was oxidized to NiO and $NiTiO_3$ during the POM reaction.

Another way to modify catalyst surface and metal-support interaction is through tuning support acidity [44]. Al_2O_3, SiO_2-Al_2O_3, H-Y Zeolite and SiO_2-ZrO_2 were tested (Table 3) [44]. The best results were achieved on SiO_2-ZrO_2 support with 5% Ni loading (96.1% CH_4 conversion, 97.2% CO selectivity and 99.4% H_2 selectivity). On the contrary, H-Y zeolite achieved the lowest conversion and syngas selectivity. The low acidity of silica-zirconia promoted high CH_4 conversion and syngas selectivity, while high acidity of zeolites supports reduced conversion and selectivity. In particular, the addition of 25% CeO_2-ZrO_2 to ZSM-5 supported Ni reduced POM equilibrium temperature. Moreover, CH_4 conversion up to 90% was achieved at 700 ºC [45].

Table 3. CH_4 conversion (X_{CH4}) and syngas selectivity (S) in partial oxidation over Ni supported catalysts at 780 ºC. Reproduced with permission from reference [44]. Copyright 2018, Elsevier.

Support	Metal loading (wt.%)	X_{CH4} (%)	S_{CO} (%)	S_{CO2} (%)	S_{H2} (%)
Al_2O_3	1	95.3	96.3	3.7	99.4
Al_2O_3	5	95.7	95.7	4.3	99.9
SiO_2-Al_2O_3	1	13	33.8	66.2	-
SiO_2-Al_2O_3	5	94.6	96.1	3.9	99.1
SiO_2-ZrO_2	1	95.6	96.1	3.9	99.6
SiO_2-ZrO_2	5	96.1	97.2	2.8	99.4
H-Y zeolite	1	25.9	52.4	47.8	-
H-Y zeolite	5	90	92.5	7.5	98.2

Aluminosilicate support was studied for POM with different active metals (Ni, Co, Fe, Cr, and Cu) [46]. Ni on the support yielded (93% CH_4 conversion, 94% CO and 95% H_2 selectivities) at 800 ºC. However, Co, Fe, Cr and Cu turned to favor CO_2 formation with no significant syngas production. Berrocal et al. investigated zirconia-alumina supported Ni catalysts at 450-750 ºC and 1 atm [47]. The best performance achieved was up to 85% of CH_4 conversion and 82% of H_2 selectivity at 750 ºC by catalyst with an Al/Zr ratio of 2. Moreover, $NiAl_2O_4$ species was detected by XRD and 23% coke deposition was noticed on the catalyst, leading to the low conversion and syngas selectivity. Apart from zeolites, the effect of acidity and calcination temperature have been studied on Ni/Y_2O_3 catalysts [48]. Decreased acidity has been reported at low calcination temperature and consequently lower Ni-Y_2O_3 interaction. Consequently, low support acidity leads to active sites migration and agglomeration, which decreases CH_4 conversion from 84% to 77% due to reduced active site availability for the reaction.

As well as support acidity, basicity has a significant effect on POM reaction. Particularly, high support basicity decreases carbon deposition due to the facile oxidation of carbon species on the basic sites. [42]. Ozmedir et al. reported that the carbon deposition rate on Ni/Al_2O_3 catalyst was increased when the basicity was decreased by doping the catalyst with Mg. High support basicity to enhances the reverse Boudouard reaction, which oxidizes carbon species on the catalyst surface. Similarly, the high concentration of Lewis basic acid sites of O_2-anions on Ni/ZrO_2 catalyst increases the adsorption of CO_2 and its conversion to CO [49]. However, this high rate of the reverse Boudouard reaction decrease H_2/CO ratio simultaneously. Furthermore, the effect of catalyst basicity on the formation of CO could not be observed at a temperature higher than 700 ^oC due to the high desorption rate of CO_2 [42].

Support reducibility affects catalyst activity as well as acidity and basicity. The disproportionation of CO on the catalyst surface depends on support reducibility [50]. This reaction can lead to CO_2 formation Equation 14 and a reduction in syngas selectivity. Tang et al. [50] studied CH_4 decomposition and support reducibility on Ni/MgO, Ni/CaO, and Ni/CeO_2 catalysts. Due to its low reducibility, Ni/MgO catalyst showed higher resistance to CO disproportionation and CH_4 decomposition over 100 h compared to Ni/CeO_2 and Ni/CaO. CeO_2 has been widely investigated as Ni catalyst support due to its high reducibility. Pantaleo et al. reported excellent performance of Ni/CeO_2 by using hydrothermal, microwave-assisted co-precipitation and impregnation techniques for synthesis [51].

$$2CO \leftrightarrow CO_2 + C \quad (14)$$

Methane conversion reached 98% with 95% CO selectivity at 800 ^oC. This high performance was attributed to CeO_2 facile reduction and CH_4 dissociation on the catalyst surface, which is beneficial to CO formation rather than carbon deposition. It worth noticing that Ce presence enhanced oxygen mobility, which increased CO formation. Pantaleo et al. also reported

modifying Ni/CeO_2 catalyst support with La_2O_3 decreased catalyst activity temperature as supported by TPR studies because of decreased reducibility. Likewise, Singha et al. reported nano-scaled Ni-CeO_2 excellent performance in POM [52]. The nano-scaled catalyst had high reducibility according to TPR analysis and achieved 98% CH_4 conversion and 95%> syngas selectivity. The catalyst was stable over 100 h operation showing a slight decrease in conversion due to the small amount of carbon deposition. Peymani et al. [53] reported a high surface area for CeO_2 supported Ni catalyst, which achieved up to 90% CH_4 conversion and 90% CO selectivity. In addition to the positive effect in catalysts reduction, it has been shown that CeO_2 increases Ni dispersion, which resulted in higher syngas production over Ni/CeO_2-SiO_2 catalyst [54]. In the same prospect, CeO_2 was reported to play an important role in CH_4 decomposition, in the case of CeO_2-supported La_xNiO_y catalyst. Furthermore, methane conversion to CO was shifted to a lower temperature with no carbon accumulation in the presence of CeO_2 interacting with the nickel phases [55].

In order to further enhance ceria supported Ni catalyst reducibility in POM, several studies reported the catalytic performance of Ni dispersed on ceria-doped supports such as $(Ce_{0.88}La_{0.12})O_{2-x}$, $(Ce_{0.91}Gd_{0.09})O_{2-x}$, $(Ce_{0.71}Gd_{0.29})O_{2-x}$, $(Ce_{0.56}Zr_{0.44})O_{2-x}$ and pure ceria [56]. In these studies, catalysts reducibility was assessed by H_2-TPR. Ni/$(Ce_{0.56}Zr_{0.44})O_{2-x}$ showed higher hydrogen production than the Ni/Gadolinium-doped catalysts, which may be due to its higher reducibility and surface area. By enhancing the support reducibility in Ni/doped-ceria catalysts, their catalytic activity was promoted correspondingly due to the availability of lattice oxygen, which increased the formation of CO and H_2. Moreover, the reducibility of Ni/Ce-ZrO_2 catalyst was also investigated by Larimi and Alavi [57]. It was found that increasing ZrO_2 content tent to improve catalyst activity, accordingly, at Ce/Zr ratio of 3, >98% CH_4 conversion was achieved with >92% syngas selectivity at 850 ºC. However, syngas selectivity decreased

with time. Moreover, ZrO_2 addition to Ni/SiO_2 can be an effective way of increasing carbon deposition resistance and catalyst surface area [29, 58, 59].

Turning to the effect of promoters on Ni-based catalysts activity, they were reported to enhance Ni-based catalyst activity by lowering ignition temperature and reducing carbon deposition. Noble metals and metal oxides were reported to reduce NiO_x/Al_2O_3 ignition temperature [38, 60]. The addition of Pt to Ni/Al_2O_3 reduced the ignition temperature from 790 to 530 ºC. $Ni/Li/La_2O_3/Al_2O_3$ catalyst was reported to be stable during 200 h methane partial oxidation reaction with 96% CH_4 conversion and 98% CO selectivity at 900 ºC [61]. Carbon was formed on the catalyst surface by pyrolysis and then reacted with lattice oxygen to for CO. However, the activation energy for this reaction was higher than conventional carbon pyrolysis [62], which was the rate-determining step. The catalyst reduction temperature was 700-900 ºC as evidenced by TPR, which can explain the high POM temperature. It is worth noticing that despite the high temperature, the catalyst showed high resistance to carbon deposition [63]. These findings are in agreement with the reported reduced ignition temperature of NiO/Al_2O_3 when it was promoted with La_2O_3. It was found that La_2O_3 reduced carbon deposition on NiO/Al_2O_3 catalyst while CaO addition reported inhibiting carbon deposition completely as well [60, 64, 65].

As well, promoters have a key role in enhancing reducibility. For example, Ce, Na, Sr and La addition to the support has been reported to enhance $Ni/\gamma\text{-}Al_2O_3$ reducibility. Ce addition resulted in a 92% CH_4 conversion due to the prevention of strong metal-support interaction [16]. Therefore, it can be concluded that Ce addition tends to decrease catalyst reduction temperature [38]. Ir, La, and Cr, was also investigated as promoters to reduce carbon deposition [66, 67]. The catalyst with 0.25%wt and 0.5%wt Ni gave 25% CH_4 conversion with 80% syngas selectivity at 600 ºC. On the other hand, Ni/La_2O_3 and Ir/La_2O_3 catalyst did not yield syngas at the same conditions. Ferreira et al. reported the synergetic effect of Ln_2O_3 on NiO

catalyst by studying the effect of Gd, Lu, and Pr as promoters. Syngas selectivity reached up to 80% and CH_4 conversion up to 90% at 750 ºC [68]. Similar observations have been reported on La_2O_3 effect on Ni/Ce-ZrO_2 [69].

The catalytic activity can be increased further by utilizing promoters in combination with suitable support. For instance, various supports such as Y_2O_3, ZrO_2, Al_2O_3, MgO, SiO_2, and TiO_2 have been also considered to support Ni-Ir system. However, no significant syngas yield was achieved within a temperature range of 400-600 ºC except for TiO_2 support. Ni–Yb/Al_2O_3 catalyst (Ni/Yb = 1) proved to be more active, giving CH_4 conversion of 98%, CO selectivity of 98% and H_2 selectivity of 83% (800 °C and space velocity of 5 × 104 $mL.g^{-1}.h^{-1}$). In addition, the addition of Yb was deduced to facilitate adsorption of CO_2 and catalyze methane combustion, which was the first step of POM reaction, thus reducing carbon deposition and improving methane conversion [29, 70]. $(Ni_xMg_{1-x})Al_y$ catalyst was studied with the addition of Cu and Fe [71]. The addition of Cu improved the selectivity to CO and H_2 up to 53% and 41% respectively. On the contrary, Fe addition favored total combustion and water-gas shift reactions. Cu effect catalyst reducibility has been reported as well for Cu-Ni-Mg/Al catalyst [71]. Similarly, Rh-promoted Ni catalysts were tested on various supports including Al_2O_3, MgO, CeO_2, ZrO_2 and La_2O_3. It has been reported that Rh addition enhanced Ni reduction and carbon deposition, which resulted in up to 90% syngas selectivity and 90% CH_4 conversion at 750 ºC [72]. Moreover, the activity of Ni/Al_2O_3 catalyst in POM was improved by the addition of Re (100 CH_4 conversion was achieved) due to carbon deposition resistance [73].

Moreover, less common promoters such as PrO_2 have been impregnated in Ni/ZrO_2 system. The result suggested that PrO_2 contributed to the formation of Ni^0 active phases due to high metal dispersion and metal-support interaction in contrast [74].

Overall, Ni-based catalysts have higher activity than Co-based catalysts in terms of CH_4 conversion and syngas selectivity. Yet their stability still requires improvement to reduce carbon deposition. In addition to promoters doping and selecting suitable support, recent studies showed that tuning catalyst structure could reduce carbon deposition since carbon deposition is structure-sensitive to Ni catalyst [37, 75].

2.3 Rhodium and Ruthenium Catalysts

Compared to Ni-based catalysts, Ru and Rh-based catalysts have higher activity in POM. Ru and Rh catalysts were reported to have better metal-support interaction, facile reduction and higher resistance to coke formation [3]. Similar to Ni catalysts, different supports were investigated for Rh-based catalysts. For example, partial oxidation of methane (POM) was also studied over Rh/$(Ce_{0.56}Zr_{0.44})O_{2-x}$, Rh/ $(Ce_{0.91}Gd_{0.09})O_{2-x}$, Rh/$(Ce_{0.71}Gd_{0.29})O_{2-x}$ and Rh/$(Ce_{0.88}La_{0.12})O_{2-x}$ [76, 77]. Rh/$(Ce_{0.56}Zr_{0.44})$ showed the best performance at 750 ^oC due to good reducibility introduced by Ce addition.

The promoter effect on Rh/Al_2O_3 catalyst has been studied. High CH_4 conversion over Rh-Pt catalyst was obtained with syngas selectivity > 95% at 800 ^oC [78]. Pt was reported to promote Ru/Al_2O_3-ZrO_2-CeO_2 catalyst by trigger POM at lower temperature and achieve near 100% CH_4 conversion at 750 ^oC [79]. Compared to Ru/γ-Al_2O_3, hydroxyapatite supported Rh showed good performance (90% CH_4 conversion and 90% CO selectivity) at a lower temperature of 700 ^oC. However, a syngas ratio higher than 3 has been reported in most of the reaction experiments. This indicates increased CH_4 dissociation over Rh^0, which was detected by XPS [80].

Analogous to Rh, Ru-based catalysts on different supports have been studied Ru/La_2O_3 and Ru/Al_2O_3 [81. Carbon formation on catalyst surface reported being more uniform and reactive. Furthermore, CH_4 decomposition on the Ru catalyst surface yielded surface carbon and low

coverage of CH_4. This indicates that Ru catalysts are different in terms of CH_4 dissociation in comparison with Rh catalysts. However, direct CO formation was reported on Ru/TiO_2 catalyst [82, 83], while Ru/Al_2O_3 did not directly form CO. Furthermore, on Ru/Al_2O_3 catalyst, CH_4 conversion remained below 25%. Direct syngas formation for Ru/TiO_2 was also claimed by Elmasides et al.[84, 85]. The reason for the excellent properties of Ru/TiO_2 was later studied by XPS and FTIR and compared to Ru/Al_2O_3. It was found that while Ru supported on alumina was incompletely reduced by hydrogen treatment at 550 ^oC, the titania supported catalyst was completely reduced and stabilized in its reduced state even when exposed to methane and oxygen at temperatures above 700 ^oC. The ability of Ru/TiO_2 to remain completely reduced was claimed to be the reason why it catalyzed a direct route to synthesis gas. In addition, a kinetic model based on the direct formation of CO and H_2 has been reported to describe the catalytic behavior of Ru/TiO_2 [86]. Compared to Al_2O_3, TiO_2 and ZrO_2, CeO_2-ZrO_2 supported Ru shows better reducibility and consequently higher conversion at 850 ^oC due to CeO_2 doping [87]. These results agree with Oleveira et al. study which reported that different Ru species formed on different supports which affect Ru dispersion, which consequently affects syngas production. DIRFT analysis showed γ-Al_2O_3 supported Ru catalyst tent to chemically adsorb CO contrary to CeO_2 supported Ru, which affect syngas ratio [88]. Ru catalysts have been tested at low-temperature POM as well. For instance, Zeolite-encaged Ru phthalocyanine catalyst was implemented in POM at 375 ^oC. CH_4 conversion reached 60% despite Ru good catalytic activity in POM [89]. This indicates that CH_4 activation is more difficult at a low temperature.

2.4 Other POM Catalysts

Apart from Ni, Co, Rh and Ru based catalysts, other catalysts based on Fe, Pd, Pt, Cu, and Mo were also reported[34, 46]. Fathi et al. reported a Pd/SiO_2 catalyst for POM in a continuous flow reactor [90]. Since the combustion-reforming mechanism is dominant on Pd/SiO_2

catalyst, syngas was produced as a secondary product [91]. Pt-based catalysts have been tested for POM. and CeO_2 was used for modification of Pt/Al_2O_3 [92]. CeO_2 addition increased Pt dispersion, promoting CH_4 oxidation and syngas selectivity. Compared to Pt/Al_2O_3, Pt/CeO_2 catalyst was reported to have better performance in POM at 800 ºC[93]. Several methods have been implemented for Pt/CeO_2 synthesis including controlled deposition, co-precipitation, hydrothermal and impregnation. Pt/CeO_2 by controlled deposition had excellent yield (98% CH_4 conversion and 97% CO selectivity and syngas ratio of 2 [94].

Similar studies on $Pt/CeO_2/Al_2O_3$ and $Rh/CeO_2/Al_2O_3$ reported good activity in POM [95, 96]. According to the observations, CH_4 dissociates to CH_x on noble metal active sites (i.e. Pt) and then the CH_x gets oxidized by the lattice oxygen from CeO_2, which is the rate-determining step [62]. This implies that oxygen concentration on the surface/lattice significantly affects syngas selectivity as indicated by CH_4 pulse reaction. Contrary to conventional CeO_2 and Al_2O_3 supports, dispersed Pt over the surface of fercalloy foam microlith coated with α-Al_2O_3 and α-Al_2O_3/CeO_2 was reported as well. The conversion and selectivity to syngas of these FA-microlith was reported to reach 90% and 60% respectively at 900 °C [97].

Other supports have been used to load Pt for POM. For example, TiO_2 [98], CaO [32], Y_2O_3, Al_2O_3-MgO, LnO_x [99] , $Ce\text{-}ZrO_2/Al_2O_3$ [100], $MgAl_2O_4$ [101] and rare earth oxide (namely, La_2O_3, Pr_6O_{11}, Nd_2O_3, Sm_2O_3, Gd_2O_3, Dy_2O_3 and Er_2O_3). These catalysts have been compared for their performance in the oxidative conversion of methane to CO and H_2 at 700 and 800°C. The best performance was obtained on Al_2O_3/CeO_2 supports (>95% conversion > 96% syngas selectivity at 700-800 ºC).

Moreover, Verlato et al. reported a different type of support comprising fecralloy foam loaded with Ru as an active site [102]. Although better dispersion was achieved, the performance was lower in comparison with $Ru/AlPO_4$-fercalloy catalyst due to Ru- fecralloy foam interaction.

Nickel nanowire catalyst showed high CH_4 conversion and syngas selectivity with good stability. With the increase in CH_4/O_2 ratio, the methane conversions on both catalysts decrease and the selectivity for syngas increases. It was suggested that nickel nanowire catalyst had more NiO dispersed species and thus higher activity. However, the combustion reforming reaction (CRR) mechanism may be dominant due to conversion decrease with increasing reactant flow rate[103, 104]. Although gold is more expensive compared with other metals, Au-Pd/TiO_2 catalyst has shown good activity in POM at 650 ^oC due to its ability to dissociate CH_4 and O_2 [105]. Table 4 shows less common catalysts and their relevant performances in POM.

Table 4. Summary of non-common metals-based catalysts activity in POM

Catalyst	Support	$XCH_4/SH_2/SCO$ (%)	T (^oC)	Reference
Fe	Al_2O_3/ La_2O_3	<36/<60/-	-	[34]
Cu, Cr, Fe, Mn	Mayenite	<40/<30/<30	-	[36]
Pt	FA-CeO_2-Al2O_3	90/60/60	900	[74]
Ru	fecralloy foam	65/85/85	800	[102]
Ni nanowires	-	90/99/97	900	[103]
Cu-Ni	$Al_2O_3/ZrO_2/La_2O_3$	3/-/-		[106]
La_2O_3	-	35/65/45	900	[107]
Mo_2C	-	98/-/95	950	[108]
Mo_2C-Ni	Al_2O_3	96/95/95	850	[109]
Y_2O_2	ZrO_2	25 (syngas yield)	900	[110]
Au-Pd	TiO_2	35/(25 TON)/(0.6 TON)	650	[105]

In summary, plenty of supported metal oxide catalysts were considered for POM. However, handful showed high activity and stability such as Ni, Co, Cu, Mn, Ru and Rh based catalysts. Among these supported metal oxide catalysts, Ni, Co and Rh based catalysts reported having the highest activity among supported metal oxide catalysts. Nevertheless, Ni catalysts suffer from significant coke deposition issues contrary to Rh and Co. In addition, there still stability issues, including active site sintering and aggregation. One of the common approaches to reduce carbon deposition and active site aggregation is utilizing prompters such as Ru, which

showed drastic improvement in coke formation reduction [111]. Another approach is support modification with dopants as Ce, Mg or Zr. Ceria was proved to have the most positive effect in catalyst performance due to the facilitation of catalyst reduction and hence, lower reaction temperature. However, since high syngas yield can only be obtained at a temperature higher than 800 ^{o}C, there is still room for improving supported metal oxide activity in POM.

2.5 Perovskite Catalysts for POM

The research on mixed ionic-electronic conducting materials has led to the exploration of the potential of perovskites in catalysis. This has opened the door for such materials for both membranes and catalysis purposes with no compatibility problems. A feature of perovskite structured oxides $ABO_{3-\delta}$, as shown in Figure 5, is the high mobility of the oxygen sub-lattice [21]. The presence of transition metals with variable oxidation states in these compounds promotes the appearance of defects in the anion sublattice. These defects could increase the mobility of lattice oxygen resulting in high oxygen flux and benefiting POM reaction in membrane reactors [112].

For perovskites-based catalytic POM, many catalytic properties have to be investigated apart from oxygen transport including; surface active sites, morphology, acidity, adsorption, desorption and REDOX properties. In this regard, different perovskite-type catalysts have been investigated for POM with B-site cations such as Ni, Co, Al and Fe [113]. Table 5 shows the common perovskite catalysts used for POM.

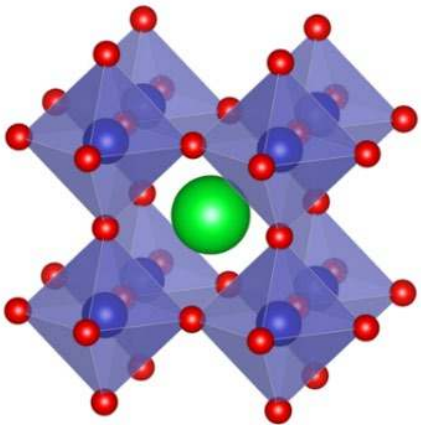

Figure 5. Chemical structure of perovskites $ABO_{3-\delta}$.

2.5.1 B-site Cation Selection

Due to good catalytic properties in POM (as illustrated in Sections 2.1 and 2.2), Ni and Co are common metals for B-site occupation in perovskites catalysts, with partial substitution with other metals. On the subject of Ni-based perovskites, Fe as co-dopant in B-site is commonly utilized to stabilize their catalytic activity. For instance, Mishra et al. reported catalytic performance of $AMn_xB_{1-x}O_3$ (A = Ca or Ba; B = Fe/Ni) and its REDOX properties [114]. Conversion and syngas selectivity were found to be dependent on Ni contents in B-site. Overall, 95% CO selectivity was achieved on $BaMn_{0.5}Fe_{0.5}O_3$ catalyst at 900 ºC. Moreover, Mg doping in $LaGa_{0.6}5Mg_{0.15}Ni_{0.2}O_{3-\delta}$ (LGMN) improved CH_4 conversion to 100% due to the increased catalyst reducibility [115]. Yet, syngas selectivity was 81% at 900 °C, which is lower than the $BaMn_{0.5}Fe_{0.5}O_3$ catalyst.

Moreover, Provendier et al. reported the effect of Ni/Fe ratio in $LaNi_xFe_{1-x}O_3$ perovskites in POM [116]. It was reported that decreasing Fe ratio in B-site enhances REDOX properties of $LaFeO_3$ perovskite by lowering reduction temperature from 950 ºC to 550 ºC due to Ni-Fe alloy formation. This resulted in significant improvement in the catalytic performance during CH_4 partial oxidation, which indicates that active species in CPO of methane are the reduced metal present at the surface of the catalyst. It should be mentioned that TPR analysis showed

that Fe doping in B-site of $LaNiO_3$ (i.e. forming $LaNi_{1-x}Fe_xO_{3-\delta}$) tends to increase catalyst reduction temperature from 500 ºC to 700 ºC [113].

Beside Fe partial substitution in Ni-based perovskites, Ni and Co combination in B-site has been reported as well. Partial substitution of Ni with Co in $LaNiO_3$, $La_{0.8}Ca(or\ Sr)_{0.2}NiO_3$ and $LaNi_{1-x}Co_xO_3$ (where x = 0.2–1) perovskites was reported by Choudhary et al. [117]. Low CH_4 conversion of 60% was achieved when Co content was increased, indicating that Co has less activity in POM than Ni in $LaNi_{1-x}Co_xO_3$ perovskites catalysts. Similarly, a decrease in syngas selectivity over mesoporous $NiCo–Gd_{0.1}Ti_{0.1}Zr_{0.1}Ce_{0.7}O_2$ occurred when Co/Ni ratio was increased from 1:4 to 4:1 [118].

Table 5. Perovskite catalysts and their activity in POM

Perovskite catalyst	$X_{CH4}/S_{H2}/S_{CO}$ (%)	T (ºC)	Reference
$BaMn_{0.5}Fe_{0.5}O_3$	98/-/95	900	[114]
$La_{0.75}Sr_{0.25}FeO_3$	65/100/-	850	[119]
$LaNi_{0.3}Fe_{0.7}O_3$	95/-/96	800	[116]
$LaCo_{0.5}Fe_{0.5}O_3$	17.1/59.2/30.9	700	[120]
$La_{0.8}Sr_{0.2}Fe_{0.9}Co_{0.1}O_3$	85/-/93	900	[121]
$LaCoO_3$ /$LaMnO_3$	35/-/0	800	[110]
$Ca_{0.8}Sr_{0.2}Ti_{0.6}Ni_{0.4}O_3$	97/98/97	800	[122]
$LaNiO_3$	85/90/95	800	[117]
$LaNiO_3$-CeO_2	93/-/100	800	[55]
$LaNi_{0.8}Co_{0.2}O_3$	60/75/90	800	[117]
$NiCo–Gd_{0.1}Ti_{0.1}Zr_{0.1}Ce_{0.7}O_2$	95/95/-	900	[118]
$Ca_{0.8}Sr_{0.2}TiO$	34/21/42	800	[123]

$Ca_{0.8}Sr_{0.2}Ti_{0.8}Ni_{0.2}O_3$	97/99.5/97.8	800	[123]
$NdCaCoO_{3.96}$	90/-/100	860	[124]
$GdCoO_3$	73/81/79	750	[125]
$SmCoO_3$	40/55/75	750	[125]
$Ni/CaTiO_3$	93.8/98.2/98.3	750	[126]
$Ni/SrTiO_3$	94.4/97.9/97.9	750	[126]
$Ni/BaTiO_3$	94.7/95.9/96.5	750	[126]
$BaTi_{0.8}Ni_{0.2}O_3$	95/-/98	950	[127]
$LaCo_{0.5}Ni_{0.5}O_3$	30/70/75	750	[128]
$LaCrO_3$	26/-/2	800	[129]
$LaNiO_3$	89/-/46	800	[129]
$LaNiO_3/CeO_2$	60/-/100	800	[55]
$LaRhO_3$	96/-/93	800	[130]
$LaRhNiO_3$	81/-/69	800	[130]
$LaCoO_3$	25/-/76	800	[129]
$LaCoCuO_3$	68/70/-	900	[130]
$Ni_{0.8}Co_{0.2}/La2O_3$	74/63/29	800	[131]
La-Ca-Co-(Al)-O	98.2/99.8/99.9	850	[132]
La-Ca-Cr-(Al)-O	56.2/75.1/79.5	850	[132]
La-Ca-Fe-(Al)-O	78.6/88.1/88.1	850	[132]
La-Ca-Mn-(Al)-O	74.3/81.4/83.6	850	[132]
$Pt/La_{0.7}Sr_{0.3}AlO_{2.85}$	605/-/78	800	[59]
$La_{0.5}Sr_{0.5}FeO_3$	70/95/90	850	[133]
$LaFeO_3$	96/-/98	900	[134]
$LaMnO_3$	20/-/70	850	[135]

$LaCrO_3$	38/1.4/4.7	850	[136]
$LaCr_{0.85}Ru_{0.15}O_3$	100/46/65	850	[136]
$NdCaCoO_{3.96}$	90/-/90	920	[137]
$Pr_{0.7}Zr_{0.3}O_{4-\delta}$	-/88/-	850	[138]

Similarly, Araujo et al. reported the substitution of Ni by Co in $LaCo_xNi_{1-x}O_3$ perovskite catalyst and its effect on catalyst activity in POM[128]. They found that increasing Co ratio (x=0 to 1.0) resulted in decreasing CH_4 conversion (from 60% to 20%) and syngas selectivity by 10%, agreement with Choudhary et al. findings [117].

Apart from Ni, perovskites with a combination of Co and Fe in B-site was an attractive option as well. Partial substitution of Fe with Co in $LaCo_{0.5}Fe_{0.5}O_3$ was reported to have a low CH_4 conversion of 17.1% and 59.2% H_2 selectivity at 700 ^oC. In the same way, Dai et al. observed that CO selectivity in the case of Sr and Co doping into $LaFeO_3$ [121]. Syngas selectivity was decreased with the addition of Co in the order $LaFeO_3$>$La_{0.8}Sr_{0.2}FeO_3$ > $La_{0.8}Sr_{0.2}Fe_{0.9}Co_{0.1}O_3$, while conversion was increased in this order. The low performance of Co/Fe perovskites can be attributed to lower activity of Co and Fe in POM compared to Ni [133, 139].

Less common elements such as Rh, Ru, Al, Ti, Ga, Cu, and Cr as B-site holders were examined for POM. As mentioned in Section 2.3, Rh conventional catalysts were shown to have high selectivity to syngas. Therefore, Rh was considered as B-site occupant as well. Catalytic partial oxidation of methane to synthesis gas was performed over La-M-O, (M = Co, Cr, Ni, Rh) [129]. The best system was found to be La-Rh-O, which gave 95% CH_4 conversion with 98% CO selectivity even after 120 h on stream at 800°C. It should be noticed that Rh has been reported to have high performance in POM and better coke resistance thane Ni [3, 16]. Compared to La-Rh-O, La_xNiO_y/CeO_2 showed higher activity (100% CH_4 conversion and CO selectivity at 800 ^oC) due to positive Ce role in carbon deposition resistance [55].

As for Al as B-site partial occupant, up to 98% syngas selectivity at 850 ^{o}C was achieved on La-Ca-Co-(Al)-O perovskite [132]. Similar to Al, Zr in B-site of $Pr_{0.7}Zr_{0.3}O_{4-\delta}$ perovskite catalyst was reported to give 88% syngas selectivity [138]. Regarding Ti effect as B-site occupant, Hayakawa et al. reported the effect of Ti substitution with Ni in POM using $Ca_{0.8}Sr_{0.2}Ti_{l-y}Ni_y$ catalyst [133]. Ti as B-site holder gives a low conversion of 34 %, which was improved via Ti partial substitution with Ni [117, 122, 126, 127]. Ni addition enhanced catalyst activity as CH_4 conversion increased from 34% to 97.4% as Ni content from 0-0.4% at 800 ^{o}C. A part from Ti and Al, Ru-doped perovskites have also been investigated for POM. In particular, Melchiori et al. reported the catalytic activity of $LaCr_{0.85}Ru_{0.15}O_3$ perovskite in POM. $LaCrO_3$ showed low CH_4 conversion up to 16% at 850 ^{o}C with 55% CO selectivity[136]. However, Ru addition improved CH_4 conversion up to 100% with 65% CO selectivity due to RuO_2 presence. Similarly, 35% CH_4 conversion of $Nd_{0.95}CrO_3$ was reported indicating poor Cr performance as perovskite B-site holder [140].

In summary, there have been several metals studied for perovskites B-site occupants. Nevertheless, only a few were found to be highly active in POM. There was no surprise that high conversion and syngas selectivity (>90%) were achieved on perovskites with Ni, Co and Rh in B-site. This is due to their high activity as an active site for POM over conventional metal oxides. The underline factor, which explains Ni, Co and Rh high activity is their facile reducibility similar to conventional metal oxides. In contrast, Fe, Ti, Al, Zr and Al as whole B-site occupants were reported to have relatively low conversion and syngas selectivity (<90%), which was improved via partial substitution with Ni or Co. Moreover, the co-doping of Al and Fe in B-site was reported to improve the stability of perovskites in POM [141-143].

2.5.2 A-site Doping in Perovskite Catalytic Activity

A-site affects oxygen mobilization and flux, which can influence CH_4 conversion and syngas selective ultimately. In this prospect, several studies investigated the A-site doping role in perovskite catalytic performance [133]. For illustration, it was reported that doping in $La_{1-x}Sr_xFeO_3$ improves CH_4 conversion from 70% to 95%. Sr facilitates Fe reduction, which is crucial for CH_4 oxidation. Facile reduction of Fe increases bulk lattice oxygen was responsible for Fe^{+3} oxidation from Fe^{+2}, which favors CH_4 partial oxidation to CO and H_2 [134, 144]. Likewise, Khine et al. reported partial oxidation of methane using $(La_{0.7}A_{0.3})BO_3$ where, (A= Ba, Ca, Mg, Sr, and B = Cr or Fe) [127]. Near 100% CO and H_2 selectivity were achieved on $(La_{0.75}Sr_{0.25})FeO_3$ catalyst due to its facile reduction. Similarly, Sr was reported to enhance oxygen mobility in the $LaSrCoO_3$ lattice significantly compared to $LaCoO_3$ [145, 146]. In the same prospect, $NdCoO_3$ is more active as a POM catalyst than $LaCoO_3$. It was observed that the catalytic activity of rare-earth cobaltates increases with decreasing radii of rare-earth elements in the following sequence: $LaCoO_3 > PrCoO_3 > NdCoO_3 > SmCoO_3 > GdCoO_3$. It was proposed also that the low activity of these perovskite-based catalysts could be associated with their high stability and the ability to re-oxidize into the initial phase. In the same frame, Dedov 2015 also reported the effect of Nd and Ca on $NdCaCoO_3$ perovskites catalyst. Nevertheless, a higher temperature of 930 ^oC was required to achieve 90% CH_4 conversion and 90% CO selectivity [137]. On the contrary, Ln substitution has no effect on shifting catalyst reduction temperature in the case of $LnCoO_3$ perovskite catalysts (Ln=La, Pr, Nd, Sm, and Gd).

In brief, studies agree that alike earth doping in A-site was reported to facilitate B site element reduction[147]. Facile B-site reduction increases lattice oxygen mobility at a lower temperature. Consequently, the degree of lattice oxygen mobility and concentration affect syngas selectivity. As well, high lattice oxygen mobility decreases the required temperature for syngas production [119]. Numerous alkali and rear-earth elements such as can be utilized as

A-site dopants. However, in most cases, a combination of La and Sr was proved to have the most positive effect on perovskite oxygen mobility and consequently increasing its activity [148]. Table 6 compares the oxygen mobility of some catalysts and support with perovskites with A-site dopants.

Table 6. Comparison of oxygen mobility of catalysts in the presence of A-site dopant. Reproduced with permission from reference [127]. Copyright 2002, Elsevier.

Catalyst	Mobile oxygen ($mmol.g^{-1}$)
$CaTiO_3$	143
$SrTiO_3$	285
$BaTiO_3$	76.4
MgO	4.0
α-Al_2O_3	0.7
$Ni/CaTiO_3$	468
$Ni/SrTiO_3$	277
$Ni/BaTiO_3$	148
Ni/α-Al_2O_3	11

3. Membrane Reactor Configurations for POM

Dense membranes for oxygen separation have been developed in the past decade for partial oxidation of methane. The permeation of O_2 from the oxygen-enrich side will be utilized to oxidize methane to syngas [28]. Using air reduces operation cost and minimizes the safety hazard associated with pure oxygen. An additional advantage of catalytic membrane reactors is assigned to their uniform temperature profile distribution [28, 149, 150], which solves the problem of overheating the inlet part of catalysts bed where the gas phase oxygen is consumed in the total oxidation of methane. Overheating the inlet part of catalysts leads to the sintering of active components, corrosion of metal substrates, spallation of supported layers, and cracking of ceramic substrates [150, 151].

Research activities in POM using membrane reactors include; (1) membrane stability at high temperature to maintain high oxygen flux in presence of reducing gases such as H_2, CO, and CH_4; (2) membrane catalytic properties and surface modification for high CH_4 conversion and syngas selectivity; (3) designing new membrane configurations for POM. This review paper deals with the simplest membrane module (disk-shaped) mixed ionic-electronic membranes reactors to focus on the effect of membrane and catalyst layer composition on POM. Furthermore, membranes under discussion are divided into (1) symmetric (without catalyst layer or coating) and (2) asymmetric (with catalyst layer or coating). In the case of the asymmetric membrane (without catalyst layer), it is importing to consider modifying the membrane itself for methane oxidation. On the other hand, in the asymmetric membrane, the reaction side is coated with a catalyst layer, which mainly responsible for POM.

3.1 Symmetric Membranes

In the absence of a catalyst layer on the reaction side, oxygen flux plays a major rule in POM via symmetric membranes, and different membrane compositions give different oxygen fluxes. Table 7 summarises the reported symmetric mixed ionic and electronic membrane materials and their relevant POM performance.

Several membrane composites have been considered for POM such as BCFT ($BaCo_xFe_yTa_z$) and BCFZ ($BaCo_xFe_yZr_z$), which were reported to have higher POM performance. The high POM performance of BCFT is due to higher oxygen flux [152-160]. In addition, BCFT membrane is more stable than $BaCo_{0.7}Fe_{0.2}Nb_{0.1}O_{3-\delta}$ (BCFN), which is regarded as one of the highest oxygen flux perovskite materials until now [152]. Dense $BaCo_{0.7}Fe_{0.2}Ta_{0.1}O_{3-\delta}$ membrane has been considered for POM as well. High CH_4 conversion and CO selectivity were achieved at 900 ^oC due to good oxygen flux for CH_4 conversion. Figure 6 shows the effect of temperature and oxygen flux on CH_4 conversion and CO selectivity. BCFT membrane has

been modified by various B-site holders. Luo et al. reported Ta substitution to Zr and $BaCo_{0.7}Fe_{0.2}Ta_{0.1}O_{3-\delta}$ (BCFT) presented high oxygen flux and good stability during POM to syngas [105].

$SrFe_{0.7}Al_{0.3}O_{3-\delta}$ and $La_{0.3}Sr_{0.7}Co_{0.8}Ga_{0.2}O_{3-\delta}$ have been considered for POM in membrane reactors as well [153]. The catalytic performance was far from thermodynamic equilibrium as reported. Only 60% CH_4 conversion was achieved at 800 °C and CO selectivity was up to 8%. Kharton et al. suggested the low surface area of the membranes resulted in low catalytic activity. However, Fe and Ga have low catalytic activity in POM as indicated in Section 3 [153].

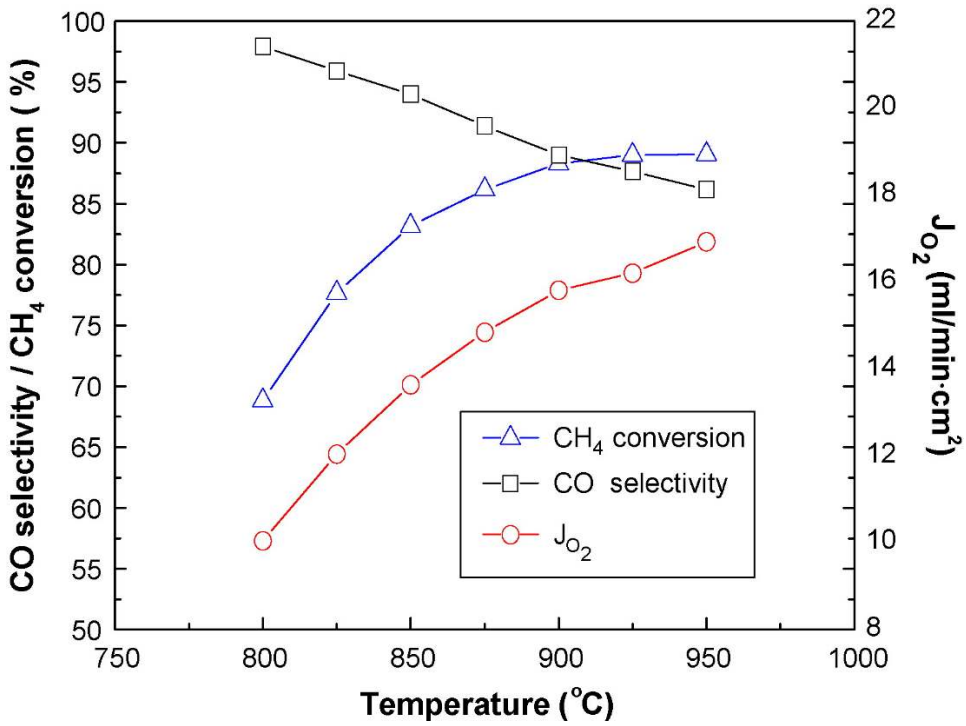

Figure 6. Temperature influence on CH_4 conversion, CO selectivity and O_2 permeation flux in $BaCo_{0.7}Fe_{0.2}Ta_{0.1}O_{3-\delta}$ (BCFT) symmetric membrane reactor. Reproduced with permission from reference[152]. Copyright 2010, Elsevier.

An alternative to using membrane without individual catalyst layer, catalyst and membrane materials can be integrated into one phase. In this prospect, Evdou et al. reported syngas

production using $LaSrFeO_3$ membrane mixed with NiO catalyst as on phase [161]. It was observed that during the CH_4 pulse reaction, more oxygen was removed. In addition, CH_4 decomposition was increased and therefore H_2 and CO production increased. It should be noticed that since NiO was mixed with the perovskite, CH_4 was in direct contact with the membrane, which decomposes on vacant oxygen sites [134].

Table 7. Symmetric membranes (without catalyst coating) performance in POM

Membrane	O_2 flux ($ml.min^{-1}.cm^{-2}$)	$XCH_4/SCO/SH_2$ (%)	T (ºC)	Stability (hours)	References
$BaCo_{0.7}Fe_{0.2}Ta_{0.1}O_{3-\delta}$	4.2	99/94/-	900	60 injections	[154]
$La_{0.2}Ba_{0.8}Co_{0.2}Fe_{0.8}O_{3-\delta}$	-	88/97/-	850	-	[155]
$SrFe_{0.5}Co_{0.5}O_3$	4	99/98/-	850	850	[156]
$Ba_{0.5}Sr_{0.5}Co_{0.8}Fe_{0.2}O_{3-\delta}$	11.5	97/95/-	875	7	[157]
$BaCo_{0.7}Fe_{0.2}Zr_{0.1}O_{3-\delta}$	5.6	98/97/-	850	1000	[158]
$BaCo_{0.7}Fe_{0.2}Nb_{0.1}O_{3-\delta}$	20	88/97/-	850	2200	[159]
$SrFe_{0.8}Co_{0.2}O_3/SrAl_2O_4$	8	75/-/91	850	300	[160]
$La_{0.7}Sr_{0.3}FeO_3/NiO$	(20 pulse injection)	20/99/99	1000	1200	[161]
$SrFe_{0.7}Al_{0.3}\ O_{3-\delta}$	-	60/-/8	950	100	[162]
$La_{0.3}Sr_{0.7}Co_{0.8}Ga_{0.2}O_{3-\delta}$	-	30/-/6	950	100	[162]

Likewise, Dong et al reported improved hydrogen production over $SrCo_{0.8}Fe_{0.2}O_{3-\delta}$ (SCF) doped with $SrAl_2O_4$ (3, 5,7 and 9%) system[160]. The reported CH_4 conversion and H_2 selectivities were 75% and 91% respectively at 850 ºC. Although $SrAl_2O_4$ enhancement of

membrane stability over 1200 hours of operation, the catalytic performance was lower than other membranes in Table 7. This can be attributed to $SrAl_2O_4$ nature, since species such as $NiAl_2O_4$, $CoAl_2O_4$ has a negative effect on catalyst activity in POM as discussed in Section 2. Hu et al. reported the performance of Co-doped $YBa_2Cu_3O_{3-\delta}$ (YBCO) membrane reactor for POM [163]. The results showed that doping YBCO membrane with a little Co can enhance its oxygen permeation flux and improve its stability in a reducing environment noticeably. At 900 ^oC (feed flow at 50 $ml.min^{-1}$, CH_4 6.0 v%, SV = 12,000 h^{-1}) CH_4 conversion rate, CO selectivity, and oxygen permeation flux can reach to 98%, 92% and 1.41 $ml.min^{-1}.cm^{-2}$ respectively. Co addition can also be the reason for high syngas production due to its good catalytic activity as a catalyst as B-site holder in perovskites catalysts [3, 16, 138]. It can be concluded that high oxygen mobility in membrane structure can cause high lattice strain which reduces metal-oxygen structure. Obviously, the continuous REDOX process in POM can impose the same lattice strain on perovskite structure which leads to its failure. The continuous reduction of perovskite structure during POM will eventually result in unstable catalyst performance due to sintering [164].

3.2 Asymmetric Membranes

3.2.1 Porous Catalysts Toward Membrane Catalytic Activity in POM

Asymmetric membranes herein contain thin and porous catalyst layers as shown in figure 4. For asymmetric membrane in POM, a number of membrane/catalyst combinations have been proposed (Table 8). Both Single-phase and dual-phase (composed of perovskite and fluorite) membranes reactor were investigated for POM.

Single-phase membranes were intensively studied due to their high oxygen separation capability. For example, Babakhani et al. instigated $Ba_{0.5}Sr_{0.5}Co_{0.8}Fe_{0.1}Ni_{0.1}O_{3-\delta}$ membrane reactor coated with a Ni/Al_2O_3 catalyst for POM [165]. They reported 98% methane conversion

and 96% CO selectivity at 850 ºC, which is the best performance at the lowest temperature so far. Other groups have investigated different ceramic membranes with Ni-based catalysts at a temperature of 875 ºC [164-168]. CO yield over NiO/MgO coated on a $BaCo_xFe_yNb_zO_{3-\delta}$ membrane reactor was obtained at 85%-96% [168]. Moreover, POM was investigated in a relatively higher temperature of 900 ºC [152, 169-172]. High CO selectivity over bulk Ni catalyst of 99% and 96% CH_4 conversion on $BaCo_{0.6}Fe_{0.2}Ta_{0.2}O_3$ and $Sr_{1.7}La_{0.3}GaZO_{3-\delta}$ membrane respectively [173] Luo et al. reported a high oxygen flux in a $BaCo_{0.7}Fe_{0.2}Ta_{0.1}O_3$ membrane coated with Ni catalysts, which resulted in excellent CH_4 conversion with 94% CO selectivity at 900 ºC [152,174]. In this case, the high oxygen flux was attributed to the positive role of Ta in the membrane phase. While the highest stability achieved on a bulk Ni catalyst was 7500 hours on $La_{0.5}Sr_{0.5}FeO_{3-\delta}$ at 850 ºC [175].

Al_2O_3-supported Ni oxides were extensively utilized as catalysts in POM in membrane reactors. For example, Li-La modified Ni/γ-Al_2O_3 catalyst (backed on $BaCo_{0.4}Fe_{0.4}Zr_{0.2}O_{3-\delta}$) activity has been reported by Tong et al. By utilizing LiLaNiO/γ-Al_2O_3 catalyst, higher selectivity up to 99% to CO was achieved with 98% CH_4 conversion [159]. In that case, at the beginning of the reaction, CO_2 was observed due to the presence of NiO. Afterward, Ni reduction to Ni^0 contributed to CO and H_2 production. Moreover, after 60 minutes of operation, catalyst induction occurred, and membrane lattice oxygen became the rate-determining step. POM and oxygen permeation in a dense $SrCoFeO_x$ membrane reactor were studied with the reaction side of the membrane packed with 10 wt % Ni/γ-Al_2O_3) [175]. The highest CH_4 conversion (~90%), CO selectivity (97%) was achieved at 900 ºC. Overall, although $LiLaNiO_x$/γ-Al_2O_3 has high performance in POM, an induction period (reduction of NiO to Ni^0) was required for syngas production.

In the same manner, LiLaNi/γ-Al_2O_3 catalyst was coated on several membranes such as $Ba_{0.15}Ce_{0.85}O_{3-\delta}$. Good syngas selectivity was obtained (96% CO selectivity). In contrast, in the

case of the blank membrane, only C and CO_2 were produced [157, 176]. Moreover, Li et al. reported the performance of $BaCe_{0.1}Co_{0.4}Fe_{0.5}O_{3-\delta}$ in POM [169]. The membrane was coated with LiLaNiO/g-Al_2O_3 catalyst and evaluated for POM. During membrane operation, catalyst induction occurred by NiO reduction to Ni^0. Afterward, 99% CH_4 conversion was achieved with 93% CO selectivity at 875°C. It was reported that reduced catalysts are more selective to syngas than oxidized catalysts [3, 16, 168, 177].

Table 8. Asymmetric membranes (with catalyst coating) activity in POM

Membrane	Catalyst	O_2 flux (ml.cm^{-2}.min^{-1})	$XCH_4/SH_2/SCO$ (%)	T (°C)	Stability (hours)	Catalyst layer thickness (mm)	References
$Ce_{0.8}Sm_{0.2}O_{2-\delta}$-$La_{0.8}Sr_{0.2}CrO_{3-\delta}$	$La_4Sr_8Ti_{12}O_{38-\delta}$		34/89/88	950	600	1.07	[10]
$Ba_{0.5}Co_{0.7}Fe_{0.2}Ta_{0.1}O_{3-\delta}$	Ni	16.2	99/-/94	900	400	0.7	[152]
$Ba_{0.5}Sr_{0.5}Co_{0.8}Fe_{0.2}O_{3-\delta}$	LiLaNiO_x/γ-Al_2O_3	11	97/-/96	875	500	-	[158]
$BaCo_{0.4}Fe_{0.4}Zr_{0.2}O_{3-\delta}$	LiLaNiO/γ-Al_2O_3	5.8	98/-/99	850	2200	1.0	[159]
$Ba_{0.5}Co_{0.7}Fe_{0.2}Nb_{0.1}O_{3-\delta}$	NiO/MgO	12.3	96/78.9/104	875	100	-	[168]
$BaCe_{0.1}Co_{0.4}Fe_{0.5}O_{3-\delta}$	LiLaNiO/γ-Al_2O_3	8.9	94/-/95	875	1000	1.0	[169]
$SrCoFeO_x$	Ni/Al_2O_3	3.0	98/90/90	850	7500	1.0	[175]
$Ba_{0.1}Ce_{0.85}Co_{0.4}FeO_{3-\delta}$	LiLaNiO/γ-Al_2O_3	3	96/-/96	850	160	1.5	[176]
YSZ-$SrCo_{0.4}Fe_{0.6}O_{3-\delta}$	NiO/γ-Al_2O_3	6.2	86.7/-/100	900	1000	0.2	[178]
$La_{0.7}Sr_{0.3}Ga_{0.6}Fe_{0.4}O_{3-\delta}$-$La_{0.6}Sr_{0.4}CoO_{3-\delta}$	NiO/$NiAl_2O_4$	18	88/42/100	850	100	0.1	[179]
$Ce_{0.2}Sm_{0.8}O_{2-\delta}$-$Sr_2Fe_{1.5}Mo_{0.5}O_{5+\delta}$	Ni/Al_2O_3	2.7	97/-/98	950	500	1.3	[180]
$SrCo_{0.4}Fe_{0.4}Zr_{0.2}O_{3-\delta}$	Ni/Al_2O_3	6.2	85/-/95	850	1000	0.2	[180]
$La_{0.8}Sr_{0.2}Cr_{0.5}Fe_{0.5}O_{3-\delta}$-YSZ	Ni/Al_2O_3	1.4	90/-/95	850	220	1.8	[181]
$Ba_{0.5}Sr_{0.5}Co_{0.8}Fe_{0.2}O_{3-\delta}$	Ni/ZrO_2	11.4	98.8/-/91.4	850	-	-	[182]
$Ba_{0.5}Sr_{0.5}Zn_{0.2}Fe_{0.8}O_{3-\delta}$	Ni	2.55	64/-/98.3	900	65	1.25	[184]
$BaCo_{0.7}Fe_{0.2}Nb_{0.1}O_{3-\delta}$	$Ru_{0.2}$wt%$_{Rh0.2}$wt%/$Co_{0.3}Mg_{0.7}O$	18	98/-/-	900	700	1.0	[185]
$La_{0.2}Ba_{0.8}Fe_{0.8}Ga_{0.2}O_{3-\delta}$	Rh/Al_2O_3	-	97/-/100	850	696	0.15	[186]
$SrCo_{0.8}Fe_{0.2}O_{3-\delta}/Al_2O_3$	NiO/Al_2O_3	2.97	80/-/100	850	500	1.3	[187]

$Sm_{0.5}Sr_{0.5}CoO_3$-$Sm_{0.15}Ce_{0.85}O_{1.92}$	LiLaNiO/c-Al_2O_3	7.27	98/-/98	950	30	3.0	[188]
GDC-$La_{0.2}Ca_{0.8}FeO_{3-\delta}$	NiO-GDC-($La_{0.3}Sr_{0.7}TiO_{3-\delta}$)	3.2	80/100/-	900	100	-	[189]
$(SrFe)_{0.7}(SrAl_2)_{0.3}O_z$	Ferrite	0.3	24/-/16	950	200	0.003	[190]
$(SrFeO_{3-\delta})_{0.7}(SrAl_2O_4)_{0.3}$	Pt/$LaNiO_3$/Al_2O_3	0.2	95/-/96	900	50	-	[191]

Apart from Al_2O_3-supported Ni catalysts, Ni/ZrO_2 catalyst was coated on $Ba_{0.5}Sr_{0.5}Co_{0.8}Fe_{0.2}O_{3-\delta}$ membrane and evaluated for POM. CH_4 conversion reached 98.8% at 850 ºC with 91.4% CO selectivity. However, they reported that that CH_4 can be oxidized to CO_2 by surface lattice oxygen and gas-phase oxygen near the permeation surface. Similar observations have been reported by Wang et al. regarding CH_4 combustion near the membrane surface of $Ba_{0.5}Sr_{0.5}Co_{0.8}Fe_{0.2}O_{3-\delta}$ backed with $LiLaNiO/\gamma$-Al_2O_3 catalyst [158]. Co and Rh conventional catalysts showed good activity in POM as discussed in Section 2. Therefore, they have been an attractive choice for membrane POM [191]. Harada et al. reported a high CH_4 conversion of 99% on $BaCo_{0.7}Fe_{0.2}Nb_{0.1}O_{3-\delta}$ membrane coated with $Ru_{0.2}wt\%Rh_{0.2}wt\%/Co_{0.3}Mg_{0.7}O$ catalyst [185]. The observed high activity was attributed to the catalyst layer, which brought methane immediately into the reaction in a short induction time.

Dual-phase ceramic-ceramic membranes have been investigated for POM at a temperature range of 800-950 ºC. For example, Ruiz-Terejo et al. reported POM using Ag/GDC composite membrane coated with Ni mesh [190]. The obtained CH_4 conversion was 20.8 % with 98% CO selectivity. Yet, the addition of fluorites such as YSZ (yttria doped zirconia), SDC (Sm-doped ceria) and GDC (Gadolinium-doped ceria) improved membrane perovskites stability [191]. As well, POM on $La_{0.7}Sr_{0.3}Fe_{0.4}Ga_{0.6}O_{3-\delta}$ (LSGF) perovskite membrane coated with

$La_{0.6}Sr_{0.4}CoO_{3-\delta}$ (LSC) has been investigated as well [179]. $NiO/NiAl_2O_4$ catalyst was coated on the membrane reaction side to improve syngas production. CH_4 conversion up to 88% was obtained with 100% CO selectivity at 850 °C. In comparison, Ga doped $La_{0.2}Sr_{0.8}Fe_{0.8}Ga_{0.2}O_{3-\delta}$ membrane reactors reported by Ritchie et al. [186]. Approximately 100% CO selectivity at 850 °C was achieved by utilizing Rh catalyst and CH_4 conversion reached 97%. Yet, membrane decomposed at 780 °C. As can be noticed, Rh based catalyst has better performance than $NiO/NiAl_2O_4$ when they were coated on LSGF membrane, which can be related to the negative effect of $NiAl_2O_4$ on catalyst activity [38].

Similarly, high performance was obtained over SDC-$Sm_{0.6}Sr_{0.4}FeO_{3-\delta}$ dual-phase membrane doped with LSC ($La_{0.6}Sr_{0.4}CoO_{3-\delta}$) catalyst [192]. Of course, LSC perovskite catalyst has lower performance than Ni-based perovskite $LaSrNi_xCo_{1-x}O_{3-\delta}$ an also more difficult to be reduced, therefore, a higher temperature is required for high syngas production. Consequently, although a high CO selectivity of 96% was obtained, the required temperature was 950 °C. In addition, soot deposition on the reaction side of the membrane was detected by XRD analysis of the reduced sample. Similar to SDC doped perovskites, Gu et al. investigated YSZ-SCF ($SrCo_{0.4}Fe_{0.6}O_{3-\delta}$) dual-phase membrane backed with NiO/Al_2O_3 catalyst [178]. Long-term stability for 240 hours with 84.7% CH_4 conversion and 100% CO selectivity. On the contrary, only CO_2 and H_2O observed with no syngas detected using YSZ-SCF membrane without a catalyst. Compared to NiO/Al_2O_3 catalyst, supported membrane composed of $La_{0.8}Sr_{0.2}Cr_{0.5}Fe_{0.5}O_{3-\delta}$ /YSZ was tested at 800°C. In this case, CH_4 throughput conversion over 90%, CO and H_2 selectivity both over 95%, and an equivalent oxygen permeation rate 1.4 $mL.cm^{-2}.min^{-1}$ [181].

In the same manner, $Ce_{0.2}Sm_{0.8}O_{2-\delta}$-$Sr_2Fe_{1.5}Mo_{0.5}O_{5+\delta}$ in a dual-phase membrane and coated with Ni/Al_2O_3 catalyst was reported to achieve 98% CO selectivity and 97% CH_4 conversion at 950 °C [187]. As well Zhu et al. reported high POM performance using $Sm_{0.15}Ce_{0.85O1.9}$-

$Sm_{0.6}Sr_{0.4}Fe_{0.7}Al_{0.3}O_{3-\delta}$ dual-phase membrane [188]. CH_4 conversion and CO selectivity were above 98% at 950 °C by implementing LiLaNiO/c-Al_2O_3 catalyst. In the same frame, POM over perovskite, catalyst $La_4Sr_8Ti_{12}O_{38-\delta}$ backed on $Ce_{0.2}Sm_{0.8}O_{2-\delta}$-$La_{0.8}Sr_{0.2}CrO_{3-\delta}$ dual-phase composite membrane reactor was reported investigated. Approximately 88% CO and 89% H_2 selectivity at 30% CH_4 conversion were observed under the optimized membrane reactor operating conditions at 950 °C and CH_4 feed rate of 20 mL.min^{-1}[10]. Likewise, high selectivity to CO was achieved by utilizing NiO-GDC-($La_{0.3}Sr_{0.7}TiO_{3-\delta}$) catalyst coated on GDC-$La_{0.2}Ca_{0.8}FeO_{3-\delta}$ membrane at 900 °C [189].

Apart from fluorites materials, dual-phase membranes reactors can be synthesized by modifying perovskites with other thermally stable metal oxides such as Al oxides. Yaremchenko et al. reported up to 24% CH_4 and 16% CO selectivity on $(SrFe)_{0.7}(SrAl_2)_{0.3}O_z$ membrane reactor at 950 °C [193]. This poor syngas yield can be attributed to the utilization of ferrite-based catalyst. On the other hand, coating the $(SrFeO_{3-\delta})_{0.7}(SrAl_2O_4)_{0.3}$ membrane with Pt/$LaNiO_3$/Al_2O_3 catalyst improved CH_4 conversion to 95% and CO selectivity to 96% at 950 °C [194].

Although different asymmetric membrane reactors were used to improve membrane reactor POM, still a high temperature is required for high syngas yield. In most cases, membrane reactors can achieve >90% syngas yield only at a high temperature (850-950 °C), which increases their energy consumption. Therefore, there is a strong drive to develop membrane reactors that operate at a lower temperature without sacrificing syngas yield. Recently, there are considerable studies reported membrane reactors with meaningful syngas yield at a reduced temperature <800 °C. For instance, 80% CH_4 conversion and 90% CO selectivity were observed on $Ba_{0.5}Sr_{0.5}Co_{0.8}Fe_{0.2}O_{3-\delta}$ membrane coated with Ni/ZrO_2 catalyst at 800 °C [195]. In the same manner, above 87% syngas selectivity and 38% CH_4 conversion were observed on $La_4Sr_8Ti_{12}O_{38-\delta}$ catalyst coated on $Ce_{0.8}Sm_{0.2}O_{2-\delta}$-$La_{0.8}Sr_{0.2}O_{3-\delta}$ membrane at 800 °C [10]. It

should be pointed that hollow fiber membranes have the potential to produce a high yield of syngas at a reduced temperature. For example, high CO and H_2 selectivity of 91% and 74% respectively, with CH_4 conversion of 97% were achieved at 750 ^oC on $La_{0.6}Sr_{0.4}Co_{0.8}Ga_{0.2}O_{3-\delta}$ hollow fiber membrane coated with $Ni/LaAlO_3$-Al_2O_3 catalyst [196]. Similarly, Wang et al. were able to obtain up to 80% CH_4 conversion and 85% CO selectivity at a reduced temperature of 730 ^oC with the stability of 100 hours of POM [197].

It can be noticed that there are two challenges that encounter the development of low-temperature membrane reactors for POM: (1) The low oxygen permeation rate at low temperature, which reduces CH_4 conversion since POM strongly affected by oxygen flux as mentioned in Section 4. Consequently, it is challenging to obtain high oxygen flux at a temperature below 800 ^oC, which necessitates reducing the CH_4 flow rate and compromising the suitability of the system for large-scale syngas production. (2) The limitation imposed by the catalyst itself as it produces syngas via reforming mechanism, which requires a high temperature above 800 ^oC for high syngas yield. Therefore, the development of membrane material and configurations that supply high oxygen flux at low temperature, and catalysts produces syngas via direct partial oxidation can facilitate the operation of membrane reactors at low temperature.

As well as catalyst layer composition, catalyst layer thickness significantly influences syngas yield. Generally, increasing catalyst layer thickness provides more reaction sites for CH_4 conversion, which intern increases syngas yield. For example, the observed CH_4 conversion on $LiLaNiO/Al_2O_3$ catalyst layer (1mm thickness) coated on $Ba_{0.5}Sr_{0.5}Co_{0.8}Fe_{0.2}O_{3-\delta}$ membrane was 94%, while for the same system, the observed conversion was 98% when the thickness was increased to 3mm [198]. Nevertheless, the increment of catalyst layer thickness can result in reactant diffusion resistance, and non-uniform temperature gradient (hot spots) similar to fixed bed reactors, which can decrease syngas yield [199].

Succinctly, metal oxides and perovskites were evaluated as a membrane catalyst layer for POM. Ni and Rh based metal oxide catalysts showed the highest activity, which is expected due to their excellent performance in fixed bed reactors. Co-based catalysts showed lower syngas yield but higher coke deposition resistance in contrast with Ni catalysts. On the other hand, Perovskite catalysts were reported to have high POM activity (>85% syngas yield). However, they still suffer from stability issues in the form of phase decomposition.

3.2.2 Dual-Functional Membranes Reactors

Dual-functional membranes reactors are an emerging trend in membrane reactors design. The dual-function membranes combine two or more reactions in one membrane reactor [200]. In this case, multiple reactions can take place in several zones in one membrane. In the dual-function membrane reactor, products from one zone undergo a second reaction in a different reaction zone. Therefore, different types of catalysts can be utilized depending on the reaction in that specific zone.

A typical case is the coupling of the decomposition of oxygen-containing gases such as CO_2, NO_x, and H_2O with partial oxidation of methane [200,201]. For example, Wang et al. reported NO decomposition reaction coupled with POM in $BaBi_{0.05}Co_{0.8}Nb_{0.15}O_{3-\delta}$ membrane coated with Ni-phyllosilicate catalyst (Figure 7). The membrane benefited both reactions since the consumption of oxygen by POM increased NO decomposition rate. At the same time, the produced oxygen form NO decomposition increased POM reaction rate at a low temperature of 700 ^oC[197]. As well, Liang et al. combined CO_2 reforming of methane with N_2O decomposition using $BaFe_{0.9}Zr_{0.05}Al_{0.05}O_{3-\delta}$ membrane coated with Ni/Al_2O_3 catalyst [202]. Likewise, Jiang et al. combined water-splitting reaction with POM in BCFZ membrane coated with Ni/Al_2O_3 [201].

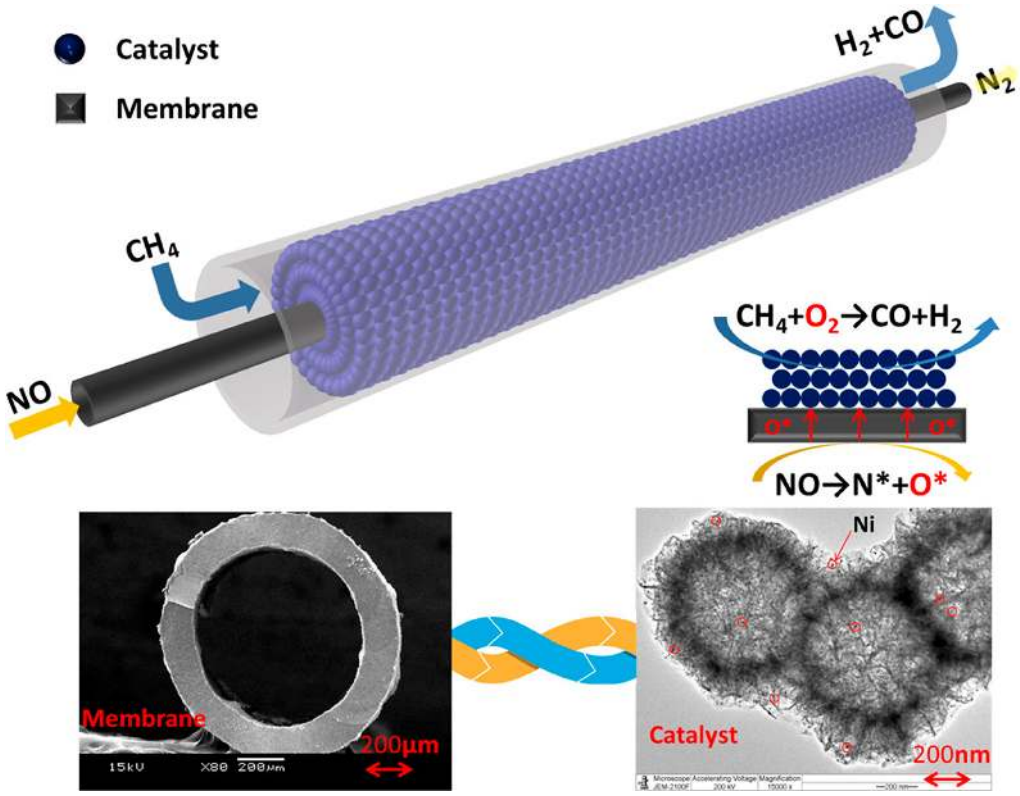

Figure 7. Schematic diagram of a dual-functional membrane for NO decomposition and POM. Reprinted with permission from Reference [197]. Copyright 2019, American Chemical Society.

Overall, A dual-function membrane reactor is designed mainly to combine exothermic and endothermic reactions [200]. The heat produced from the exothermic reaction such as POM can be utilized by the endothermic reaction. In addition, the products of one reaction such as oxygen form NO_x decomposition benefits POM reaction by increasing oxygen supply. In exchange, consumption of oxygen vis POM or dry reforming increases the reaction rate of NO_x decomposition. This can increase efficiency, reduce cost and produce high-value chemicals [200].

3.2.3 Overview of Catalyst Layer Coating Methods

Catalyst layer fabrication on membranes is important for the performance of reactors. Catalyst can be coated on membrane reaction using several methods, which include spraying, pressing,

electrodeposition, impregnation, sputter, screen painting [203-205]. In the spraying method, catalyst powder or ink is deposited on membrane material via a rolling process. Following to catalyst powder/ink mixing in a knife mill, it is sprayed using nitrogen stream through a slit nozzle directly on membrane material. In the case of catalyst ink coating, an organic medium with the addition of rice starch is used. Similar to spraying, painting of catalyst ink is a simple method for catalyst layer deposition. Catalyst ink in this method is brush-painted directly onto the membrane surface. The advantage of spraying and painting methods is the ability to control catalyst layer porosity by using pore former agent. Nevertheless, in this method, it is difficult to form a homogenous catalyst layer since distortion occurs during the drying step [206, 207]. Screen-printing is also a common method by which the catalyst layer is coated on the membrane reaction side. In this method, a screen is used for a specific catalyst pattern on the membrane surface, which can be considered as an advantage of this method. However, the limitation of this method is that larger particles tend to get obstructed, which forms distorted patterns. Besides, the decal method is a common way for catalyst coating. In this method, catalyst ink is coated on a decal with the same dimensions of the membrane surface. Fiberglass reinforced Teflon is the widely used decal material as a decal. Moreover, vapor deposition is another method for catalyst layer coating. In this method, a catalyst is deposited on the membrane from its vapor phase. As well, the electrically assisted catalyst layer deposition is one of the common methods. In this technique, a catalyst is deposited via electrochemical processes such as electro-spraying, electrophoretic deposition. In vapor and electrochemical deposition, a thin catalyst layer as low as 1 μm can be obtained. Nevertheless, these two methods often yield a non-uniform catalyst layer.

3.2.4 Effect of Catalyst Layer on Oxygen Permeation

In catalytic asymmetric membranes, the presence of a catalyst will affect membrane oxygen flux as well as POM reaction. CH_4/O_2 ratio during POM is determined by the catalyst state.

During POM reaction on membrane side, products and reactants partial pressure changes, which cause pressure variation across the membrane. Consequently, oxygen flux changes and thus CH_4/O_2 ratio can not be considered to be constant in the case of membrane reactor POM [157, 208]. In this frame, several studies reported that oxygen permeation flux depends on the extent of the reaction on the reaction side of the membrane[157]. For example, Gu et al. reported oxygen flux was increased by applying Ni-based catalyst in comparison with a plane membrane. Figure 8 shows oxygen flux variation for LSCF membrane with reactant flow rate at a fast reaction (complete conversion) and no reaction [20, 180]. In the same prospect, different catalyst compositions affect POM reaction and oxygen flux as shown in Table 9 [175]. For instance, in the case of γ-Al_2O_3 coated on $SrCoFeO_x$ membrane, lower oxygen flux was obtained compared to $La_{0.6}Sr_{0.4}Co_{0.8}Fe_{0.2}O_{3-\delta}$ and Ni/γ-Al_2O_3 catalysts.

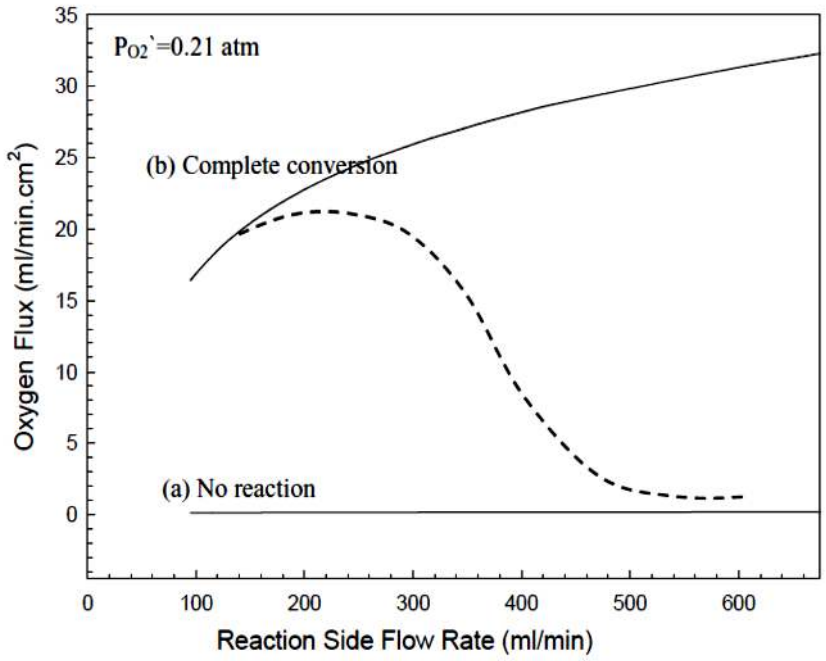

Figure 8. Comparison of modeling of oxygen flux through LSCF membrane as a function of reaction side flow rate: (a) No reaction (inert influent); (b) Complete conversion. Reprinted with permission from Reference [208]. Copyright 2004, Elsevier.

Table 9. Effect of catalyst coating on oxygen flux

Membrane	Catalyst	T (°C)	Oxygen flux ($ml.cm^{-2}.s^{-1}$)	Reference
$SrCoFeO_x$	-	900	0.75	
	γ-Al_2O_3	900	0.75	[175]
	$La_{0.6}Sr_{0.4}Co_{0.8}Fe_{0.2}O_{3-\delta}$	900	1.75	[175]
	Ni/γ-Al_2O_3	900	2.40	[175]
$BaCo_{0.7}Fe_{0.2}Nb_{0.1}O_{3-\delta}$	Ru-Rh/ $Co_{0.3}Mg_{0.7}O$	900	17.6	[185]
	Ni-Rh/ $Co_{0.3}Mg_{0.7}O$	900	11.0	[185]
	Ru-Rh/$BaAl_2O_4$	900	6.5	[185]
	Ni-Rh/ $BaAl_2O_4$	900	7.0	[185]

3.2.5 Effect of Oxygen Flux on Syngas Production

Oxygen flux has a significant effect on CH_4 conversion and syngas selectivity as well. Nevertheless, oxygen flux depends significantly on membrane thickness. Oxygen flux is controlled by the surface exchange reaction (i.e. membrane elements reduction and oxidation rate) at a small membrane thickness. On the other hand, bulk diffusion controls oxygen flux at thicker membranes [21]. Higher oxygen flux can be obtained by decreasing membrane thickness. Comparable results were obtained by Harada et al. higher oxygen flux resulted in higher performance [185]. In the case of $BaCo_{0.7}Fe_{0.2}$ $Nb_{0.1}O_{3-\delta}$, CH_4 conversion significantly increased from 73% to 97% when the oxygen flux was increased from 6.3 to 17.6 ($ml.cm^{-2}.s^{-1}$). Regarding syngas selectivity, although during POM reaction in membrane reactors Ni^0, Co^0 and Fe^0 active sites can be obtained by catalyst induction [120, 147], these species have lower syngas selectivity except for Ni^0 active sites [3, 20, 209]. On oxygen activation on the reaction side, Gu et al. suggested that surface oxygen ions exposed to the reducing atmosphere (CH_4,

CO and H_2) could be transformed by four routes described below by adopting the Kröger-Vink mechanism [178]. In the case of symmetric membrane reactor, Equations 15 and 18 occur at the membrane surface, and the oxygen flux was enhanced by Equation 15 compared with the oxygen permeation measurement. When the flow rate of methane was controlled at a constant rate, the increase in the helium flow rate would result in a decrease in the methane partial pressure in the reactive side. On the other hand, in the case of membrane reactors with catalyst packing, there are more significant amounts of reducing gases such as CO, H_2, and CH_4 in the reaction side. Reactions in Equations 15 and 18 would coincide at the catalyst layer. Because of the stronger reducing potential of H_2 and CO, the rates of the reactions in Equations 16 and 17 were substantially higher than that of the reaction in Equation 15. Consequently, the oxygen flux of the membrane reactor packed with the catalyst would be substantially higher than that of the membrane reactor without the catalyst [178].

$$CH_4 + 4O^* + 8h' \rightarrow CO_2 + 2H_2O + 4O_{\square} (15)$$

$$CO + 4O^* + 2h' \rightarrow CO_2 + 2O_{\square} (16)$$

$$H_2 + O^* + 2h' \rightarrow 2H_2O + O_{\square} (17)$$

$$2O^* + 4h' \rightarrow 2O_{\square} (18)$$

4. Thermodynamic Analysis and Mechanism of POM in Membrane Catalysis

4.1 Overview of POM Thermodynamics

Generally, partial oxidation of methane is a mildly exothermic reaction (Figure 9), which is an advantage over steam methane reforming. Based on thermodynamic calculations, reaction conditions such as inlet flow rate, reaction temperature and O_2/CH_4 ratio affect POM mechanism (Figure 9) and syngas yield. Membrane reactors happen to be significantly dependent on the feed flow rate, reaction temperature and O_2/CH_4 ratio based on

thermodynamic studies. For example, the reactant flow rate affects reaching the equilibrium. High pressure decreases both CH_4 conversion and syngas selectivity [3]. Equilibrium conditions are reached at a lower flow rate rather than a higher one. At a high flow rate, the elementary reactions for partial oxidation do not reach their equilibrium, which affects the mechanism of the overall reaction and becomes the limiting factor [3].

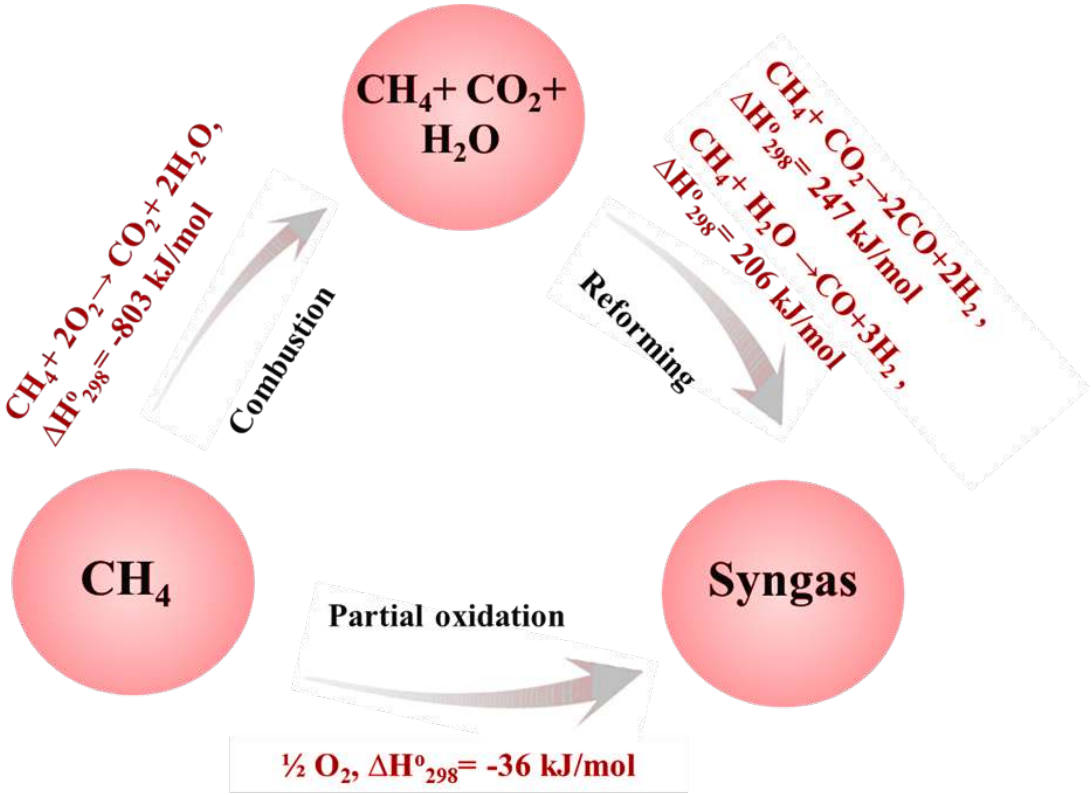

Figure 9. POM to syngas reaction pathways

Figure 10. summarizes the effect of O_2/CH_4 ratio and temperature on CH_4 conversion and syngas ratio [210]. Reaction temperature has a major impact on CH_4 conversion and syngas yield. Increasing reaction temperature above 750 °C results in a high syngas yield as the equilibrium conversion is nearly reached as in Figure 9. Below 750 °C CH_4 conversion drops significantly, which consequently decreases syngas yield. As well, POM reaction is highly dependant on O_2/CH_4 ratio. Syngas yield increases in proportion with the O_2/CH_4 ratio at fixed reaction temperature. The optimum O_2/CH_4 ratio from a thermodynamic viewpoint is 2. At

O_2/CH_4 ratio higher than 2, the excess O_2 causes complete CH_4 oxidation takes place, which is not beneficial to POM as no syngas will be produced. On the other hand, at an O_2/CH_4 ratio of less than 0.5 CH_4 conversion is low due to low O_2.

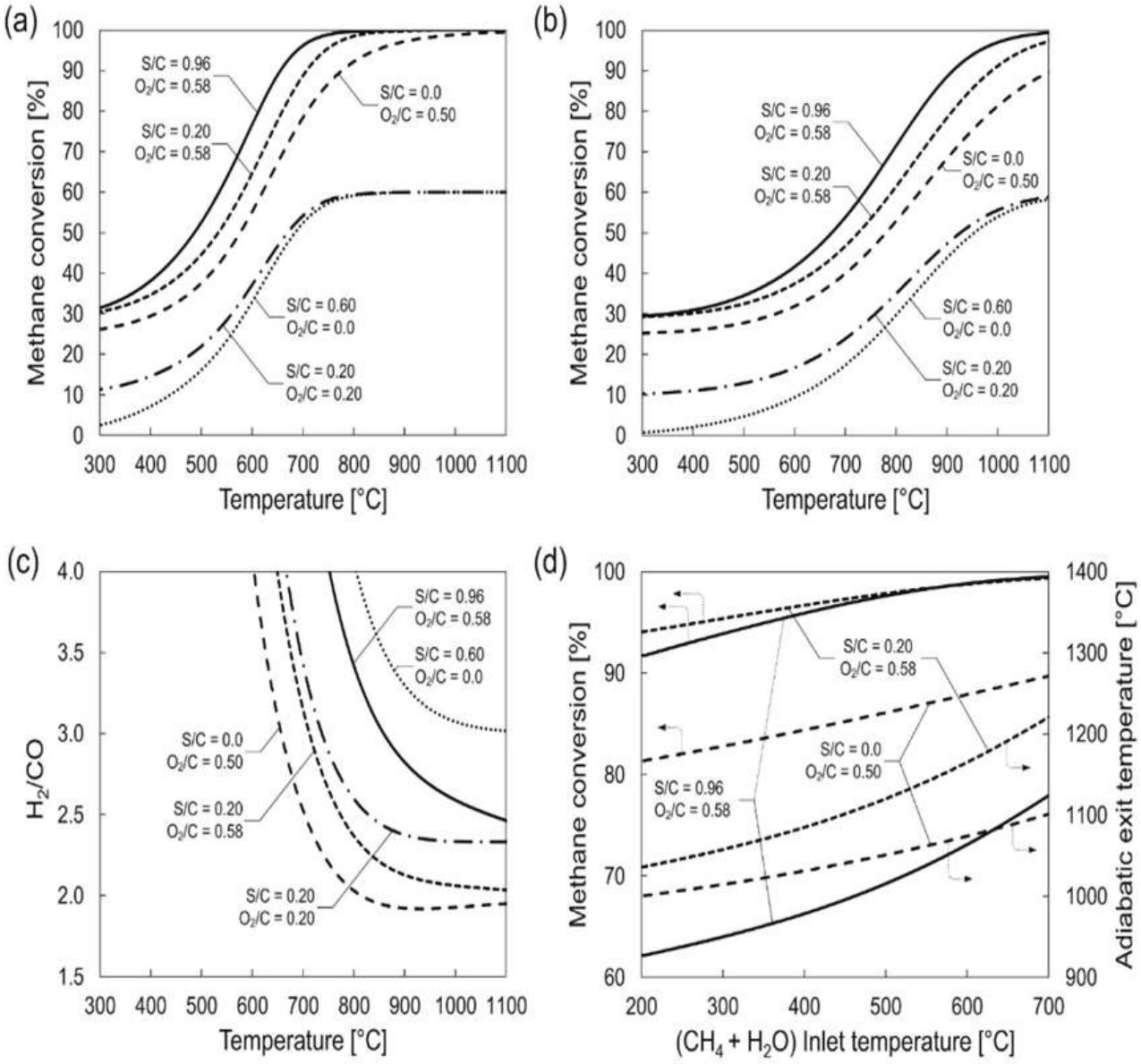

Figure 10. CH_4 reforming as a function of operating variables: Effect of S/C and O_2/C ratios on methane conversion as a function of constant exit reactor temperature at (a) 1 bar and (b) 25 bar, (c) Syngas H_2/CO ratio at 25 bar; (d) Effect of inlet temperature on adiabatic exit temperature and conversion at 25 bar, T =220 ºC for O_2. Reprinted with permission from Reference [210]. Copyright 2014, Elsevier.

4.2 POM Reaction Mechanism

Partial oxidation of methane is reported to follow two mechanisms [16]: (1) Indirect mechanism includes total CH_4 combustion and CO_2/H_2O reforming as shown in figure 8, which is called combustion and reforming reaction mechanism "CRR". (2) A direct mechanism as in figure 8, which involves methane decomposition and oxidation to CO and H_2, which is called direct partial oxidation mechanism "DPO".

In "CRR", initially, part of methane reacts with oxygen to produce CO_2 and H_2O as shown in figure 8. Afterward, CH_4 is reformed by CO_2/H_2O to produce syngas [3]. Evidenced by experiment, hot spots were reported at the front of the catalyst during POM over Ni/MgO catalyst [3]. In that case, this indicates a high exothermic reaction followed by an endothermic reaction which implies that the CRR mechanism has taken place. An additional observation from the CRR mechanism that initially CO_2 is produced with no trace of CO, afterward, CO_2 concentration is decreased and CO is produced at the same time. Furthermore, CRR explains the observation of increased CO_2 and H_2O production at the expense of syngas at high reactant flow rates or high CH_4/O_2 ratio. It should be noticed that Ni and noble metals catalysts in their oxidized forms are reported to enhance indirect CH_4 conversion to syngas via CO_2 and steam reforming [18]. Conversely, the direct partial oxidation mechanism involves CH_4 dehydrogenation and oxidation to CO as proposed initially by Heckman and Schmidt [211]. The following sets of equations (19-34) show the elementary steps of methane steam, dry reforming and POM :

Steam reforming:

$$CH_{4(g)} + \square \rightarrow CH_{4-x(S)} + xH_{(s)}, where\ x\ is\ 1,2,3,4 \quad (19)$$

$$H_2O_{(g)} + \square \rightarrow H_{2(g)} + O^*_{(S)} \ (20)$$

$$CH_{4-x(S)} + O^*_{(S)} \rightarrow CO_{(s)} + 4 - x\ H_{(s)} \ (21)$$

$$CO_{(s)} \rightarrow CO_{(g)} + \square \ (22)$$

$$2H_{(s)} \rightarrow H_{2(g)} (23)$$

Dry reforming:

$$CH_{4(g)} + \square \rightarrow CH_{4-x(S)} + xH_{(s)}, where\ x\ is\ 1,2,3,4 \ (24)$$

$$CO_{2(g)} + \square \rightarrow CO_{2(s)} \ (25)$$

$$CO_{2(s)} + \square \rightarrow CO_{(s)} + O^*_{(S)} \ (26)$$

$$CH_{4-x(S)} + O^*_{(S)} \rightarrow CO_{(s)} + 4 - x\ H_{(s)} \ (27)$$

$$CO_{(s)} \rightarrow CO_{(g)} + \square \ (28)$$

$$2H_{(s)} \rightarrow H_{2(g)} (29)$$

Partial oxidation:

$$CH_{4(g)} + \square \rightarrow CH_{4-x(S)} + xH_{(s)}, where\ x\ is\ 1,2,3,4 \ (30)$$

$$O_{2(g)} + 2\square \rightarrow 2O^*_{(S)} \ (31)$$

$$CH_{4-x(S)} + O^*_{(S)} \rightarrow CO_{(s)} + 4 - x\ H_{(s)} \ (32)$$

$$CO_{(s)} \rightarrow CO_{(g)} + \square \ (33)$$

$$2H_{(s)} \rightarrow H_{2(g)} (34)$$

Heckman and Schmidt (1992) showed that on increasing the reactant flow rate, an increase in the synthesis gas selectivity was seen, contrary to the results presented in the literature. These

observations support the proposed mechanism in Equations (30-34) and cannot be readily explained using the CRR mechanism [211].

Regarding the POM mechanism in perovskites catalysts and symmetric membranes, the type of oxygen and oxygen vacancies concentration affect the mechanism of syngas production significantly as mentioned in Sections 3 and 4. In this theme, He et al. suggested that there are two types of oxygen on oxides: surface adsorbed oxygen and bulk lattice oxygen. Surface oxygen contributes to CH_4 complete oxidation to CO_2 and H_2O while lattice oxygen is selective to CO and H_2. Therefore, initially, CO_2 and H_2O are observed during POM reaction, then as surface oxygen is depleted, lattice oxygen diffuses to the surface and thus CO and H_2 are formed [148]. In the same way, Santos et al. investigated the POM mechanism over $LaNi_{1-x}Co_xO_{3-\delta}$. A temperature-programmed surface reaction of CH_4 experiment revealed that both CH_4 and oxygen were adsorbed on the surface resulting in the formation of CO, CO_2 and H_2O [135]. When the temperature was increased, CH_4 and CO_2 consumption rates were observed and consequently, H_2 and CO formation rate increased. It was suggested that two phenomena were present; First oxygen and CH_4 consumption are relatives to combustion and metal re-oxidation. Secondly, syngas was produced by POM and CO_2 reforming and/or steam reforming.

Moreover, in-situ catalyst characterization showed different types of species present including Ni^0, La_2O_3 and NiO. La_2O_3 and NiO species contribute to CH_4 combustion, while Ni^0 contributes to CH_4 dissociation and reforming as shown in Figure 11. A similar conclusion was suggested by Mihai et al. over $LaFeO_3$ catalyst [134]. Furthermore, Luo et al. also reported that during POM over $BaCo_{0.7}Fe_{0.2}Ta_{0.1}O_{3-\delta}$ membrane reactor, oxygen permeation is controlled by the surface exchange, which leads to CO_2 formation and thus CRR [152]. Therefore, in the case of perovskites and symmetric membrane, the surface concentration and oxygen mobility are high, which leads to the combustion reforming mechanism.

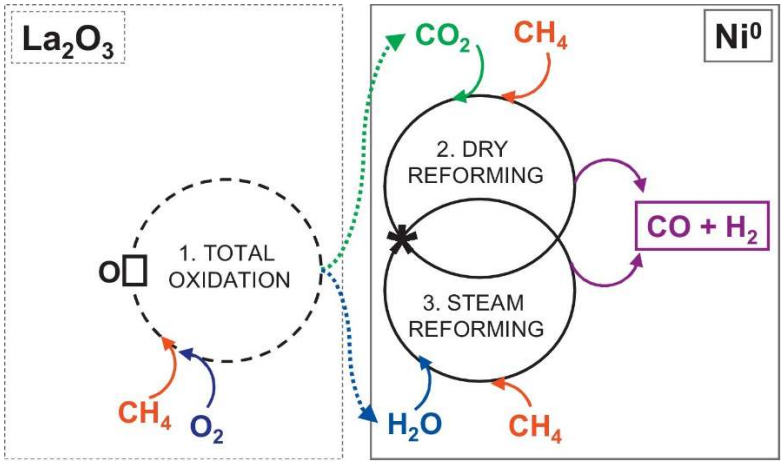

Figure 11. Classical POM kinetics over Ni^0/La_2O_3 catalyst

In agreement with the Luo et al. conclusion on CRR, Richie et al. reported thermodynamic calculations of POM equilibrium which showed only CO_2 formation followed by syngas production as the temperature was increased [186]. Wang et al. observed CH_4 combustion near the membrane surface of $Ba_{0.5}Sr_{0.5}Co_{0.8}Fe_{0.2}O_{3-\delta}$ membrane backed with $LiLaNiO/\gamma\text{-}Al_2O_3$ catalyst. Similar findings were presented by Cihlar et al. The study reported that during POM, La-Co-O perovskite catalyst gave mainly carbon dioxide during the first 30 h of the test [132]. Then the activity changed to give mainly carbon monoxide. Some deactivation was observed during 50 hours test. La-Cr-O produced mainly carbon dioxide. These observations are consistent with the combustion reforming mechanism. Accordingly, the catalytic POM process in membrane reactors likely proceeds through a combustion-reforming pathway when the oxidation of CH_4 to CO_2 and H_2O is followed by the reforming reactions of CH_4 with steam and CO_2 leading to the syngas formation as in figure 8 [165].

For asymmetric membranes with a catalyst layer, catalyst controls the reaction mechanisms since CH_4 does not come in contact with membrane surface in asymmetric membrane reactors. In addition, as mentioned earlier, catalyst activation in the membrane reactor is different from the fixed-bed reactor. This affects the type of active species in POM reaction depending on the catalyst oxidation state in the presence of oxygen flux. Consequently, in asymmetric membrane

reactors, the activity of catalysts in POM is associated with the amount of oxygen adsorbed on the catalyst surface due to constant oxygen flux [137]. A considerable number of reports on POM using membrane reactor with catalyst layer reported CRR mechanism. For example, Wang et al. studied catalyst distribution on $Ba_{0.5}Sr_{0.5}Co_{0.8}Fe_{0.2}O_{3-\delta}$ and concluded that POM mechanism would follow CRR [212]. Similarly, Shen et al. investigated the effect of feed space velocity on CO selectivity on $Ba_{0.5}Sr_{0.5}Co_{0.8}Fe_{0.2}O_{3-\delta}$ membrane reactor coated with Ni/ZrO_2 catalyst [182]. It was suggested that if POM follows DPO mechanism, the high methane flowrate will avoid the full oxidation of methane, and the CO selectivity will increase. However, their results are contrary to this mechanism. In addition, catalyst layer activation is an important step before syngas production in membrane reactors [157, 158]. Therefore, complete combustion was observed on $LiLaNiO_x/\gamma\text{-}Al_2O_3$ backed on $Ba_{0.5}Sr_{0.5}Co_{0.8}Fe_{0.2}O_{3-\delta}$ prior to syngas production similar to observation. It was suggested that the catalyst need to be activated before syngas is produced. It worth mention that due to the delay in catalyst reduction (Ni^0 formation), CO was observed after 5 hours of operations.

Furthermore, Zhan et al. reported a POM mechanism over $La_4Sr_8Ti_{12}O_{38-\delta}$ backed on $Ce_{0.8}Sm_{0.2}O_{2-\delta}$-$La_{0.8}Sr_{0.2}CrO_{3-\delta}$ [179]. Then the reaction mechanism is explored by a comparative study with a conventional fixed-bed reactor, suggesting a direct CH_4 partial oxidation route below 800 ºC and obvious CO_2 and steam reforming activities above 850 ºC. This observation has been confirmed by results of oxidation and reforming of CH_4 in a fixed-bed reactor, as an appreciable yield of syngas was observed before 750 ºC, at which all oxygen is converted. At the same time, both CO_2 and steam reforming of methane may only be possibly initiated after 800 ºC. These facts evidently indicate that the primary products CO and CO_2 are not interconvertible at reaction temperature below 800 ºC. Moreover, the obvious activities of reforming reactions at rather high temperatures greater than 850 ºC, which increases the yield

of CO and H_2 at the expense of the CO_2 yield. This suggests that both direct and indirect mechanisms take effect under this condition.

On the other hand, DPO mechanism was reported only on a few catalysts such as Rh/SiO_2 [3], reduced Ni on $LiLaNiO_x/Al_2O_3$ [132], Ru, Pt and Rh [212]. Therefore, reduced catalyst favors DPO contrary to the oxidized catalyst as reported by Au et al. [213]. Therefore, keeping the catalyst surface in the reduced state is the precondition of high conversion of CH_4 and high selectivity to CO and H_2. In particular, the surface state of the catalyst decides the reaction mechanism and plays a very important role in the conversions and selectivity of partial oxidation of CH_4. In particular, the suitable composition of active and support material leads to the formation of smaller active particles, which are reported to be capable of activating methane at lower temperatures [52].

As an alternative to Heckman et al. proposed a DPO mechanism, the direct partial oxidation of methane (DPO) over the oxide catalyst has been proposed to proceed via the decomposition of the surface formaldehyde intermediate, resulting from the activation of methane by surface lattice oxygen species. On the other hand, CO_2 may be formed by the decomposition of carbonate species, which originated from the further oxidation of the surface intermediate. According to these reaction mechanism schemes, the formation of CO requires less surface lattice oxygen species than CO_2 formation and a lower concentration of gas-phase oxygen results in less full oxidation of the desorbed surface formaldehyde intermediate [179].

Combustion reforming and direct oxidation mechanisms can also occur simultaneously on membrane reactors coated with a catalyst. A few studies reported the co-production of CO and CO_2 at the beginning of POM reaction over membrane reactors. Gu et al. POM studies showed CO production can occur without a catalyst induction period. This may be due to the direct POM mechanism over NiO/Al_2O_3 [178]. Similarly, constant CH_4 conversion and CO

selectivity were reported over time by using NiO/Al_2O_4 catalyst and concluded that the reaction followed the direct partial oxidation mechanism [179]. However, Gu et al. and Kim et al. results, CO_2 was detected over the reaction period indication methane combustion also has taken place. Above all, by proper modification of the catalyst layer on membrane reactor, CH_4 activation and oxidation can be facilitated then the POM mechanism can be altered toward DPO.

5. Membrane Reactor Stability in POM

The applicability of the membrane reactor for POM to syngas is not only determined by catalytic performance (i.e. conversion, selectivity) but also by its stability. Membrane stability is a broad term and can account for several aspects, which have been investigated extensively and reported in the literature. This section mainly discusses membrane stability during POM, which involves harsh and reducing conditions (i.e. presence of reducing gases such as syngas and CH_4, Co and H_2). In this frame, several aspects are overviewed including structural, thermodynamic and chemical stability. In particular, the light will be shed on structure stability, material and catalyst stability during partial oxidation of methane reaction at high temperature.

5.1 Membrane Structure and Thermodynamic Stability

Depending on material type, structure stability may vary during membrane operation which affects oxygen flux and ultimately CH_4/O_2 ratio during POM. Fluorite based membranes are known for their higher stability such as yttria-stabilized zirconia YSZ, Sm-stabilized ceria SDC and Gd-stabilized ceria GDC. However, fluorites membranes have low oxygen permeation flux compared to perovskites [21]. Several studies investigated modifying fluorites for higher oxygen flux in order to benefit from their stability. On the contrary, perovskite membranes have higher oxygen fluxes and lower stability. Several approaches have been considered for developing and improving MIEC membrane structural stability. For instance, the substitution

of Co with Fe or Zn elements in MIEC, however, tends to reduce oxygen flux [214]. Partial substation of B-site by Zr, which gives better stability only in limited compounds [215]. Another option is the introduction of higher valence cation in A or B sites, yet, this approach reduced electronic conductivity and hence oxygen flux [216]. In particular cases partial substitution of A or B sites with larger radius cations, which tends to improve membrane stability without affecting oxygen flux [217]. Furthermore, as mentioned earlier, perovskites stability can be improved by the addition of fluorites such as YSZ, SDC and GDC. Therefore, dual-phase ceramic-ceramic membranes have been reported to be stable during POM at a temperature range of 900-950 ºC [192, 218].

Thermodynamic stability is another important aspect to be taken into account since it affects overall structural stability. A thermal expansion mismatch of membrane materials can lead to thermal stress. Membranes comprise perovskites composites suffer from chemical expansion due to the variation of oxygen partial pressure during POM [219]. This effect arises when B-site cations such as Co or Fe partially reduces, while oxygen vacancies are formed. The ionic radii increases with the decreasing valence state resulting in lattice expansion due to distortion of the oxygen octahedral. The oxygen partial pressure gradient over the membrane leads to a vacancy concentration gradient and consequently in gradients of lattice elongation and mechanical stress respectively [219, 220]. As a result, the membrane may crack eventually accompanied by decomposition [220].

5.2 Stability of Perovskite Catalysts and Membrane Reactors During POM

There are several factors affect the stability of perovskite catalysts and membrane reactor materials during POM, which impact their long term operation and their scale-up process. Herein, we discuss common stability aspects.

5.2.1 Stability in a Reducing Environment

Stability in reducing the environment that contains CH_4, CO, CO_2, H_2, and H_2O gases is an important requirement for the membrane reactors and perovskites catalysts to endure long term operation. During POM, several reducing gases come in contact with membrane surface or catalyst layer (in case of the coated membrane). These gases include CH_4, CO, CO_2, H_2, and H_2O, which cause structural instability and phase change [178, 220]. Among these gases, CO_2 has a great negative impact on membrane operation as it can be absorbed on the surface leading to the formation of a carbonate layer on the surface. The carbonation process is more common with membranes that contain alkaline-earth elements. Based on the Ellingham diagram in Figure 12, Ba and Sr have more stable carbonate and thus membrane with Ba and Sr dopant have more potential to form carbonate layer compared to Ca or La [221].

In addition, Co-containing membranes suffer from poisoning with H_2O, CO and CO_2 due to the weaker Co-O bond compared to Zr-O, Ti-O and Fe-O. Accordingly, substituting Co with elements such as Ti or using A-site Ca/La dopants has improved poisoning tolerance [21]. Several studies reported porous layer formation due to carbonate deposition on the surface during POM [165, 169, 178]. Gu et al. suggested that the formed porous layer increased the surface area of the SCFZ membrane exposed to the reaction side, which would be beneficial to the oxygen permeation through the SCFZ membranes. On the other hand, Wu et al. suggested that when this porous layer was reduced into metal oxides, such as Fe_3O_4 [188]. Consequently, oxygen permeation flux should begin to decrease again because the perovskite structure on a new permeate-side surface begins to be destructed. The acidic environment is another issue that encounters membrane reactors especially sulfur-containing feed.

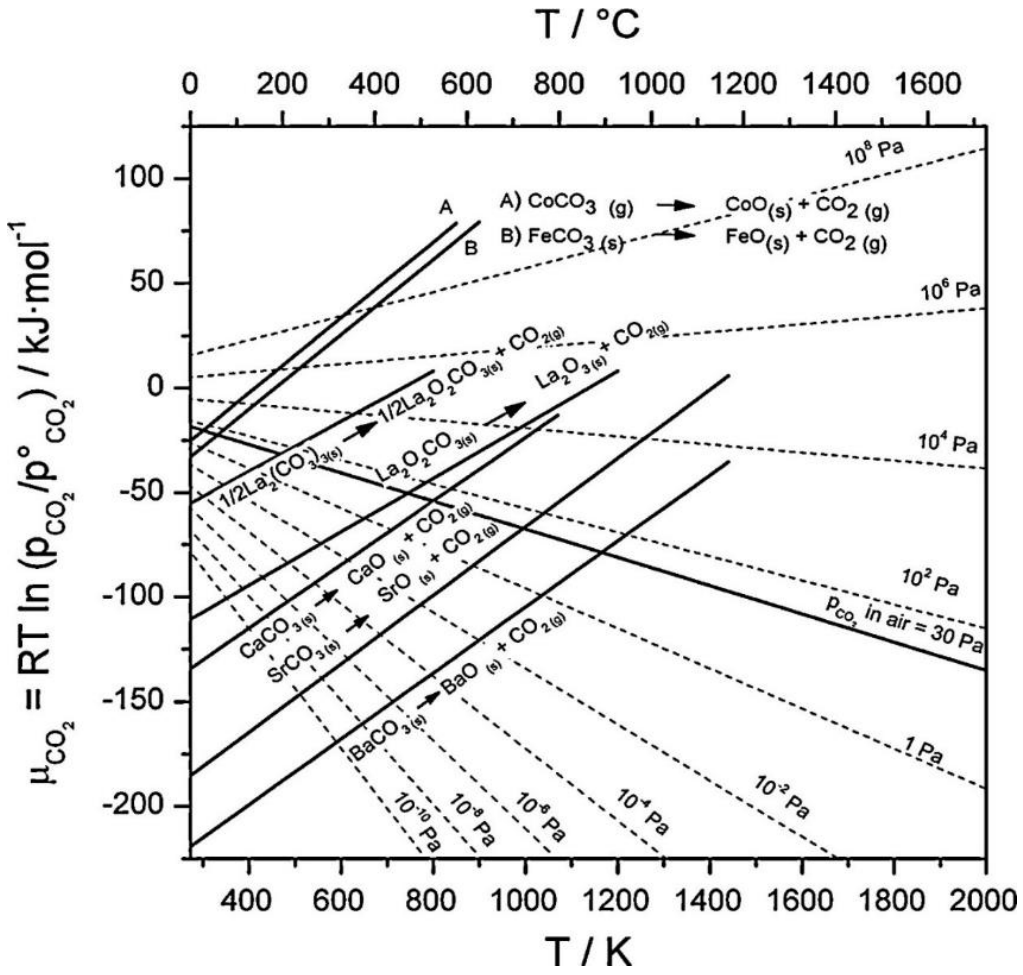

Figure 12. Ellingham diagram for the decomposition of common perovskites elements (CO, Fe, La, Ba, Sr, Ca) under different CO_2 partial pressures and operating temperatures. Reprinted with permission from Reference [221]. Copyright 2012, Elsevier.

Membranes contain Zr and La elements have more potential to form their sulfur compounds due to their low heat of formation (-1260, -1205 kJ.mol^{-1} respectively) compared to Ba and Sr, which have relatively higher heat of formation (-406 and -472 kJ.mol^{-1} respectively), hence membranes doped with Ba and Sr are more stable in the environment with acidic gases [221, 222].

Apart from elements doping, membrane stability during POM can be improved by re-designing the membrane reactor configuration. For instance, the tubular membrane module has higher stability in the presence of reducing gases such as CO, CO_2, H_2O [19, 223-226]. However,

porous layers can be coated on the dense perovskite membranes to improve their stability. As an example, Praxair developed a pilot-scale multi-tubular reactor for syngas production with >1000 hours of stability. A $(La_{0.825}Sr_{0.175})_{0.94}Cr_{0.72}Fe_{0.26}V_{0.02}O_{3-\delta}$-YSZ dense membrane was utilized for oxygen separation, which coated with a porous layer of $(La_{0.8}Sr_{0.2})_{0.98}Mn_{0.02}O_{3-\delta}$-YSZ for reforming reaction. The YSZ porous layer allowed such long term structural stability in the presence of reducing gases. The reactor combines steam and auto-thermal reforming, which provides the required heat for the steam reforming section and consequently reduces the operation cost [226].

5.2.2 Phase Decomposition due to Partial Pressure Gradient

Phase decomposition due to partial pressure gradient is a common issue associated with long term membrane operation. Phase decomposition can occur due to the stress associated with the oxygen chemical potential gradient across the membrane and the variation of reactant/products partial pressure during POM [157]. For instance, perovskite unit cells undergo expansion as a result of the reduction of the transition metals to their larger lower valence ions. In addition, the part of the membrane exposed to higher oxygen flux also decomposes due to the fast mobility of the metal cations in that part as a consequence of the partial pressure gradient [222].

Oxygen partial pressure gradient itself causes metal reduction across the membrane. For example, Pei et al. reported two types of $Sr(Co, Fe)O_3$ membrane failure during POM [227]. It should be noticed that the catalyst layer on the membrane surface also is subjected to this sort of reduction, during which reduced metal acts as active reaction sites [3, 18, 209]. Ten Elshof et al. detected Fe and Co metal phases on $La_{0.6}Sr_{0.4}Co_{0.8}Fe_{0.8}O_{3-\delta}$ membrane during the oxidative coupling of methane [215]. Pei et al. reported Fe/Co phases on $Sr(Co,Fe)O_3$ membrane surface [227]. As well, Luo et al. reported that BCFT membrane surface in contact with syngas was eroded significantly and large amounts of small particles were observed [152].

It should be pointed that, Co-containing perovskites are known as one of the most reducible perovskites, and the cobalt extraction by reduction of cobalt cations from the "precursor" perovskite to generate Co-enriched surface phases has been reported as well. In this case, due to the reducing atmosphere (synthesis gas), cobalt cations in the perovskite BCFT lattice might be partly reduced, leading to the formation of Co-enriched particles on the membrane surface exposed to synthesis gas. These findings indicate that a strongly reducing atmosphere (H_2, CO and CH_4) and eroding gases such as steam and CO_2 have a negative effluence on the membrane stability during the POM to syngas [228]. Furthermore, TPR analysis indicated that for membrane, second reduction peaks at high temperature (500-800 ºC) is due to a partial reduction of Fe^{+3} to Fe^{+2}/Fe^0 and Co^{+2} to Co^0 [113]. These results are in agreement with the detection of reduced metal phase on the membrane surface during POM at a high temperature. It worth mentioning that partial substitution of B-site with different metals combinations can enhance phase stability as indicated by Cihlar et al. (Figure 13) [132].

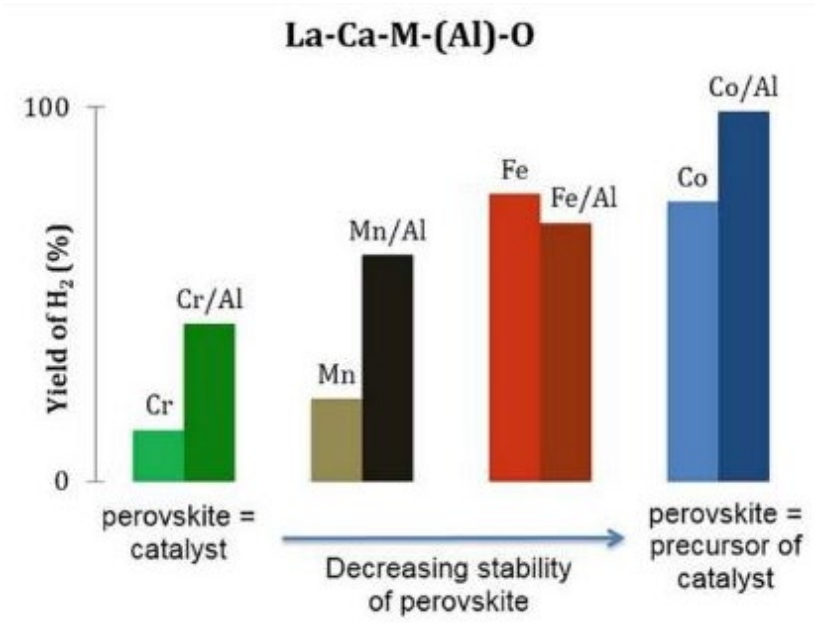

Figure 13. Effect of partial substitution on stability and H_2 yield of La-Ca-M-(Al), where M= Cr,Mn,Fe orCo. Reprinted with permission from Reference [132]. Copyright 2017, Elsevier.

In general, the presence of reduced metal phases or metal oxides due to phase change can affect the POM reaction mechanism and syngas selectivity. For example, following to perovskite $LaNi_{1-x}Co_xO_3$ perovskite decomposition to La_2O_3 and NiO in POM, increased CO_2 formation was reported by De Santana Santos et al. In addition, the presence of reduced metal phases such as Ni can also lead to carbon deposition [3, 153, 169].

5.3 Carbon Deposition

Carbon deposition is a significant issue regarding the practical application of catalytic POM. It should be noticed that carbon deposition can occur with or without having a catalyst layer on the membrane surface. In the case of catalyst coating on the membrane surface, the catalyst layer should be designed to resist carbon deposition. Some catalysts have been reported to have a higher tendency toward carbon deposition (Table 10) such as Ni-based catalyst [3, 18, 169]. This is due to the presence of reduced active metal phases on the catalyst surface. Similarly, as mentioned in the previous section, membrane surface can be reduced in the presence of syngas, and CH_4 (Equations 35 and 36) This reduction leads to reduced metal phase on the membrane surface, which also can result in carbon deposition on membrane surface similar to catalyst active phases. In addition, as reported earlier, POM can follow the combustion reforming mechanism or direct partial oxidation mechanism. In either case, carbon deposition can occur according to the below reactions [3, 229]:

$$CH_4 \leftrightarrow C + 2H_2\ , \Delta H^o_{298} = 75\ kJ.mol^{-1} (35)$$

$$2CO \leftrightarrow C + CO_2\ , \Delta H^o_{298} = -171\ kJ.mol^{-1} (36)$$

Table 10. Carbon formation over catalysts after stoichiometric methane partial oxidation at 1 atm and 777 ºC (all experiments were run for 24 h, except the Ni catalysts 150 min). Reproduced with permission from reference [3]. Copyright 2003, Elsevier.

Catalyst active metal	1% Ir	1% Ru	1% Pt	1%Rh	5%Ru	5%Rh	5%Pt	5%Ni
Carbon formation (mg/g_{cat})	0	0.35	0	0.24	0.6	0.1	7	21

Several studies on membrane POM reported carbon formation on membrane/catalyst surface. Kharton et al. compared $SrFe_{0.7}Al_{0.3}O_{3-\delta}$ and Pt/SiO_2 catalysts coated on $La_{0.3}Sr_{0.7}Co_{0.8}Ga_{0.8}O_{3-\delta}$ membrane [162]. The $SrFe_{0.7}Al_{0.3}O_{3-\delta}$ catalyst showed no carbon deposition contrary to Pt/SiO_2 at high temperature. This can be attributed to the prevention of phase change as XRD inspection showed that $SrFe_{0.7}Al_{0.3}O_{3-\delta}$ perovskite phase in the catalyst was kept essentially unchanged (i.e. no metal phases detected on catalyst surface). Similarly, Palcheva et al. reported no carbon deposition during methane pulses on contrary to Rh/Ga catalysts [142]. This observation is in agreement with Li et al. conclusion, which reports that the reason for POM catalyst deactivation was that the coke accumulating on Ni^0 grain surface after LiLaNiO/g-Al_2O_3 catalyst activation and reduction. Zhu et al. also detected graphite formation on membrane surface after implementation of LiLaNiO/Al_2O_3 catalyst.

In the same manner, carbon deposition occurring for perovskite $La_4Sr_8Ti_{12}O_{38-\delta}$ was much less serious than that for the Ni-based catalyst after testing for 100 h in the membrane reactor at 950 ºC and CH_4 feed rate of 20 $mL.min^{-1}$. However, in this case, $La_4Sr_8Ti_{12}O_{38-\delta}$ perovskites catalyst was reported to be reduced to oxides phases which contribute to CH_4 decomposition and CO_2 formation [180]. D.S Santos et al. reported that $LaNi_{0.8}Co_{0.2}O_3$ was reduced during

TPSR, resulted in several phases. These phases produced reaction products such as CO_2 and syngas by CH_4 decomposition. The activity of these phases in methane decomposition was in the order: $Ni_{0.8}Co_{0.2}/La_2O_3 \geq Ni/La_2O_3 > Ni_{0.5}Co_{0.5}/La_2O_3 > Co/La_2O_3$.

5.4 Stability of Membrane Catalyst Layer in the Asymmetric Membrane Reactor

Catalyst layer stability is important for syngas selectivity as well. Similar to membrane material, the catalyst layer, which coated on the membrane experiences phase decomposition during POM. During membrane reactors operation, catalysts undergo an induction process before syngas production. Catalyst induction leads to the reduction of metal oxides and consequently phase decomposition. This observation has been reported in many studies on LiLaNiO/γ-Al_2O_3 and NiO/Al_2O_3 catalysts [158, 169, 178]. Similarly, Nguyen et al. showed that $LaNiO_3$ catalyst also undergoes phase decomposition into Ni_0/La_2O_3, which acts as an actual catalyst during POM. Similarly, decomposition of $NdCaCoO_3$ perovskite catalyst to CaO and Nd_2O_3 at a high reaction temperature during POM was reported [137]. Consequently, catalyst phase change can result in undesirable oxides and pure metal phases that can lead to CO_2 formation which ultimately decreases syngas selectivity.

6. Conclusions and Future Perspective

6.1 Conclusions

Natural gas is one important source of syngas, which can be can be converted via partial oxidation. In addition, the discoveries on its resources have been increased recently. Nevertheless, most of the natural gas resources are stranded in remote areas, either onshore or offshore. Therefore, due to their advantages of combining oxygen separation and POM reaction, light-weight MIEC membrane reactors can be designed for remote natural gas resource utilization.

Mixed ionic-electronic conducting perovskite membranes have been an attractive option for catalytic POM due to high oxygen flux. Membrane reactors without catalyst coating showed good performance up to 95% CH_4 conversion and syngas selectivity at 850 ºC to 950 ºC temperature range. This high performance was attributed to the reduction of B-site in its structure. However, despite their excellent performance in catalytic POM, MIEC membranes suffer from instability issues in an environment containing reducing gases such as CH_4, CO and H_2. Accordingly, the development of highly stable MIEC materials is required. On the other hand, in the presence of catalyst layer coated on the membrane reaction side, higher catalytic performance (up to 98% CH_4 conversion and 99% syngas selectivity) was achieved. Yet, in both cases, the required temperature for high catalytic activity for POM was between 850 ºC and 950 ºC. Consequently, since one of the disadvantages of steam reforming is energy consumption, membrane reactors operation in POM at a high temperature can lead to the same situation.

One factor controlling the performance is the REDOX behavior of membrane material, which in some cases requires high temperature for B-site reduction such as Fe. In addition, most of the studies on POM using membrane reactors suggest the indirect CH_4 conversion route (via dry or steam reforming) is dominant over long contact time. The endothermic nature of dry or steam reforming reaction may explain the requirement for high temperature for syngas production. Therefore, it is beneficial to develop a membrane system to produce syngas via DPO route, which requires lower energy as DPO is an exothermic reaction.

As well as membrane REDOX properties, membrane/catalyst oxidation state and morphology during POM plays an important role. The catalyst or membrane oxidation leads to the formation of undesired species that affect catalytic activity. These oxides/metal phases contribute to lowering syngas production and carbon deposition as well as affecting the POM mechanism.

In addition, membrane reactors still showing other stability issues in partial oxidation reaction such as soot formation on the reaction side.

Given the factors mentioned above, there is still room for developing and improvement of membrane reactors for better POM performance. Thus, one important factor to be considered is catalyst/membrane status during continuous reduction-oxidation induced by oxygen flux and POM reaction. This phenomenon can be observed on the membrane reaction side. Furthermore, it should be taken into account that POM effects oxygen flux in two ways: (1) oxygen consumption by CH_4 lower its partial pressure, which increases the permeation rate. (2) The reducing chemicals such as CO, CH_4, and H_2 react with membrane surface oxygen which also affects the permeation rate.

6.2 Future Prospective

6.2.1 Understanding POM Mechanism in Membrane Reactors

In Section 4.2, several studies reporting POM mechanism in membrane reactors were mentioned, however deep understanding of the factors controlling the mechanism is yet to be established. The reported studies suggest that indirect syngas production via CRR mechanism in membrane reactors is more dominant than direct partial oxidation. However, there are also evidences that DPO and CRR mechanism may occur simultaneously as indicated earlier in Section 4.2.

Emphasizing DPO mechanism benefits membrane operation in term of operating temperature since DPO is mildly exothermic. Although many factors can affect the POM mechanism, in this section, we cast some light on catalyst layer behavior in case of membrane coated with a catalyst. POM in membrane reactors is different from the fixed bed reactor due to continuous oxygen flux and the nature of oxygen transport in MIEC membranes. Continues oxygen flux induces continuous REDOX cycles during oxygen transportation, which affect catalyst state in

case of membranes with a catalyst layer. Consequently, CH_4/O_2 ratio is determined by the catalyst state, which is constant in fixed bed reactors. On the other hand, due to partial pressure variation across the membrane, oxygen flux changes and thus CH_4/O_2 and catalyst active species are changed consequently in continuous REDOX cycles (Figure 14) [18, 157, 208]. Furthermore, to improve membrane/catalyst activity, it is crucial to understanding membrane reactors involve several types of active sites (oxygen vacancies, reduced metals sites, and oxidized metals phases).

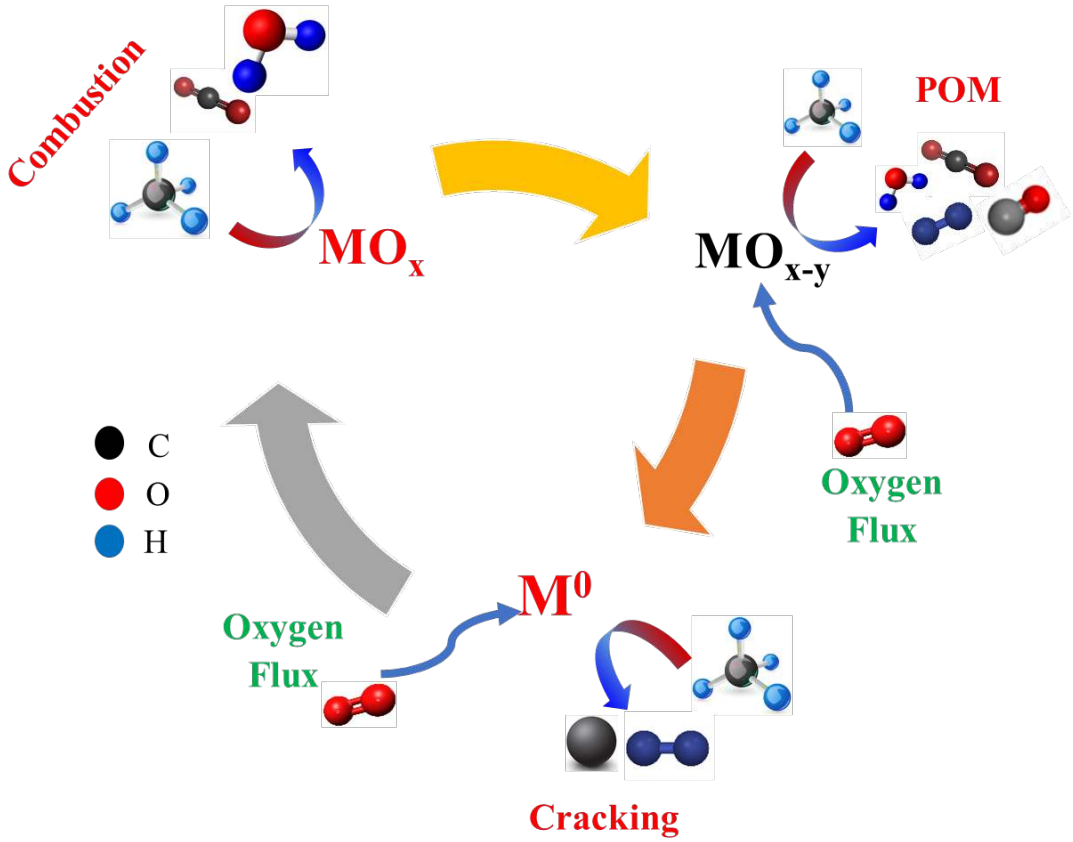

Figure 14. Catalyst continuous reduction-oxidation cycles during POM in a membrane reactor (M^0: reduced, MO_{x-y} : partially oxidized, MO_x : fully oxidized)

6.2.2 Taking Advantages of Oxygen Vacancies in POM Membrane Reaction

As discussed in Section 3.5, the desorption of adsorbed oxygen is responsible for CH_4 combustion, while bulk lattice oxygen favors CH_4 partial oxidation to CO and H_2 [230, 231]. Moreover, some oxides such as CeO_2 were reported to play a vital role in oxygen activation during reaction with methane and enhances catalyst activity [52]. Nonstoichiometric structure of cerium oxide expressed as CeO_{2-x}, with high oxygen release and storage properties, enhances reversible activation of oxygen in CeO_{2-x} lattice, and this oxygen activates methane. In particular, oxygen vacancies can act as active sites for O−O bond cleavage [232, 234]. Activated oxygen species such as in superoxo state (O_2^-), or peroxo state (O_2^{2-}) tend to partially oxidize methane following to its activation according to Equations 37 and 38:

$$CH_4 + O^* + 2e' \rightarrow CO_{(g)} + H_{2(g)} + O_{\square} + 2e' \quad (37)$$

$$O_{\square} + \frac{1}{2}\, O_{2\,(g)} + 2e' \rightarrow O^* \quad (38)$$

Accordingly, oxygen vacancies concentration can lead to the formation of different types of active sites, which can enhance syngas formation via DPO. Hence, the coating of the membrane reactor with a catalyst layer comprises a suitable combination of active sites and oxygen vacancies is beneficial for POM reaction. In this regard, Based on the catalyst reduction degree, it can be concluded that there are different surface domains (active sites) leading to CO_2, CO or C formation [132]. These domains cannot be assigned to specific metal sites responsible for catalytic properties in the perovskite, but the oxygen coordination with the surface atoms. Mihai et al. suggested three types of domains in $LaFeO_3$ perovskite catalyst, Mihai 2012, which are defined as Fe^{I}, Fe^{II}, Fe^{III} [132]. Fe^{I} active sites with high O coordination correspond to CO_2 formation, while Fe^{II} sites with moderate O coordination correspond to CO and H_2 formation. The Fe sites with low coordinated O (i.e. Fe^{III}) lead to carbon formation. The rate of carbon formation increases remarkably with increasing O vacancy (Figure 15). Thus, the

nature of the active sites is highly dynamic, and oxygen close to the Fe sites plays an important role in surface kinetics. Fe^{III} sites are responsible for the carbon formation from either methane dissociation and/or Boudouard reaction. The reduction in the reaction rate at a relatively high amount of O removed could be either the consequence of less O available or carbon covering the active sites.

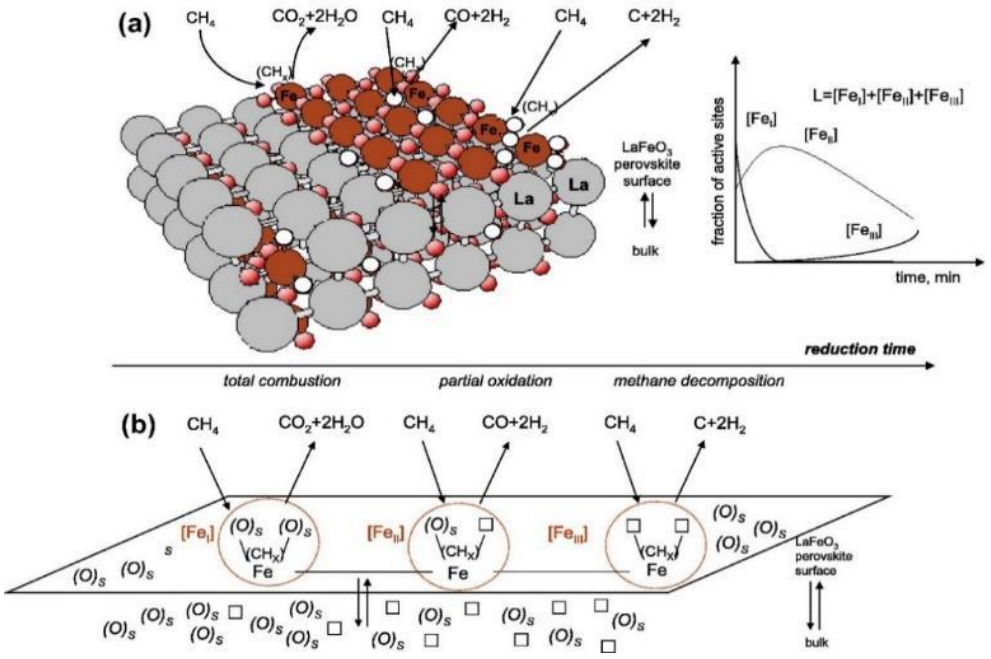

Figure 15. (a) Schematic illustration of the $LaFeO_3$ (100) perovskite surface. (b) Simplified scheme of the total combustion, partial oxidation, and methane decomposition on different active sites of $LaFeO_3$ perovskite. O_s – Surface oxygen species, $O_{\square}$ – oxygen vacancy, L – number of total active sites on the surface. Reprinted with permission from Reference [132]. Copyright 2012, Elsevier.

Hence, POM can be affected by the presence of oxygen vacancies in term of adsorption and activation of oxygen which is consumed in oxidization of activated methane [235]. Since these oxygen vacancies are inherent in MIEC membrane, membrane reactors can be designed to operate with the DPO mechanism.

6.2.3 Bridging Electronic Properties with Catalytic POM Reaction

Defining the relationship between membrane/catalyst electronic properties (ionic and electronic conductivity, formation/migration of oxygen vacancies, oxygen binding to membrane and catalyst surface) and the catalytic performance would provide a fundamental understanding of POM in membrane reactors. Electronic properties were reported to give insight about catalytic activity trends, and even mechanistic insights for reactions involving O_2 activation such as oxygen evolution reaction [223, 234]. Electronic properties such as charge transfer affect surface-oxygen bonding and therefore, dictate the activity of oxidation reactions. Additionally, as we pointed out the importance of oxygen vacancies for oxygen activation for the oxidation reaction. The formation of these oxygen vacancies is related to the electronic structure of oxides and oxygen binding in the structure (Figure 16)[233, 235]. This also affects the oxidation rate of CH_4 and ultimately syngas formation in membrane reactors [236]. Similarly, the charge transfer between Pt and the support in Pt/Tin catalyst was reported to affect metal-support interaction and Pt optimum loading, which ultimately affect overall activity [237].

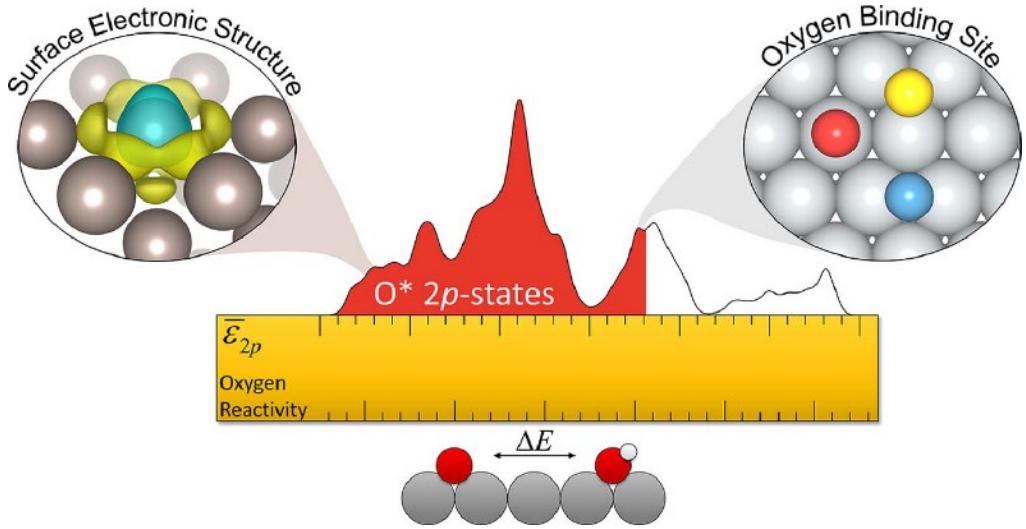

Figure 16. Oxygen reactivity dependence on the surface electronic structure. Reprinted with permission from reference [235]. Copyright 2015, Elsevier.

Furthermore, in order to highlight the importance of electronic properties in catalysis, here we take CO oxidation over perovskites catalysts as an example. In this vein, studying perovskites molecular orbits descriptors gave more insights regarding the nature of the metal-oxygen bond in the perovskite structure. Metal-oxygen bond nature provides a basis for tuning perovskite electronic structure to control oxygen-binding energetics on the catalyst surface. Since CO oxidation can be considered as a template reaction for the oxidation of other hydrocarbons such as CH_4, the energetics of surface carbon and surface-oxygen bonding can similarly dictate the activity of these reactions[237].

7. Funding Details

This work was supported by the Australian Research Council (ARC) under the discovery project DP160104937.

8. Acknowledgment

We acknowledge the scientific and technical assistance of the Australian Microscopy and Microanalysis research facility at the University of Queensland. We acknowledge the financial support from the University of Queensland Graduate School Research Training Scholarship.

9. Appendix: Notation

Abbreviations

ATR Auto-thermal reforming

CPOM Catalytic partial oxidation of methane

CRR Combustion reforming reaction

DMR Dry Methane Reforming

DPO Direct partial oxidation

EDS Energy-dispersive x-ray spectroscopy

MIEC Mixed ionic-electronic conducting membranes

POM Partial oxidation of methane

REDOX Reduction oxidation cycles

SMR Steam Methane Reforming

SCT-CPO Short contact time catalytic partial oxidation

STEM Scanning transmission electron microscopy

TON Turnover number per minuet

TPD Temperature-programmed desorption

TPR Temperature-programmed reduction

TPSR Temperature-programmed surface reaction

Symbols

□ Reaction site

ΔH^{o}_{298} Heat of reaction at 298 K

CH_x Activated methane molecule (i.e. x= 1,2, or 3)

e' Electron

h' Free electron hole

h Hours

L Number of total active sites on the catalyst surface

M^0 Reduced metal active site

min Minuets

MO_x Metal oxide

MO_{x-y} Reduced metal oxide

$O_{\square}$ Oxygen vacancy

O^{2-} Activated oxygen in peroxo state

O_2^{2-} Activated oxygen in superoxo state

O^* Activated oxygen

O_2/C oxygen to methane ratio

Po Oxygen partial pressure at air side

Po_2 Oxygen partial pressure at reaction side

sec Seconds

S/C Steam to methane ratio

SH_2 H_2 selectivity

SCO CO selectivity

T Temperature

WGS Water-gas shift reaction

XCH_4 Methane conversion

Subscripts

aq Aqueous

g Gas phase species

s Surface adsorbed species

x,y,z Ratios of perovskite components in A or B sites

10. References

[1] Aasberg-Petersen,K.; Dybkjær,I.; Ovesen, C.V.; Schjødt, N.C.; Sehested, J.; Thomsen, S.G. Natural gas to synthesis gas – Catalysts and catalytic processes, *J. Nat. Gas Sci. Eng.* 3, **2011**, 423-459. https://doi.org/10.1016/j.jngse.2011.03.004

[2] Ghoneim, S.A.; El-Salamony, R.A.; El-Temtamy, S.A. Review on Innovative Catalytic Reforming of Natural Gas to Syngas. *World Journal of Engineering and Technology.* **2016**, 4, 116-139. DOI: 10.4236/wjet.2016.41011

[3] Andrew, T.X.; York, P.E.; Malcolm, L.H. Green, Brief overview of the partial oxidation of methane to synthesis gas. *Top. Catal.* **2003** , 22, 345-358. https://doi.org/10.1023/A:1023552709642

[4] Kalamaras, C.M.; Efstathiou, A.M.; Hydrogen Production Technologies: Current State and Future Developments. *Conference Papers in Energy*. **2013**, 1-9. http://dx.doi.org/10.1155/2013/690627

[5] Rostrupnielsen, J.R.; Hansen, J.H.B. CO_2-Reforming of Methane over Transition Metals, *J. Catal.* **1993**, 144, 38-49. https://doi.org/10.1006/jcat.1993.1312

[6] Ahmed , B.; Gadalla, M. The role of catalyst support on the activity of nickel for reforming methane with CO_2. *Chem. Eng. Sci.* **1988** ,43, 3049-3062. https://doi.org/10.1016/0009-2509(88)80058-7

[7] Kumar, N.; Shojaee, M.; Spivey, J. Catalytic bi-reforming of methane: from greenhouse gases to syngas. *Current Opinion in Chemical Engineering.* **2015**, 9:8–15. https://doi.org/10.1016/j.coche.2015.07.003

[8] Olah, G.A.; Goeppert, A.; Czaun, M.; Mathew, T.; May, R.; Surya Prakash G. K. Single Step Bi-reforming and Oxidative Bi-reforming of Methane (Natural Gas) with Steam and Carbon Dioxide to Metgas ($CO\text{-}2H_2$) for Methanol Synthesis: Self-Sufficient Effective and Exclusive Oxygenation of Methane to Methanol with Oxygen. *J. Am. Chem. Soc.* **2015**, 137, 27, 8720-8729. https://doi.org/10.1021/jacs.5b02029

[9] Velasco, J.A.; Lopez, L.; Cabrera, S.; Boutonnet, M.; Järås, S. Synthesis gas production for GTL applications: Thermodynamic equilibrium approach and potential for carbon formation in a catalytic partial oxidation pre-reformer. *J. Nat. Gas Sci. Eng.* **2014**, 20, 175-183. https://doi.org/10.1016/j.jngse.2014.06.021

[10] Zhan, M.-C.; Wang, W.-D.; Tian, T.-F.; Chen, C.-S. Catalytic Partial Oxidation of Methane over Perovskite $La_4Sr_8Ti_{12}O3_{8-\delta}$ Solid Oxide Fuel Cell (SOFC) Anode Material in an Oxygen-Permeable Membrane Reactor. *Energ. Fuels.* **2010**, 24, 764-771. https://doi.org/10.1021/ef900995t

[11] Ji, Y.; Li W.; Xu, H.; Chen, Y. Catalytic partial oxidation of methane to synthesis gas over Ni/Al_2O_3 catalyst in a fluidized-bed, *Appl. Catal., A.* **2001**, 21, 325-31. https://doi.org/10.1016/S0926-860X(00)00887-5

[12] Bharadwaj, S.S.; Schmidt, L.D. Synthesis gas formation by catalytic oxidation of methane in fluidized bed reactors, *J. Catal.* **1994**, 146, 11-21. https://doi.org/10.1016/0021-9517(94)90003-5

[13] Bhavsar, S.; Veser, G. Chemical looping beyond combustion: production of synthesis gas via chemical looping partial oxidation of methane, *RSC Adv.* **2014**, 4, 47254-47267. DOI: 10.1039/c4ra06437b

[14] Kang, D.; Lee, M. ; Lim, H.S. ; Lee, J.W. Chemical looping partial oxidation of methane with CO_2 utilization on the ceria-enhanced mesoporous Fe_2O_3 oxygen carrier, *Fuel.* **2018** , 215, 787-798. https://doi.org/10.1016/j.fuel.2017.11.106

[16] Enger, B. C. ; Lødeng, R. ; Holmen, A. A review of catalytic partial oxidation of methane to synthesis gas with emphasis on reaction mechanisms over transition metal catalysts, *Appl. Catal., A.* **2008**, 346, 1-27. https://doi.org/10.1016/j.apcata.2008.05.018

[17] Zhang, J.; He, T.; Wang, Z.; Zhu, M.; Zhang, K.; Li, B.; Wu, J. The search of proper oxygen carriers for chemical looping partial oxidation of carbon, *Appl. Energy.* **2017**, 190, 1119-1125. https://doi.org/10.1016/j.apenergy.2017.01.024

[18] Caro, .; Wang, H.H.; Tablet, C.; Kleinert, A.; Feldhoff, A.; Schiestel, T.; Kilgus, M.; Koelsch, P.; Werth, S. Evaluation of perovskites in hollow fibre and disk geometry in catalytic membrane reactors and in oxygen separators. *Catal. Today.* **2006**, 118, 128–135. https://doi.org/10.1016/j.cattod.2005.12.015

[19] Wang, Z.; Li, Z.; Cui, Y.; Chen, T.; Hu, J.; Kawi, S. Highly Efficient NO Decomposition via Dual-Functional Catalytic Perovskite Hollow Fiber Membrane Reactor Coupled with Partial Oxidation of Methane at Medium-Low Temperature, *Environ. Sci. Technol.* **2019**, 53, 16, 9937-9946. https://doi.org/10.1021/acs.est.9b02530

[20] Shelepova, E.; Vedyagin, A.; Sadykov, V.; Mezentseva, N.; Fedorova, Y.; Smorygo, O.; Klenov, O.; Mishakov, I. Theoretical and experimental study of methane partial oxidation to syngas in catalytic membrane reactor with asymmetric oxygen-permeable

membrane, *Catal. Today.* **2016,** 268, 103-110. https://doi.org/10.1016/j.cattod.2016.01.005

[21] Sunarso, J.; Baumann, S.; Serra, J.M. ; Meulenberg, W.A. ; Liu, S.; Lin, Y.S. ; Diniz da Costa, J.C. Mixed ionic–electronic conducting (MIEC) ceramic-based membranes for oxygen separation. *J. Membr. Sci.* **2008**, 320, 13-41. https://doi.org/10.1016/j.memsci.2008.03.074

[22] Prettre, C.E. M. ; Perrin, M. The catalytic oxidation of methane to carbon monoxide and hydrogen, *J. Chem. Soc. Faraday Trans.* **1946**, 42, 335-339. DOI: 10.1039/TF946420335B

[23] Rostrup-Nielsen, J.R. Production of synthesis gas. *Catal.Today.* **1993**, 18, 305-324. https://doi.org/10.1016/0920-5861(93)80059-A

[24] Wang, H.Y. ; Ruckenstein, E.R. Conversions of Methane to Synthesis Gas over Co/γ-Al_2O_3 by CO_2 and/or O_2. *Catal. Lett.* **2001** ,75, 13-18. https://doi.org/10.1023/A:1016719703118

[25] Marnasidou, K.G.; Voutetakis, S.S.; Tjatjopoulos, G.J.; Vasalos, I.A.Catalytic partial oxidation of methane to synthesis gas in a pilot-plant-scale spouted-bed reactor. *Chem. Eng. Sci.* **1999**, 54, 3691-3699. https://doi.org/10.1016/S0009-2509(98)00455-2

[26] Sokolovskii, V.D.; Jeannot, J.C.; Coville, N.J.; Glasser, D.; Hildebrandt, D.; Makoa, M. High yield syngas formation by partial oxidation of methane over Co-alumina catalysts, *Stud. Surf. Sci. Catal.* **1997**, 107, 461-465. https://doi.org/10.1016/S0167-2991(97)80377-1

[27] Choudhary, V.R.; Sansare, S.D.; Mamman, A.S. Low-temperature selective oxidation of methane to carbon monoxide and hydrogen over cobalt-MgO catalysts. *Appl. Catal., A.* **1992**, 90, 1-5. https://doi.org/10.1016/0926-860X(92)80242-5

[28] Wang, H.Y.; Ruckenstein E. Partial Oxidation of Methane to Synthesis Gas over Alkaline Earth Metal Oxide Supported Cobalt Catalysts. *J. Catal.* **2001,** 199, 307-317. https://doi.org/10.1006/jcat.2001.3190

[29] Ding, C.; Ai, G.; Zhang, K. ;Yuan, Q.; Han, Y. ;Ma, X.; Wang, J.; Liu, S. Coking resistant Ni/ZrO_2@SiO_2 catalyst for the partial oxidation of methane to synthesis gas. *Int. J. Hydrog. Energy.* **2015**, 40, 6835-6843. https://doi.org/10.1016/j.ijhydene.2015.03.094

[30] Iwasakia, Na-o.; Miyake, T.; Yagasakib, E.; Suzuki, T. Partial oxidation of ethane to synthesis gas over Co-loaded catalysts. *Catal.Today.* **2006**, 111, 391-397. https://doi.org/10.1016/j.cattod.2005.10.050

[31] Nishimoto, H.; Nishimoto, K.N.; Ikenaga, N.; Nishitani-Gamo, M.; Ando, T. Toshimitsu Suzuki, Partial oxidation of methane to synthesis gas over oxidized diamond catalysts, *Appl. Catal. A.* **2004**, 264, 65-72. https://doi.org/10.1016/j.apcata.2003.12.029

[32] Choudhary, V.R.; Rajput, A.M.; Prabhakar, B.; Mamman, A.S. Partial oxidation of methane to CO and H_2 over nickel and/or cobalt containing ZrO_2, ThO_2, UO_2, TiO_2 and SiO_2 catalysts, *Fuel.* **1998**, 77, 1803-1807. https://doi.org/10.1016/S0016-2361(98)00072-6

[33] Fakeeha, A.H.; Arafat, Y.; Ibrahim, A.A.; Shaikh, H.; Atia, H.; Abasaeed, A.E.; Armbruster, U.; Al-Fatesh, A.S. Highly Selective Syngas/H_2 Production via Partial Oxidation of CH_4 Using (Ni, Co and Ni–Co)/ZrO_2–Al_2O_3 Catalysts: Influence of Calcination Temperature. *Processes.* **2019**, 7 (144). https://doi.org/10.3390/pr7030141

[34] Swaan, H.M.; Widyananda, P.; Mirodatos, C. Partial oxidation of methane over nickel- and cobalt-based catalysts. *Stud. Surf. Sci. Catal.* **1997**, 107, 447-453. https://doi.org/10.1016/S0167-2991(97)80375-8

[35] Tang, S.; Lin, J.; Tan, K.L. Partial oxidation of methane to synthesis gas over α-Al_2O_3-supported bimetallic Pt–Co catalysts. *Catal. Lett.* **1999**, 59, 129–135. https://doi.org/10.1023/A:1019001428159

[36] Moral, A.; Reyero, I.; Llorca, J.; Bimbela, F.; Gandía, L.M. Partial oxidation of methane to syngas using Co/Mg and Co/Mg-Al oxide supported catalysts. *Catal. Today.***2018**, 333, 259-267. https://doi.org/10.1016/j.cattod.2018.04.003

[37] Bengaard, H.S.; Nørskov, J.K.; Sehested, J.; Clausen, B.S.; Nielsen, L.P.; Molenbroek, A.M.; Rostrup-Nielsen, J.R. Steam Reforming and Graphite Formation on Ni Catalysts, *J. Catal.* **2002**, 209, 365-384. https://doi.org/10.1006/jcat.2002.3579

[38] Choudhary, V. R.; Uphade, B. S.; Mamman, A. S. Large enhancement in methane-to-syngas conversion activity of supported Ni catalysts due to precoating of catalyst supports with MgO, CaO or rare-earth oxide. *Catal. Lett.* **1995**, 32, 387–390. https://doi.org/10.1007/BF00813233

[39] Choudhary, V. R.; Uphade, B. S.; Mamman, A. S. Oxidative Conversion of Methane to Syngas over Nickel Supported on Commercial Low Surface Area Porous Catalyst Carriers Precoated with Alkaline and Rare Earth Oxides. *J.Catal.* **1997**, 172, 281-293. https://doi.org/10.1006/jcat.1997.1838

[40] Wang, Z.; Cheng, Y.; Shao, X.; Veder, J.-P.; Hu, X.; Ma, Y.; Wang, J.; Xie, K.; Dong, D.; Ping Jiang, S.; Parkinson, G.; Buckley, C.; Li, C.-Z. Nanocatalysts anchored on

nanofiber support for high syngas production via methane partial oxidation. *Appl. Catal. A.* **2018**, 565, 119-126. https://doi.org/10.1016/j.apcata.2018.08.001

[41] Boukha, Z.; Jiménez-González, C.; Gil-Calvo, M.; de Rivas, B.; González-Velasco, J.R.; Gutiérrez-Ortiz, J.I.; López-Fonseca, R.; $MgO/NiAl_2O_4$ as a new formulation of reforming catalysts: Tuning the surface properties for the enhanced partial oxidation of methane. *Appl. Catal. B.* **2016**, 199, 372-383. https://doi.org/10.1016/j.apcatb.2016.06.045

[42] Özdemir, H.; Öksüzömer, M.A.; Gürkaynak, M. Preparation and characterization of Ni based catalysts for the catalytic partial oxidation of methane: Effect of support basicity on H_2/CO ratio and carbon deposition. *Inte. J. Hydrogen Energy*. **2010**, 35, 12147-12160. https://doi.org/10.1016/j.ijhydene.2010.08.091

[43] Yan, Q.G.; Weng, W.Z.; Wan, H.L.; Toghiani, H.; Toghiani, R.K.; Pittman Jr., C.U.; Activation of methane to syngas over a Ni/TiO_2 catalyst. *Appl. Catal. A.* **2003**, 239, 43-58. https://doi.org/10.1016/S0926-860X(02)00351-4

[44] Vermeiren, W.J.M.; Blomsma, E.; Jacobs, P.A.; Catalytic and Thermodynamic Approach of the Oxyreforming Reaction of Methane. *Catal. Today.* **1992**, 13, 427-436. https://doi.org/10.1016/0920-5861(92)80168-M

[45] Osman, A.I.; Meudal, J.; Laffir, F.; Thompson, J.; Rooney, D. Enhanced catalytic activity of Ni on η-Al_2O_3 and ZSM-5 on addition of ceria zirconia for the partial oxidation of methane. *Appl. Catal. B.* **2017**, 212, 68-79. https://doi.org/10.1016/j.apcatb.2016.12.058

[46] Sato, K.; Fujita, S.; Suzuki, K.; Mori, T. High performance of Ni-substituted calcium aluminosilicate for partial oxidation of methane into syngas. *Catal. Commun.* **2007**, 8, 1735-1738. https://doi.org/10.1016/j.catcom.2007.02.006

[47] Berrocal, G.P.; Da Silva , A.; Assaf, J.M.; Alboronz, A.; Rangel, M. Novel supports for nickel-based catalysts for the partial oxidation of methane. *Catal. Today.* **2010**, 149, 240–247. https://doi.org/10.1016/j.cattod.2009.06.005

[48] Liu, H.; Wu, H.; He, D. Methane conversion to syngas over Ni/Y_2O_3 catalysts — Effects of calcination temperatures of Y_2O_3 on physicochemical properties and catalytic performance. *Fuel Process. Technol.* **2014**, 119, 81-86. https://doi.org/10.1016/j.fuproc.2013.11.001

[49] Consuelo, A.; Mayra, M.; Laura, R.; Luis, E.; Rufino, N.; Mahdi, A.; Beatriz, R.; Fierro, J. Partial Oxidation of Methane to Syngas Over Nickel-Based Catalysts: Influence of

Support Type, Addition of Rhodium, and Preparation Method, *Front. Chem.* **2019,** 7, https://doi.org/10.3389/fchem.2019.00104

[50] Tang, S.; Lin, J.; Tan, K. L.; Partial oxidation of methane to syngas over Ni/MgO, Ni/CaO and Ni/CeO_2. *Catal. Lett.* **1998**, 51, 169-175. https://doi.org/10.1023/A:1019034412036

[51] Pantaleo, G.; Parola, V.L.; Deganello, F.; Singha, R.K.; Bal, R.; Venezia, A.M. Ni/CeO_2 catalysts for methane partial oxidation: Synthesis driven structural and catalytic effects. *Appl. Catal. B.* **2016**, 189, 233-241. https://doi.org/10.1016/j.apcatb.2016.02.064

[52] Singha, R.K.; Shukla, A.; Yadav, A.; Sivakumar Konathala, L.N.; Bal, R. Effect of metal-support interaction on activity and stability of Ni-CeO_2 catalyst for partial oxidation of methane. *Appl. Catal. B.* **2017**, 202, 473-488. https://doi.org/10.1016/j.apcatb.2016.09.060

[53] Peymani, M.; Alavi, S.M.; Rezaei, M.; Preparation of highly active and stable nanostructured Ni/CeO_2 catalysts for syngas production by partial oxidation of methane. *Int. J. Hydrogen Energy.* **2016**, 41, 6316-6325. https://doi.org/10.1016/j.ijhydene.2016.03.033

[54] Hu, J.; Yu, C.; Bi, Y.; Wei, L.; Chen, J.; Chen, X. Preparation and characterization of Ni/CeO_2-SiO_2 catalysts and their performance in catalytic partial oxidation of methane to syngas. *Chin. J. Catal.* **2014**, 35, 8-20. https://doi.org/10.1016/S1872-2067(12)60723-2

[55] La Parola, V.; Pantaleo, G.; Deganello, F.; Bal, R.; Venezia, A.M. Plain and CeO_2–Supported La_xNiO_y catalysts for partial oxidation of CH_4. *Catal. Today.* **2018**, 307,189-196. https://doi.org/10.1016/j.cattod.2017.04.045

[56] Salazar-Villalpando, M.D.; Reyes, B. Hydrogen production over Ni/ceria-supported catalysts by partial oxidation of methane. *Int. J. of Hydrogen Energy.* **2009**, 34, 9723-9729. https://doi.org/10.1016/j.ijhydene.2009.10.019

[57] Larimi A. S.; Alavi, S. M. Partial Oxidation of Methane over Ni/$CeZrO_2$ Mixed Oxide Solid Solution Catalysts, *International Journal of Chemical Engineering and Applications*. **2012**, 3. https://DOI: 10.7763/IJCEA.2012.V3.150

[58] Leroi, P.; Madani, B.; Pham-Huu, C.; Ledoux, M.-J.; Savin-Poncet, S.; Bousquet, J.L.; Ni/SiC: a stable and active catalyst for catalytic partial oxidation of methane. *Catal.Today.* **2004**, 91-92, 53-58. https://doi.org/10.1016/j.cattod.2004.03.009

[59] Mukai D.; Tanaka K.; Kikuchi E.; Sekine Y. Low temperature ingnition of methane partial oxidation over Ni/$LaAlO_3$ catalyst. *Journal of japan petroleum institute.* **2012**,56, 156-164.

[60] Cao, Y.; Chin, Y.; Li, W. Effect of La_2O_3 added to NiO/Al_2O_3 catalyst on partial oxidation of methane to syngas. *Stud. Surf. Sci. Catal.* **1997** ,107, 467-471. https://doi.org/10.1016/S0167-2991(97)80378-3

[61] Liu, S.; Xiong, G.; Sheng, S.; Miao, Q.; Yang, W. Effects of Alkali and Rare Earth Metal Oxides on the Thermal Stability and the Carbon-deposition over Nickel Based Catalyst. *Proceedings of the 5th International Natural Gas Conversion Symposium.* **1998** , 747-752.

[62] Miao Q.; Xiong G.; Sheng, S.L.; Zhang,Y. Mechanistic studies of methane partial oxidation to syngas over $LiNiLaO_x/Al_2O_3$ catalyst, *Reac. Kinet. Catal. L.* **1999**, 66, 273–279. https://doi.org/10.1007/BF02475801

[63] Liu, S.; Xiong, G.; Sheng, S.; Yang, W.; Partial oxidation of methane and ethane to synthesis gas over a LiLaNiO/γ–Al_2O_3 catalyst. *Appl. Catal. A.* **2000**, 198, 261-266. https://doi.org/10.1016/S0926-860X(99)00517-7

[64] González, M.G.; Nichio N.N.; Moraweck, B.; Martin, G. Role of chromium in the stability of Ni/Al_2O_3 catalysts for natural gas reforming. *Mater. Lett.* **2000**, 45, 15-18. https://doi.org/10.1016/S0167-577X(00)00065-3

[65] Wang, H-T.; Li, Z-H.; Tian, S. Effect of promoters on the catalytic performance of Ni/Al_2O_3 catalyst for partial oxidation of methane to syngas, *Reac. Kinet. Catal. L.* **2004**, 83, 245–252. https://doi.org/10.1023/B:REAC.0000046083.76225.a0

[66] Nakagawa, K.; Ikenag, N.; Teng, Y.; Kobayashi, T.; Suzuki, T. Partial oxidation of methane to synthesis gas over iridium–nickel bimetallic catalysts. *Appl. Catal. A.* **1999**, 180, 183-193. https://doi.org/10.1016/S0926-860X(98)00336-6

[67] Omoregbe, O.; Danh, H.T.; Abidin, S.Z.; Setiabudi, H.D.; Abdullah, B.; Vu, K.B.; Vo, D.-V.N. Influence of Lanthanide Promoters on Ni/SBA-15 Catalysts for Syngas Production by Methane Dry Reforming, *Procedia Eng.* **2016**, 148, 1388-1395. https://doi.org/10.1016/j.proeng.2016.06.556

[68] Ferreira, A.C. Ferraria, A.M. do Rego, A.M.B. Gonçalves, A.P. Correia, M.R. Gasche, T.A. Branco, J.B. Partial oxidation of methane over bimetallic nickel–lanthanide

oxides. J. Alloys Compd. **2010**, 489, 316-323. https://doi.org/10.1016/j.jallcom.2009.09.082

[69] Cho, W.; Yu, H.; Ahn, W.-S.; Kim, S.-S. Synthesis gas production process for natural gas conversion over Ni–La_2O_3 catalyst, *J. Ind. Eng. Chem.* **2015**, 28, 229-235. https://doi.org/10.1016/j.jiec.2015.02.019

[70] Ding, C.; Wang, J.; Jia, Y.; Ai, G.; Liu, S.; Liu, P.; Zhang, K.; Han, Y.; Ma, X. Anti-coking of Yb-promoted Ni/Al_2O_3 catalyst in partial oxidation of methane, *Int. J. Hydrogen Energy.* **2016**, 41, 10707-10718. https://doi.org/10.1016/j.ijhydene.2016.04.110

[71] Kaddeche, D.; Djaidja, A.; Barama, A. Partial oxidation of methane on co-precipitated Ni–Mg/Al catalysts modified with copper or iron. *Int. J. Hydrogen Energy.* **2017**, 42, 15002-15009. https://doi.org/10.1016/j.ijhydene.2017.04.281

[72] Alvarez-Galvan, C.; Melian, M.; Ruiz-Matas, L.; Eslava, J.L.; Navarro, R.M.; Ahmadi, M.; Roldan Cuenya, B.; Fierro, J.L.G. Partial Oxidation of Methane to Syngas Over Nickel-Based Catalysts: Influence of Support Type, Addition of Rhodium, and Preparation Method. *Front. Chem.* **2019**, 7, 104. https://doi.org/10.3389/fchem.2019.00104

[73] Cheephat, C.; Daorattanachai, P.; Devahastin, S.; Laosiripojana, N. Partial oxidation of methane over monometallic and bimetallic Ni-, Rh-, Re-based catalysts: Effects of Re addition, co-fed reactants and catalyst support. *Appl. Catal. A.* **2018**, 563,1-8. https://doi.org/10.1016/j.apcata.2018.06.032

[74] Asencios, Y.; Marcos, F.; Assaf, J.; Assaf, E. Oxidative-reforming of methane and partial oxidation of methane reactions over NiO/PrO_2/ZrO_2 catalysts: effect of nickel content. *Braz. J. Chem. Eng.* **2016**, 33, 627-636. dx.doi.org/10.1590/0104-6632.20160333s20150056

[75] Christensen, K.O.; Chen, D.; Lødeng, R.; Holmen, A. Effect of supports and Ni crystal size on carbon formation and sintering during steam methane reforming. *Appl. Catal., A.* **2006**, 314, 9-22. https://doi.org/10.1016/j.apcata.2006.07.028

[76] Nakagawa, K.; Ikenaga, N.; Kobayashi, T.; Suzuki, T. Transient response of catalyst bed temperature in the pulsed reaction of partial oxidation of methane to synthesis gas over supported group VIII metal catalysts, Catal.Today. 64 (2001) 31-41. https://doi.org/10.1016/S0920-5861(00)00506-X

[77] Salazar-Villalpando, M.; Berry, D.; Gardner, T. Partial oxidation of methane over Rh/supported-ceria catalysts: Effect of catalyst reducibility and redox cycles. *Int. J.*

Hydrogen Energy. **2008**, 33, 2695-2703. https://doi.org/10.1016/j.ijhydene.2008.03.016

[78] Mallens, E. P. J.; Marin, G. B. The Reaction Mechanism of the Partial Oxidation of Methane to Synthesis Gas: A Transient Kinetic Study over Rhodium and a Comparison with Platinum. *J.Catal.* **1997**, 167, 43–56. https://doi.org/10.1006/jcat.1997.1533

[79] Lanza, R.; Canu, P.; Järås, S.G. Partial oxidation of methane over Pt–Ru bimetallic catalyst for syngas production. *Appl. Catal., A.* **2008**, 348, 221-228. https://doi.org/10.1016/j.apcata.2008.06.044

[80] Boukha, Z.; Gil-Calvo, M.; de Rivas, B.; González-Velasco, J.R.; Gutiérrez-Ortiz, J.I.; López-Fonseca, R. Behaviour of Rh supported on hydroxyapatite catalysts in partial oxidation and steam reforming of methane: On the role of the speciation of the Rh particles, *Appl. Catal., A.* **2018**, 556, 191-203. https://doi.org/10.1016/j.apcata.2018.03.002

[81] Eriksson, S.; Rojas, S.; Boutonnet, M.; Fierro, J.L.G. Effect of Ce-doping on Rh/ZrO_2 catalysts for partial oxidation of methane. *Appl. Catal., A.* **2007**, 326, 8-16. https://doi.org/10.1016/j.apcata.2007.03.019

[82] Boucouvalas, Y.; Zhang, Z.; Verykios, X. E. Heat transport limitations and reaction scheme of partial oxidation of methane to synthesis gas over supported rhodium catalysts. *Catal. Lett.* **1994**, 27,131–142. DOI: 10.1007/BF00806986

[83] Boucouvalas, Y.; Zhang, Z.; Verykios, X. E. Partial oxidation of methane to synthesis gas via the direct reaction scheme over Ru/TiO_2 catalyst. *Catal. Lett.* **1996**, 40, 189–195. https://doi.org/10.1007/BF00815281

[84] Elmasides, C.; Kondarides, D. I.; Grünert, W.; Verykios, X. E. XPS and FTIR Study of Ru/Al_2O_3 and Ru/TiO_2 Catalysts: Reduction Characteristics and Interaction with a Methane-Oxygen Mixture. *J. Phys. Chem., B.* **1999**, 103, 5227-5239. https://doi.org/10.1021/jp9842291

[85] Elmasides, C.; Ioannides, T.; Verykios, X.E. Kinetic behaviour of the Ru/TiO_2 catalyst in the reaction of partial oxidation of methane. *Stud. Surf. Sci. Catal.* **1998**, 119, 801-806. https://doi.org/10.1016/S0167-2991(98)80530-2

[86] Elmasides, C.; Ioannides, T.; Verykios, X.E. Kinetic model of the partial oxidation of methane to synthesis gas over Ru/TiO_2 catalyst. *AlChE J.* **2004** 461, 260-1270. https://doi.org/10.1002/aic.690460618

[87] Scarabello, A.; Dalle Nogare, D.; Canu, P.; Lanza, R. Partial oxidation of methane on Rh/ZrO_2 and $Rh/Ce–ZrO_2$ on monoliths: Catalyst restructuring at reaction conditions. *Appl. Catal., B.* **2015**, 174-175, 308-322. https://doi.org/10.1016/j.apcatb.2015.03.012

[88] Oliveira, R. L.; Bitencourt I.G.; Passos, F.B. Partial Oxidation of Methane to Syngas on Rh/Al_2O_3 and $Rh/Ce-ZrO_2$ Catalysts. *J. Braz. Chem. Soc.* **2013**, 24, 68-75. http://dx.doi.org/10.1590/S0103-50532013000100010

[89] Zhu, Y.; Barat, R. Partial oxidation of methane over a ruthenium phthalocyanine catalyst. *Chem. Eng. Sci.* **2014**, 116, 71-76. https://doi.org/10.1016/j.ces.2014.04.028

[90] Fathia, M.; Sperlea, T.; A.Rokstadb, O.; Holmena, A. Partial oxidation of methane to synthesis gas at very short contact times. *Catal.Today.* **1998** ,42, 205-209. https://doi.org/10.1016/S0920-5861(98)00093-5

[91] van Looij, F.; Stobbe, E.R.; Geus, J.W. Mechanism of the partial oxidation of methane to synthesis gas over Pd. *Catal. Lett.* **1998**, 50, 59-67. https://doi.org/10.1023/A:1019090213003

[92] Yan, Q-G.; Chu, W.; Gao, L-Z.; Yu, Z-L.; Yuan, S-Y. Reactivity of Pt/Al_2O_3 and $Pt/CeO_2/Al_2O_3$ catalysts for partial oxidation of methane to syngas. *Stud. Surf. Sci. Catal.* **1998**, 119, 855-860. https://doi.org/10.1016/S0167-2991(98)80539-9

[93] Singha, R. K.; Shukla, A.; Yadav, A.; Sain, S.; Pendem, C.; Kumar Konathala, L.N.S.; Bal, R. Synthesis effects on activity and stability of $Pt-CeO_2$ catalysts for partial oxidation of methane. *J. Mol. Catal.* **2017**, 432,131-143. https://doi.org/10.1016/j.mcat.2017.01.006

[94] Fu, G.; Xu, X.; Lu, X.; Wan, H. Mechanisms of Methane Activation and Transformation on Molybdenum Oxide Based Catalysts. *JACS.* **2005**,17, 3989-3996. https://doi.org/10.1021/ja0441099

[95] Fathi, M.; Bjorgum , E.; Viig, T.; Rokstad, O. A. Partial oxidation of methane to synthesis gas:: Elimination of gas phase oxygen. *Catal. Today.* **2000**,63, 489-497. https://doi.org/10.1016/S0920-5861(00)00495-8

[96] Otsuka, K.; Wang, Y.; Sunada, E.; Yamanaka, I. Direct Partial Oxidation of Methane to Synthesis Gas by Cerium Oxide, *J. Catal.* **1998**, 175, 152-160. https://doi.org/10.1006/jcat.1998.1985

[97] Neagoe, C.; Boffito, D.C.; Ma, Z.; Trevisanut, C.; Patience, G.S. Pt on Fecralloy catalyses methane partial oxidation to syngas at high pressure. *Catal. Today.* **2016**, 270, 43-50. https://doi.org/10.1016/j.cattod.2015.11.018

[98] Mariana, M.; Souza, M.V.M. Combination of carbon dioxide reforming and partial oxidation of methane over supported platinum catalysts. *Appl. Catal., A.* **2003**, 255, 83-92. https://doi.org/10.1016/S0926-860X(03)00646-X

[99] Passos, F. B.; Oliveira, E. R.; Mattos, L. V.; Noronha, F. B. Effect of the support on the mechanism of partial oxidation of methane on platinum catalysts. *Catal. Lett.* **2006** ,110, 161-167. https://doi.org/10.1007/s10562-006-0119-6

[100] Silva, P.P.; Silva, F.A.; Portela, L.S.; Mattos, L.V.; Noronh, F.B.; Hori, C.E. Effect of Ce/Zr ratio on the performance of $Pt/CeZrO_2/Al_2O_3$ catalysts for methane partial oxidation. *Catal. Today*. **2005**, 107-108, 734-740. https://doi.org/10.1016/j.cattod.2005.07.004

[101] Wang, F.; Li, W.-Z.; Lin, J.-D.; Chen, Z.-Q.; Wang, Y.; Crucial support effect on the durability of $Pt/MgAl_2O_4$ for partial oxidation of methane to syngas. *Appl. Catal., B.* **2018** ,231, 292-298. https://doi.org/10.1016/j.apcatb.2018.03.018

[102] Verlato, E.; Barison, S.; Cimino, S.; Dergal, F.; Lisi, L.; Mancino, G.; Musiani, M.; Vázquez-Gómez,L. Catalytic partial oxidation of methane over nanosized Rh supported on Fecralloy foams. *Int. J. Hydrogen Energy.* **2014**, 39, 11473-11485. https://doi.org/10.1016/j.ijhydene.2014.05.076

[103] Hong, X.; Li, B.; Zhang, C. Yttria Promoted Nickel Nanowire Catalyst for the Partial Oxidation of Methane to Synthesis Gas. *Advances in Materials Physics and Chemistry*. **2012**, 2, 212-215. DOI: 10.4236/ampc.2012.24B054

[104] Zhang, X.; Hayward, D.O.; Michael, D.; Mingos, P.; Further Studies on Oscillations over Nickel Wires During the Partial Oxidation of Methane. *Catal. Lett.* **2003**, 86, 235–243. https://doi.org/10.1023/A:1022672219909

[105] Luo, Z.; Kriz, D.A.; Miao, R.; Kuo, C.-H.; Zhong, W.; Guild, C.; He, J.; B. Willis, Y. Dang, S.L. Suib, P. Nandi, TiO_2 Supported gold–palladium catalyst for effective syngas production from methane partial oxidation. *Appl. Catal. A.* **2018**, 554, 54-63. https://doi.org/10.1016/j.apcata.2018.01.020

[106] Habimana, F.; Li, X.; Ji, S.; Lang, B.; Sun, D.; Li, C. Effect of Cu promoter on Ni-based SBA-15 catalysts for partial oxidation of methane to syngas. *J. Nat. Gas. Chem.* **2009**, 18, 392-398. doi:10.1016/S1003-9953(08)60130-9

[107] Fleys, M.; Shan, W.; Simon, Y.; Marquaire, P-M. Detailed Kinetic Study of the Partial Oxidation of Methane over La_2O_3 Catalyst. Part 1: Experimental Results, Ind. Eng. Chem. Res. **2007**, 41, 1063-1068. https://doi.org/10.1021/ie060342z

[108] Claridge, J. B.; York, A.; Brungs, A.J.; Marquez-Alvarez, C.; Sloan, J.; Tsang, S. C.; Green, M. L.H. New Catalysts for the Conversion of Methane to Synthesis Gas: Molybdenum and Tungsten Carbide. *J. Cat.* **1998**, 180, 85-100. https://doi.org/10.1006/jcat.1998.2260

[109] Zhu, Q.; Zhang, B.; Zhao, J.; Ji, S.; Yang, J.; Wang, J.; Wang, H. The effect of secondary metal on Mo_2C/Al_2O_3 catalyst for the partial oxidation of methane to syngas. *J. Mol. Catal. A: Chem.* **2004**, 213,199-205. https://doi.org/10.1016/j.molcata.2003.06.001

[110] Steghuis, A.G.; Van Ommen, J.G.; Seshan, K.; Lercher, J.A. New highly active catalysts in direct partial oxidation of methane to synthesis gas, Studies in Surface Science and Catalysis. **1997**, 107, 403-408. https://doi.org/10.1016/S0167-2991(97)80368-0

[111] Figen, H.E.; Baykara, S.Z. Effect of ruthenium addition on molybdenum catalysts for syngas production via catalytic partial oxidation of methane in a monolithic reactor. *Int. J. of Hydrogen Energy.* **2018**, 43, 1129-1138. https://doi.org/10.1016/j.ijhydene.2017.10.173

[112] Vella, L.D.; Villoria, J.A.; Specchia, S.; Mota, N.; Fierro, J.L.G.; Specchia, V. Catalytic partial oxidation of CH_4 with nickel–lanthanum-based catalysts. *Catal. Today.* **2011**,171, 84-96. https://doi.org/10.1016/j.cattod.2011.03.074

[113] Jahangiri, A.; Aghabozorg, H.; Pahlavanzadeh, H. Effects of Fe substitutions by Ni in La–Ni–O perovskite-type oxides in reforming of methane with CO_2 and O_2. *Int. J. Hydrogen Energy.* **2013**, 38, 10407-10416. https://doi.org/10.1016/j.ijhydene.2013.05.080

[114] Mishra, A.; Galinsky, N.; He, F.; Santiso, E.E.; Li, F. Perovskite-structured $AMn_xB_{1-x}O_3$ (A = Ca or Ba; B = Fe or Ni) redox catalysts for partial oxidation of methane. *Catal. Sci. Technol.* **2016** ,6, 4535-4544. 10.1039/C5CY02186C

[115] Meng, B. Zhang, H. Zhao, Z. Wang, X. Jin, Y. Liu, S. A novel $LaGa_{0.65}Mg_{0.15}Ni_{0.20}O_{3-\delta}$ perovskite catalyst with high performance for the partial oxidation of methane to syngas. *Catal. Today.* **2016**, 259, 388-392. https://doi.org/10.1016/j.cattod.2015.05.009

[116] Provendiera, H.; petit, C.; Estournèsb, C.; Libsa, S.; Kiennemanna, A. Stabilisation of active nickel catalysts in partial oxidation of methane to synthesis gas by iron addition. *Appl. Catal., A.* **1999** ,183, 163-173. https://doi.org/10.1016/S0926-860X(98)00343-3

[117] Choudhary, V.R.; Uphade, B.S.; Belhekar, A.A. Oxidative Conversion of Methane to Syngas over $LaNiO_3$ Perovskite with or without Simultaneous Steam and CO_2 Reforming Reactions: Influence of Partial Substitution of La and Ni. *J. Catal.* **1996**, 163, 312-318. https://doi.org/10.1006/jcat.1996.0332

[118] Zagaynov, I.V.; Loktev, A.S.; Mukhin, I.E.; Dedov, A.G.; Moiseev, I.I. Influence of the Ni/Co ratio in bimetallic NiCo catalysts on methane conversion into synthesis gas, *Mendeleev Commun.* **2017**, 27, 509-511. https://doi.org/10.1016/j.mencom.2017.09.027

[119] Khine, M.S.S.; Chen, L.; Zhang, S.; Lin, J.; Jiang, S.P. Syngas production by catalytic partial oxidation of methane over $(La_{0.7}A_{0.3})BO_3$ (A = Ba, Ca, Mg, Sr, and B = Cr or Fe) perovskite oxides for portable fuel cell applications. *Int. J. of Hydrogen Energy.* **2013** ,38, 13300-13308. https://doi.org/10.1016/j.ijhydene.2013.07.097

[120] Roseno, K.T.C.; Brackmann, R.; da Silva, M.A.; Schmal, M. Investigation of $LaCoO_3$, $LaFeO_3$ and $LaCo_{0.5}Fe_{0.5}O_3$ perovskites as catalyst precursors for syngas production by partial oxidation of methane. *Int. J. of Hydrogen Energy.* **2016**, 41, 18178-18192. https://doi.org/10.1016/j.ijhydene.2016.07.207

[121] Dai, X.; Yu, C.; Wu,Q.; Comparison of $LaFeO_3$, $La_{0.8}Sr_{0.2}FeO_3$, and $La_{0.8}Sr_{0.2}Fe_{0.9}Co_{0.1}O_3$ perovskite oxides as oxygen carrier for partial oxidation of methane. *J. nat. gas. Chem.* **2008**, 17, 415-418. https://doi.org/10.1016/S1003-9953(09)60019-0

[122] Takehira, T.H. K.; Harihara, H.; Andersen, A.G.; Suzuki, K.; Shimizua, M. Partial oxidation of methane to synthesis gas over (Ca,Sr) (Ti,Ni) oxides. *Catal. Today.* **1995**, 24, 237-242. https://doi.org/10.1016/0920-5861(95)00031-A

[123] Takehira, T.H. K.; Harihara, H.; Andersen, A.G.; Suzuki, K.; Yasuda, H.; Tsunoda, T.; Hamakawa, S.; York, A.P.; Yoon, Y.; Shimizu, M.; Takehira, K. Sustainable $Ni/Ca_{1-x}Sr_xTiO_3$ catalyst prepared in situ for the partial oxidation of methane to synthesis gas. *Appl. Catal. A.* **1997**, 149, 391-410. https://doi.org/10.1016/S0926-860X(96)00274-8

[124] Dedov, A.G.; Loktev, A.S.; Komissarenko, D.A.; Parkhomenko, K.V.; Roger, A.C.; Shlyakhtin, O.A.; Mazo, G.N.; Moiseev, I.I. High-selectivity partial oxidation of methane into synthesis gas: the role of the red-ox transformations of rare earth — alkali earth cobaltate-based catalyst components. *Fuel Process. Technol.* **2016**, 148, 128-137. https://doi.org/10.1016/j.fuproc.2016.02.018

[125] Lago, R.; Bini, G.; Peña, M.A.; Fierro, J.L.G. Partial Oxidation of Methane to Synthesis Gas Using $LnCoO_3$ Perovskites as Catalyst Precursors. *J. of Catal.* **1997**, 167, 198-209. https://doi.org/10.1006/jcat.1997.1580

[126] Takehira, K.; Shishido, T.; Kondo, M. Partial Oxidation of CH_4 over $Ni/SrTiO_3$ Catalysts Prepared by a Solid-Phase Crystallization Method. *J. Catal.* **2002**, 207, 307-316. https://doi.org/10.1006/jcat.2002.3537

[127] Guo, C.; Zhang, J.; Li, W.; Zhang, P.; Wang, Y. Partial oxidation of methane to syngas over $BaTi_{1-x}Ni_xO_3$ catalysts, *Catal. Today.* **2004**, 98, 583-587. https://doi.org/10.1016/j.cattod.2004.09.012

[128] de Araujo, G.C. Lima, S. Rangel, M.d.C. Parola, V.L. Peña, M.A. García Fierro, J.L. Characterization of precursors and reactivity of $LaNi_{1-x}Co_xO_3$ for the partial oxidation of methane. *Catal. Today.* **2005**, 107-108, 906-912. https://doi.org/10.1016/j.cattod.2005.07.044

[129] Slagtern, Å.; Olsbye, U.; Partial oxidation of methane to synthesis gas using La-M-O catalysts, *Appl. Catal., A.* **1994**, 110, 99-108. https://doi.org/10.1016/0926-860X(94)80109-6

[130] Toniolo, F.S.; Magalhães, R.N.S.H.; Perez, C.A.C.; Schmal, M.; Structural investigation of $LaCoO_3$ and $LaCoCuO_3$ perovskite-type oxides and the effect of Cu on coke deposition in the partial oxidation of methane. *Appl. Catal., B.* **2012**, 117-118, 156-166. https://doi.org/10.1016/j.apcatb.2012.01.009

[131] Santos, M.; Neto, R.C.R.; Noronha, F.B.; Bargiela, P.; Rocha, M.; Resini, C.; Carbó-Argibay, E.; Fréty, R.; Brandão, S.T. Perovskite as catalyst precursors in the partial oxidation of methane: The effect of cobalt, nickel and pretreatment. *Catal. Today.* **2018** ,299, 229-241. https://doi.org/10.1016/j.cattod.2017.06.027

[132] Cihlar, J.; Vrba, R.; Castkova, K.; Cihlar, J. Effect of transition metal on stability and activity of La-Ca-M-(Al)-O (M = Co, Cr, Fe and Mn) perovskite oxides during partial oxidation of methane. *Int. J. Hydrogen Energy.* **2017**, 42, 19920-19934. https://doi.org/10.1016/j.ijhydene.2017.06.075

[133] Zhao, K.; He, F.; Huang, Z.; Zheng, A.; Li, H.; Zhao, Z. $La_{1-x}Sr_xFeO_3$ perovskites as oxygen carriers for the partial oxidation of methane to syngas. *Chin. J. Catal.* **2014**, 35, 1196-1205. https://doi.org/10.1016/S1872-2067(14)60084-X

[134] Mihai, O.; Chen, D.; Holmen, A. Chemical looping methane partial oxidation: The effect of the crystal size and O content of $LaFeO_3$. *J. Catal.* **2012**, 293, 175-185. https://doi.org/10.1016/j.jcat.2012.06.022

[135] Wei, H.J.; Cao, Y.; Ji, W.J.; Au, C.T. Lattice oxygen of $La_{1-x}Sr_xMO_3$ (M=Mn, Ni) and $LaMnO_{3-\alpha}F_\beta$ perovskite oxides for the partial oxidation of methane to synthesis gas. *Catal. Commun.* **2008**, 9, 2509-2514. https://doi.org/10.1016/j.catcom.2008.06.019

[136] Melchiori, T.; Di Felice, L.; Mota, N.; Navarro, R.M.; Fierro, J.L.G.; Annaland, M.S.; Gallucci, F. Methane partial oxidation over a $LaCr_{0.85}Ru_{0.15}O_3$ catalyst: Characterization, activity tests and kinetic modeling. *Appl. Catal., A.* **2014**, 486, 239-249. https://doi.org/10.1016/j.apcata.2014.08.040

[137] Dedov, A.G.; Loktev, A.S.; Komissarenko, D.A.; Mazo, G.N.; Shlyakhtin, O.A.; Parkhomenko, K.V.; Kiennemann, A.A.; Roger, A.C.; Ishmurzin, A.V.; Moiseev, I.I. Partial oxidation of methane to produce syngas over a neodymium–calcium cobaltate-based catalyst. *Appl. Catal., A.* **2015**, 489, 140-146. https://doi.org/10.1016/j.apcata.2014.10.027

[138] Du, Y.-p.; Zhu, X.; Wang, H.; Wei, Y.-g.; Li, K.-z. Selective oxidation of methane to syngas using $Pr_{0.7}Zr_{0.3}O_{2-\Delta}$: Stability of oxygen carrier. *Tran. Nonferrous Met. Soc. China.* **2015**, 25, 1248-1253. https://doi.org/10.1016/S1003-6326(15)63722-0

[139] Zhou, L.; Li, X.; Yao, Z.; Chen, Z.; Hong, M.; Zhu, R.; Liang, Y.; Zhao, J. Transition-Metal Doped Ceria Microspheres with Nanoporous Structures for CO Oxidation. *Sci Rep*. **2016**, 6, 23900. doi: 10.1038/srep23900 (2016)

[140] De Roseno, K.T.; Schmal, M.; Brackmann, R.; Alves, R.M.B.; Giudici, R. Partial oxidation of methane on neodymium and lanthanium chromate based perovskites for hydrogen production, *Int. J. Hydrogen Energy.* **2019**, 44, 8166-8177. https://doi.org/10.1016/j.ijhydene.2019.02.039

[141] da Silveira, V.R.; Melo, D.M.A.; Barros, B.S.; Ruiz, J.A.C.; Rojas, L.O.A.; Nickel-based catalyst derived from $NiO–Ce_{0.75}Zr_{0.2}5O_2$ nanocrystalline composite: Effect of the synthetic route on the partial oxidation of methane. *Ceram. Int.* **2016**, 42, 16084-16089. https://doi.org/10.1016/j.ceramint.2016.07.119

[142] Palcheva, R.; Olsbye, U.; Palcut, M.; Rauwel, P.; Tyuliev, G.; Velinov, N.; Fjellvåg, H.H. Rh promoted $La_{0.75}Sr_{0.25}(Fe_{0.8}Co_{0.2})_{1-x}Ga_xO_{3-\delta}$ perovskite catalysts: Characterization and catalytic performance for methane partial oxidation to synthesis gas. *Appl. Surf .Sci.* **2015**, 357, 45-54. https://doi.org/10.1016/j.apsusc.2015.08.237

[143] Santis-Alvarez, A.J.; Büchel, R.; Hild, N.; Stark, W.J.; Poulikakos, D. Comparison of flame-made rhodium on Al_2O_3 or $Ce_{0.5}Zr_{0.5}O_2$ supports for the partial oxidation of methane.2 *Appl. Catal., A.* **2014**, 469, 275-283. https://doi.org/10.1016/j.apcata.2013.10.013

[144] He, F.; Wei, Y.; Li, H.; Wang, H. Synthesis Gas Generation by Chemical-Looping Reforming Using Ce-Based Oxygen Carriers Modified with Fe, Cu, and Mn Oxides. *Energy Fuels.* **2009**, 23, 2095-2102. https://doi.org/10.1021/ef800922m

[145] L. Borovskikh, G.Mazo, E. Kemnitz, Reactivity of oxygen of complex cobaltates $La_{1-x}Sr_xCoO_{3-\delta}$ and $LaSrCoO_4$, Solid State Sci. **2003**, 5, 409-417. https://doi.org/10.1016/S1293-2558(03)00052-9

[146] Deng, J.; Zhang, L.; Dai, H.; He, H.; Au, C. T. Preparation, characterization, and catalytic properties of $NdSrCu_{1-x}Co_xO_{4-\delta}$ and $Sm_{1.8}Ce_{0.2}Cu_{1-x}Co_xO_{4+\delta}$ (x = 0, 0.2 and 0.4) for methane combustion, Appl.Catal., B. **2009** ,89, 87-96. https://doi.org/10.1016/j.apcatb.2008.11.015

[147] Zhu, H.; Zhang, P.; Dai, S. Recent Advances of Lanthanum-Based Perovskite Oxides for Catalysis. *ACS Catal.* **2015**, 5, 6370-6385. https://doi.org/10.1021/acscatal.5b01667

[148] He, F.; Li, X.; Zhao, K.; Huang, Z.; Wei, G.; Li, H. The use of $La_{1-x}Sr_xFeO_3$ perovskite-type oxides as oxygen carriers in chemical-looping reforming of methane. *Fuel.* **2013**, 108, 465-473. https://doi.org/10.1016/j.fuel.2012.11.035

[149] Arevalo, R.L.; Aspera, S.M.; Escano, M.C.S.; Nakanishi, H.; Kasai, H. Tuning methane decomposition on stepped Ni surface: The role of subsurface atoms in catalyst design, Sci. Rep. **2017**, 7, 13963. https://doi.org/10.1038/s41598-017-14050-3

[150] Makarshin, L.L.; Sadykov, V.A.; Andreev, D.V.; Gribovskii, A.G.; Privezentsev, V.V.; Parmon, V.N. Syngas production by partial oxidation of methane in a microchannel reactor over a Ni–Pt/$La_{0.2}Zr_{0.4}Ce_{0.4}O_x$ catalyst. *Fuel Process. Technol.* **2015**, 131, 21-28. https://doi.org/10.1016/j.fuproc.2014.10.031

[151] Schneider, A.; Mantzaras, J.; Jansohn, P. Experimental and numerical investigation of the catalytic partial oxidation of of CH_4/O_2 mixtures diluted with H_2O and CO_2 in a short contact time reactor. *Chem. Eng. Sci.* **2006**, 61, 4634-4649. https://doi.org/10.1016/j.ces.2006.02.038

[152] Luo, H.; Wei, Y.; Jiang, H.; Yuan, W.; Lv, Y.; Caro, J.; Wang, H. Performance of a ceramic membrane reactor with high oxygen flux Ta-containing perovskite for the partial oxidation of methane to syngas. *J. Mem. Sci.* **2010**, 350, 154-160. https://doi.org/10.1016/j.memsci.2009.12.023

[153] Kharton, V.V.; Patrakeev, M.V.; Waerenborgh, J.C.; Sobyanin, V.A.; Veniaminov, S.A.; Yaremchenko, A.A.; Gaczyński, P.; Belyaev, V.D.; Semin, G.L.; Frade, J.R. Methane oxidation over perovskite-related ferrites: Effects of oxygen nonstoichiometry. *Solid State Sci*. **2005**, 7, 1344-1352. https://doi.org/10.1016/j.solidstatesciences.2005.08.004

[154] Evdou, A. Zaspalis, V. Nalbandian, L. $La_{1-x}Sr_xFeO_{3-\delta}$ perovskites as redox materials for application in a membrane reactor for simultaneous production of pure hydrogen and synthesis gas. *Fuel.* **2010**, 89, 1265-1273.

[155] Li, Y.; Luo, Z.Y.; Yu, C.J.; Luo, D.; Xu, Z.A.; Cen, K.F. The impact of NiO on microstructure and electrical property of solid oxide fuel cell anode. *J. Zhejiang Univ. Sci., B.* **2005**, 6, 1124-1129. DOI: 10.1631/jzus.2005.B1124

[156] Tsai , C.Y.; Dixon, A.G.; Moser, W. R.; Ma, Y. H.; Dense perovskite membrane reactors for partial oxidation of methane to syngas. *AIChE J.* 43 **1997**, 43, 2741-2750. https://doi.org/10.1002/aic.690431320

[157] W. Jin, S. Li, P. Huang, N. Xu, J. Shia, Y. SLin, Tubular lanthanum cobaltite perovskite-type membrane reactors for partial oxidation of methane to syngas. *J. Mem Sci.* **2000**, 166, 13–22. https://doi.org/10.1016/S0376-7388(99)00245-8

[158] Z.S. Hui Dong, Guoxing Xiong, Jianhua Tong, Shishan Sheng, WeishenYang, Investigation on POM reaction in a new perovskite membrane reactor. *Catal. Today.* **2001**, 167, 3-13. https://doi.org/10.1016/S0920-5861(01)00277-2

[159] Tong, W.Y.; Cai, R.; Zhu, B.; Lin, L. Novel and Ideal Zirconium-Based Dense Membrane Reactors for Partial Oxidation of Methane to Syngas. *Catal. Lett.* **2002**, 78, 129-137. https://doi.org/10.1023/A:1014950027492

[160] Harada, M.; Kazunari, D.; Michikazu, H.; Takashi, T. $Ba_{1.0}Co_{0.7}Fe_{0.2}Nb_{0.1}O_{3-\delta}$ Dense Ceramic as an Oxygen Permeable Membrane for Partial Oxidation of Methane to Synthesis Gas. *Chem. Lett.* **2006** ,35, 1326-1327. https://doi.org/10.1246/cl.2006.1326

[161] Dong, X.; Liu, Z.; He, Y.; Jin, W.; Xu, N. $SrAl_2O_4$-improved $SrCo_{0.8}Fe_{0.2}O_{3-\delta}$ mixed-conducting membrane for effective production of hydrogen from methane. *J. Mem. Sci.* **2009**, 331, 109-116. https://doi.org/10.1016/j.memsci.2009.01.023

[162] Kharton, V.V.; Yaremchenko, A.A.; Valente, A.A.; Sobyanin, V.A.; Belyaev, V.D.; Semin, G.L.; Veniaminov, S.A.; Tsipis, E.V.; Shaula, A.L.; Frade, J.R.; Rocha, J. Methane oxidation over Fe-, Co-, Ni- and V-containing mixed conductors, *Solid State Ionics.* **2005**, 176, 781-791. https://doi.org/10.1016/j.ssi.2004.10.019

[163] Hu, J.; Xing, T.; Jia, Q.; Hao, H.; Yang, D.; Guoc, Y.; Hu, X. Methane partial oxidation to syngas in $YBa_2Cu_3O_{7-x}$ membrane reactor. *Appl. Catal., A.* **2006** ,306, 29-33. https://doi.org/10.1016/j.apcata.2006.03.034

[164] Paturzo, L.; Gallucci, F.; Basile, A.; Pertici, P.; Scalera, N.; Vitulli, G. Partial Oxidation of Methane in a Catalytic Ruthenium Membrane Reactor. *Ind. Eng. Chem. Res.* **2003**, 42, 2968–2974. https://doi.org/10.1021/ie020873x

[165] Babakhani, E.G.; Towfighi, J.; Taheri, Z.; Pour, A.N.; Zekordi, M.; Taheri, A. Partial oxidation of methane in $Ba_{0.5}Sr_{0.5}Co_{0.8}Fe_{0.1}Ni_{0.1}O_{3-\delta}$ ceramic membrane reactor. *J. Nat.Gas Chem.* **2012**, 21, 519-525. https://doi.org/10.1016/S1003-9953(11)60400-3

[166] Zhang, Y.; Liu, J.; Ding, W.; Lu, X. Performance of an oxygen-permeable membrane reactor for partial oxidation of methane in coke oven gas to syngas. *Fuel.* **2011** ,90, 324-330. https://doi.org/10.1016/j.fuel.2010.08.027

[167] Liao, Q.; Chen, Y.; Wei, Y.; Zhou, L.; Wang, H. Performance of U-shaped $BaCo_{0.7}Fe_{0.2}Ta_{0.1}O_{3-\delta}$ hollow-fiber membranes reactor with high oxygen permeation for methane conversion. *Chem. Eng. J.* **2014** ,237, 146-152. https://doi.org/10.1016/j.cej.2013.09.105

[168] Yang, Z.; Zhang, Y.; Ding, W.; Investigation on the reforming reactions of coke-oven-gas to H_2 and CO in oxygen-permeable membrane reactor. *J. Mem. Sci.* **2014**, 470, 197-204. https://doi.org/10.1016/j.memsci.2014.07.041

[169] Li, Q. Zhu, X. He, Y. Yang, W. Partial oxidation of methane in $BaCe_{0.1}Co_{0.4}Fe_{0.5}O_{3-\delta}$ membrane reactor. *Catal. Today.* **2010**, 149, 185-190. https://doi.org/10.1016/j.cattod.2009.03.019

[170] Sadykov, V.; Zarubina, V.; Pavlova, S.; Krieger, T.; Alikina, G.; Lukashevich, A.; Muzykantov, V.; Sadovskaya, E.; Mezentseva, N.; Zevak, E. Design of asymmetric multilayer membranes based on mixed ionic–electronic conducting composites supported on Ni–Al foam substrate. *Catal. Today.* **2010**, 156, 173-180. https://doi.org/10.1016/j.cattod.2010.07.030

[171] Gong, Z.; Hong, L. Integration of air separation and partial oxidation of methane in the $La_{0.4}Ba_{0.6}Fe_{0.8}Zn_{0.2}O_{3-\delta}$ membrane reactor. *J. Mem. Sci.* **2011**, 380, 81-86. https://doi.org/10.1016/j.memsci.2011.06.033

[172] Wei, Y.Y.; Huang, L.; Tang, J. Y.; Zhou, L.; Li, Z.; Wang, H.H. Syngas production in a novel perovskite membrane reactor with co-feed of CO_2. *Chin. Chem. Lett.* **2011** ,22, 1492-1496. https://doi.org/10.1016/j.cclet.2011.05.040

[173] Cai, L.; Li, W.; Cao, Z.; Zhu, X.; Yang, W. Improving oxygen permeation of MIEC membrane reactor by enhancing the electronic conductivity under intermediate-low oxygen partial pressures. *J. Mem. Sci.* **2016** ,520, 607-615. https://doi.org/10.1016/j.memsci.2016.08.012

[174] Markov, A.; Mikhail V. Patrakeev, M.; Leonidov, I.; Kozhevnikov, V. Reaction control and long-term stability of partial methane oxidation over an oxygen membrane. *J. Solid. State. Electrochem.* **2011**, 15:253–257. DOI 10.1007/s10008-010-1113-x

[175] Kniep, J;. Lin, Y.S. Partial Oxidation of Methane and Oxygen Permeation in $SrCoFeO_x$ Membrane Reactor with Different Catalysts. *Ind. Eng. Chem. Res.* **2011**, 50, 7941-7948. https://doi.org/10.1021/ie2001346

[176] Zhu, X. Wang, H. Cong, Y. Yang, W. Partial oxidation of methane to syngas in $BaCe_{0.15}Fe_{0.85}O_{3-\delta}$ membrane reactors. *Catal. Lett.* **2006** ,111, 179-185. https://doi.org/10.1007/s10562-006-0145-4

[177] Nguyen, T.H.; Łamacz, A.; Krztoń, A.; Djéga-Mariadassou, G. Partial oxidation of methane over Ni^0/La_2O_3 bifunctional catalyst IV: Simulation of methane total oxidation, dry reforming and partial oxidation using the Quasi-Steady State Approximation. *Appl. Catal., B.* **2016** , 199, 424-432. https://doi.org/10.1016/j.apcatb.2016.06.034

[178] Gu, X.; Jin, W.; Chen, C.; Xu, N.; Shi, J. YSZ-$SrCo_{0.4}Fe_{0.6}O_{3-\delta}$ Membranes for the Partial Oxidation of Methane to Syngas. *AIChE J.* **2002** , 48, 2051-2060. https://doi.org/10.1002/aic.690480918

[179] Kim, J.; Hwang, G.; Lee, S.; Park, C.; Kim, J.; Kim, Y. Properties of oxygen permeation and partial oxidation of methane in $La_{0.6}Sr_{0.4}CoO_{3-\delta}$ (LSC)–$La_{0.7}Sr_{0.3}Ga_{0.6}Fe_{0.4}O_{3-\delta}$ (LSGF) membrane. *J. Mem. Sci.* **2005**, 250, 11-16. https://doi.org/10.1016/j.memsci.2004.10.012

[180] Xianfeng , Z.C.; Yanjun, H.; Xueliang, D.; Wanqin, J.; Nanping, X. A Comparative Study of the Performance of Symmetric and Asymmetric Mixed-conducting Membranes. *Chin. J. Chem. Eng.* **2009**, 17, 562-570. https://doi.org/10.1016/S1004-9541(08)60245-1

[181] Yuan, R.-h.; He, Z.; Zhang, Y.; Wang, W.-d.; Chen, C.-s.; Wu, H.; Zhan, Z.-l. Partial Oxidation of Methane to Syngas in a Packed Bed Catalyst Membrane Reactor. *AIChE J.* **2016**, 62, 2170-2176. https://doi.org/10.1002/aic.15202

[182] Shen, Z.; Lu, P.; Hu, J.; Hu, X. Performance of $Ba_{0.5}Sr_{0.5}Co_{0.8}Fe_{0.2}O_{3+\delta}$ membrane after laser ablation for methane conversion. *Catal. Commun.* **2010**, 11, 892-895. https://doi.org/10.1016/j.catcom.2010.03.016

[183] Wang, H.; Yang, W.S.; Cong, Y.; Zhu, X.; Lin, Y.S. Structure and oxygen permeability of a dual-phase membrane. *J. Mem. Sci.* **2003** ,224, 107-115. https://doi.org/10.1016/j.memsci.2003.07.003

[184] Wang, H.; Tablet, C.; Feldhoff, A.; Caro, J. A Cobalt-Free Oxygen-Permeable Membrane Based on the Perovskite-Type Oxide $Ba_{0.5}Sr_{0.5}Zn_{0.2}Fe_{0.8}O_{3-\delta}$. *Adv. Mater.* **2005**, 17,1785-1788. https://doi.org/10.1002/adma.200401608

[185] Harada, M.; Domen, K.; Hara, M.; Tatsumi, T. Oxygen-permeable Membranes of $Ba_{1.0}Co_{0.7}Fe_{0.2}Nb_{0.1}O_{3-\delta}$ for Preparation of Synthesis Gas from Methane by Partial Oxidation. *Chem. Lette.* **2006** ,35, 968-969. https://doi.org/10.1246/cl.2006.968

[186] Ritchie, J. T.; Richardson, J.T.; Luss, D. Ceramic Membrane Reactor for Synthesis Gas Production. *AIChE J.* **2001** , 47, 2092-2101. https://doi.org/10.1002/aic.690470919

[187] Wu, Z.; Jin, W.; Xu, N. Oxygen permeability and stability of Al_2O_3-doped $SrCo_{0.8}Fe_{0.2}O_{3-\delta}$ mixed conducting oxides. *J. Mem. Sci.* **2006**, 279, 320-327. https://doi.org/10.1016/j.memsci.2005.12.018

[188] Zhu, X.; Li, Q.; Cong, Y.; Yang, W. Syngas generation in a membrane reactor with a highly stable ceramic composite membrane. *Catal. Commun.* **2008** ,10, 309-312. https://doi.org/10.1016/j.catcom.2008.09.014

[189] Park, J.H.; Kwon, Y.-i.; Nam, G.D.; Joo, J.H. Simultaneous conversion of carbon dioxide and methane to syngas using an oxygen transport membrane in pure CO_2 and CH_4 atmospheres. *J. Mat. Chem., A.* **2018** ,6, 14246-14254. 10.1039/C8TA03021A

[190] Ruiz-Trejo, E. Boldrin, P. Medley-Hallam, J.L. Darr, J. A. Atkinson, N.P. Brandon, Partial oxidation of methane using silver/gadolinia-doped ceria composite membranes. *Chem. Eng. Sci.* **2015** ,127, 269-275. https://doi.org/10.1016/j.ces.2015.01.047

[191] Deibert, W.; Ivanova, M.E.; Baumann, S.; Guillon, O. ;Meulenberg, W.A. Ion-conducting ceramic membrane reactors for high-temperature applications. *J. Mem. Sci.* **2017** ,543, 79-97. https://doi.org/10.1016/j.memsci.2017.08.016

[192] Zhu, X.; Li, Q.; He, Y.; Cong, Y.; Yang, W. Oxygen permeation and partial oxidation of methane in dual-phase membrane reactors. *J. Mem. Sci.* **2010** ,360, 454-460. https://doi.org/10.1016/j.memsci.2010.05.044

[193] Yaremchenko, A.A.; Kharton, V.V.; Valente, A.A.; Veniaminov, S.A.; Belyaev, V.D.; Sobyanin, V.A.; Marquez, F. Methane oxidation over mixed-conducting $SrFe(Al)O_{3-\delta}$–$SrAl_2O_4$ composite. *Phys. Chem. Chem. Phys.* **2007,** 9, 2744–2752. DOI: 10.1039/b617409b

[194] Yaremchenko, A.A.; Kharton, V.V.; Valente, A.A.; Snijkers, F.; Cooymans, F.; Luyten, J.; Marquez, F. Performance of tubular $SrFe(Al)O_{3-\delta}$–$SrAl_2O_4$ composite membranes in CO_2- and CH_4- containing atmospheres. *J. Mem. Sci.* **2008**, 319, 141–148. doi:10.1016/j.memsci.2008.03.028

[195] Shen, Z.; Lu, P.; Hu, J.; Hu, X. Performance of $Ba_{0.5}Sr_{0.5}Co_{0.8}Fe_{0.2}O_{3+\delta}$ membrane after laser ablation for methane conversion. *Catal.comm.* **2010**, 11, 892-895. https://doi.org/10.1016/j.catcom.2010.03.016

[196] Kathiraser,. K.; Kawi, S. $La_{0.6}Sr_{0.4}Co_{0.8}Ga_{0.2}O_{3-\delta}$ (LSCG) hollow fiber membrane reactor: Partial oxidation of methane at medium temperature. *AIChE J.* **2013** 59, 3874-3885. DOI 10.1002/aic.14202

[197] Wang, Z.; Ashok, J.; Pu, Z.; Kawi, S. Low temperature partial oxidation of methane via $BaBi_{0.05}Co_{0.8}Nb_{0.15}O_{3-\delta}$-Ni phyllosilicate catalytic hollow fiber membrane reactor. *Chem. Eng. J.* **2017**, 315, 315–323. http://dx.doi.org/10.1016/j.cej.2017.01.015

[198] Shao, Z.; Xiong, G.; Dong, H.; Yang, W.; Lin, L. Synthesis, oxygen permeation study and membrane performance of a $Ba_{0.5}Sr_{0.5}Co_{0.8}Fe_{0.2}O_{3-\delta}$ oxygen-permeable dense ceramic reactor for partial oxidation of methane to syngas. *Separation and Purification Technology.* **2001 ,**25 , 97–116.

[199] Plazaola, A.; Tanaka, A.; Annaland, M.; Gallucci, F. Recent Advances in Pd-Based Membranes for Membrane Reactors. *Molecules*. **2017**, 22, 51.

[200] Zhang, G.; Jin, W.; Xu, N. Design and Fabrication of Ceramic Catalytic Membrane Reactors for Green Chemical Engineering Applications. *Engineering*. **2018**, 4, 848–860. https://doi.org/10.1016/j.eng.2017.05.001

[201] Jiang, H.; Wang, H.; Werth, S.; Schiestel, T.; Caro, J. Simultaneous Production of Hydrogen and Synthesis Gas by Combining Water Splitting with Partial Oxidation of Methane in a Hollow-Fiber Membrane Reactor. *Angew. Chem. Int. Ed.* **2008**, 47, 9341 –9344. http://dx.doi.org/10.1002/anie.200803899.

[202] Liang, W.; Megarajan, S.; Liang, F.; Zhang, Y.; He, G.; n Liu ,Z.; Jiang, H. Coupling of N_2O decomposition with CO_2 reforming of CH_4 in novel cobalt-free $BaFe_{0.9}Zr_{0.05}Al_{0.05}O_{3-\delta}$ oxygen transport membrane reactor. *Chem. Eng. J.* **2016**, 305, 176–181. http://dx.doi.org/10.1016/j.cej.2015.10.067

[203] Zhu, X.; Wang, H.; Yang, W. Relationship between homogeneity and oxygen permeability of composite membranes. *J. Mem. Sci.* **2008** ,309, 120-127. https://doi.org/10.1016/j.memsci.2007.10.011

[204] Liang, W.; Zhou, H;. Caro, J.; Jiang, H. Methane conversion to syngas and hydrogen in a dual phase $Ce_{0.8}Sm_{0.2}O_{2-\delta}$-$Sr_2Fe_{1.5}Mo_{0.5}O_{5+\delta}$ membrane reactor with improved stability. *Int. J. Hydrogen Energy.* **2018**, 43, 14478-14485. https://doi.org/10.1016/j.ijhydene.2018.06.008

[205] Chen, S.; Kucerank, A. Electrodeposition of platinum on nanometer-sized carbon electrodes, *J. Phys. Chem. B.* **2003** ,107, 8392-8402. https://doi.org/10.1021/jp0348934

[206] J. Beckers, G.; Rothenberg. Sustainable selective oxidations using ceria-based materials. *Green Chem.* **2010**, 12, 939-948. 10.1039/C000191K

[207] Sun, L.; Ran, R.; Wang, G.; Shao, Z. Fabrication and performance test of a catalyst-coated membrane from direct spray deposition. Solid State Ion. **2008**, 179, 960-965. https://doi.org/10.1016/j.ssi.2008.01.081

[208] Akin, F.T.; Lin, J.Y.S. Oxygen permeation through oxygen ionic or mixed-conducting ceramic membranes with chemical reactions. *J. Mem. Sci.* **2004**, 231, 133-146. https://doi.org/10.1016/j.memsci.2003.11.012

[209] Nguyen, T.H.; Łamacz, A.; Beaunier, P.; Czajkowska, S.; Domański, M.; Krztoń, A.; Van Le, T.; Djéga-Mariadassou, G. Partial oxidation of methane over bifunctional catalyst I. In situ formation of Ni^0/La_2O_3 during temperature programmed POM reaction over $LaNiO_3$ perovskite. *Appl. Catal., B.* **2014**, 152-153, 360-369. https://doi.org/10.1016/j.apcatb.2014.01.053

[210] Velasco, J.; Lopez, L.; Cabrer, S.; Boutonnet, M.; Järås, S. Synthesis gas production for GTL applications: Thermodynamic equilibrium approach and potential for carbon formation in a catalytic partial oxidation pre-reformer. J. Nat. Gas. Sci. Eng. **2014**, 20, 175-183. https://doi.org/10.1016/j.jngse.2014.06.021

[211] Hickman, D.A.; Schmidit, L.D. Synthesis gas formation by direct oxidation of methane over Pt monoliths. *J. Catal.* **1992** ,138, 267-282. https://doi.org/10.1016/0021-9517(92)90022-A

[212] Wang, H.; Cong, Y.; Yang, W. Investigation on the partial oxidation of methane to syngas in a tubular $Ba_{0.5}Sr_{0.5}Co_{0.8}Fe_{0.2}O_{3-\delta}$ membrane reactor. *Catal. Today.* **2003**, 82, 157-166. https://doi.org/10.1016/S0920-5861(03)00228-1

[213] Au, C. T.; Wang, H.Y.; Wan, H. L. Mechanistic Studies of CH_4/O_2 Conversion over SiO_2-Supported Nickel and Copper Catalysts. *J. Catal.* **1996**, 158, 343–348. https://doi.org/10.1006/jcat.1996.0033

[214] Ishihara, T.S.T.; Nishiguchi, H.; Takita, Y. Oxide ion conductivity in $La_{0.8}Sr_{0.2}Ga_{0.8}Mg_{0.2-x}Ni_xO_3$ perovskite oxide and application for the electrolyte of solid

oxide fuel cells. *J. Mat. Sci.* **2001**, 36, 1125–1131. https://doi.org/10.1023/A:1004821607054

[215] Ten Elshof, J.E.; Bouwmeester, H.J.M.; Verweij, H.Oxidative coupling of methane in a mixed-conducting perovskite membrane reactor. *Appl. Catal., A.* **1995** ,130, 195-212. https://doi.org/10.1016/0926-860X(95)00098-4

[216] Rebeilleau-Dassonneville, M.; Rosini, S.; Van Veen, A.C.; Farrusseng, D.; Mirodatos, C. Oxidative activation of ethane on catalytic modified dense ionic oxygen conducting membranes. *Catal. Today.* **2005**, 104, 131-137. https://doi.org/10.1016/j.cattod.2005.03.071

[217] Wang, H.; Tablet, C.; Schiestel, T.; Caro, J. Hollow fiber membrane reactors for the oxidative activation of ethane. *Catal. Today.* **2006** ,118, 98-103. https://doi.org/10.1016/j.cattod.2005.11.093

[218] Liu, J.-J.; Zhang, S.-q.; Wang, W.-d.; Gao, J.-f.; Liu, W.; Chen, C.-s. Partial oxidation of methane in a $Zr_{0.84}Y_{0.16}O_{1.92}$–$La_{0.8}Sr_{0.2}Cr_{0.5}Fe_{0.5}O_{3-\delta}$ hollow fiber membrane reactor targeting solid oxide fuel cell applications. *J. Power Sources.* **2012**, 217, 287-290. https://doi.org/10.1016/j.jpowsour.2012.06.042

[219] Hui, S.; Petric, A. Electrical Properties of Yttrium-Doped Strontium Titanate under Reducing Conditions. *J. Electrochem. Soc.* **2001**, 149, 1-10. doi: 10.1149/1.1420706

[220] Bouwmeester, H.J.M. Dense ceramic membranes for methane conversion. *Catal. Today.* **2003**, 82, 141-150. https://doi.org/10.1016/S0920-5861(03)00222-0

[221] Efimov, K.; Klande, T.; Juditzki, N.; Feldhoff, A. Ca-containing CO2-tolerant perovskite materials for oxygen separation. *J. Mem. Sci.* **2012**, 389, 205– 215. doi:10.1016/j.memsci.2011.10.030

[222] Zhang, C.; Sunarso, J.; Liu, S. Designing CO_2-resistant oxygen-selective mixed ionic–electronic conducting membranes: guidelines, recent advances, and forward directions. *Chem. Soc. Rev.,* **2017**, 46, 2941. https://doi.org/10.1039/C6CS00841K

[223] Yang, N.; Kathiraser, T.; Kawi, S. $La_{0.6}Sr_{0.4}Co_{0.8}Ni_{0.2}O_{3-\delta}$ hollow fiber membrane reactor: Integrated oxygen separatione CO_2 reforming of methane reaction for hydrogen production. *International Journal of Hydrogen Energy*. **2013**, 38, 4483-4491. https://doi.org/10.1016/j.ijhydene.2013.01.073

[224] Wang, Z.; Oemar, U.; LiAng, M.; Kawi, S. Oxidative steam reforming of biomass tar model compound via catalytic $BaBi_{0.05}Co_{0.8}Nb_{0.15}O_{3-\delta}$ hollow fiber membrane reactor, J. *Membrane Sci.* **2016**, 510, 417-425. https://doi.org/10.1016/j.memsci.2016.03.014

[225] Wang, Z.; Bian, Z.; Dewangan, N.; Xu,J.; Kawi, S. High-performance catalytic perovskite hollow fiber membrane reactor for oxidative propane dehydrogenation, J. *Membrane Sci.* **2019**, 578, 36-42. https://doi.org/10.1016/j.memsci.2019.02.012

[226] Rosen, L.; Degenstein, N.; Shah, M.; Wilson, J.; Kelly, S; Peck, J.; Christie, M. Development of oxygen transport membranes for coal-based power generation. *Energy Procedia.* **2011**, 4, 750–755. https://doi.org/10.1016/j.egypro.2011.01.115

[227] Pei, S.; Kleefisch , M. S.; Kobylinski, T.P.; Faber, J.; Udovich, C.A.; Zhang-McCoy, V.; Dabrowski, B.; Balachandran, U.; Mieville, R.L.; Poeppel, R.B. Failure mechanisms of ceramic membrane reactors in partial oxidation of methane to synthesis gas. *Catal. Lett.* **1995** ,30, 201-212. https://doi.org/10.1007/BF00813686

[228] Jianxin, Y.; Feng, S.; Zuo, Y.; Liu, W.; Chen, C. Oxygen Permeability and Stability of $Sr_{0.95}Co_{0.8}Fe_{0.2}O_{3-\delta}$ in a CO_2- and H_2O-Containing Atmosphere. *Chem. Mater.* **2005**, 17, 5856–5861. https://doi.org/10.1021/cm051636y

[229] Fouskas, A.; Kollia, M.; Kambolis, A.; Papadopoulou, C.; Matralis, H. Boron-modified Ni/Al_2O_3 catalysts for reduced carbon deposition during dry reforming of methane. *Appl. Catal., A.* **2014** ,474, 125-134. https://doi.org/10.1016/j.apcata.2013.08.016

[230] Sousa, L.F.d.; Toniolo, F.S.; Landi, S.M.; Schmal, M. Investigation of structures and metallic environment of the Ni/Nb_2O_5 by different in situ treatments – Effect on the partial oxidation of methane. *Appl. Catal., A.* **2017**, 537, 100-110. https://doi.org/10.1016/j.apcata.2017.03.015

[231] Zhao, K.; He, F.; Huang, Z.; Wei, G.; Zheng, A.; Li, H.; Zhao, Z. Perovskite-type oxides $LaFe_{1-x}Co_xO_3$ for chemical looping steam methane reforming to syngas and hydrogen co-production. *Appl. Energy.* **2016**, 168, 193-203. https://doi.org/10.1016/j.apenergy.2016.01.052

[232] Staykov, A.; Téllez, H.; Akbay, T.; Druce, J.; Ishihara, T.; Kilner, J. Oxygen Activation and Dissociation on Transition Metal Free Perovskite Surfaces. *Chem. Mater.* **2015**, 27, 8273-8281. https://doi.org/10.1021/acs.chemmater.5b03263

[233] Yang, C.; Grimaud, A. Factors Controlling the Redox Activity of Oxygen in Perovskites: From Theory to Application for Catalytic Reactions. *Catalysts.* **2017**, 7. https://doi.org/10.3390/catal7050149

[234] Hwang, J.; Rao, R.R.; Giordano, L.; Katayama, Y.; Yu, Y.; Shao-Horn, Y. Perovskites in catalysis and electrocatalysis. *Science.* **2017**, 358, 751–756. DOI: 10.1126/science.aam7092

[235] Dickens, C.F.; Montoya, J.H.; Kulkarni, A.R.; Bajdich, M.; Nørskov, J.K. An electronic structure descriptor for oxygen reactivity at metal and metal-oxide surfaces. *Surface Science.* **2019**, 681 ,122-129. https://doi.org/10.1016/j.susc.2018.11.019

[236] Yang, S.; Chung, D.Y.; Tak, Y.-J.; Kim, J.; Han, H.; Yu, J.-S.; Soon, A.; Sung, Y.-E.; Lee, H. Electronic structure modification of platinum on titanium nitride resulting in enhanced catalytic activity and durability for oxygen reduction and formic acid oxidation. *Appl. Catal., B*. **2015**,174-175, 35-42. https://doi.org/10.1016/j.apcatb.2015.02.033

[237] Freund, H.J.; Meijer, G.; Scheffler, M.; Schlogl, R.; Wolf, M. CO oxidation as a prototypical reaction for heterogeneous processes. *Angew Chem. Int. Ed.* **2011**, 50, 10064-10094. https://doi.org/10.1002/anie.201101378